

UNIVERSITY OF MANITOBA

MOISTURE AND GROUNDWATER REGIME IN A SANDY
SOIL UNDER IRRIGATION

by

Ashvani K. Madan

A THESIS

SUBMITTED TO THE FACULTY OF GRADUATE STUDIES
IN PARTIAL FULFILLMENT OF THE REQUIREMENTS FOR THE DEGREE
OF MASTER OF SCIENCE

DEPARTMENT OF AGRICULTURAL ENGINEERING

WINNIPEG, MANITOBA

April, 1979



MOISTURE AND GROUNDWATER REGIME IN A SANDY
SOIL UNDER IRRIGATION

BY

ASHVANI KUMAR MADAN

A dissertation submitted to the Faculty of Graduate Studies of
the University of Manitoba in partial fulfillment of the requirements
of the degree of

MASTER OF SCIENCE

©1979

Permission has been granted to the LIBRARY OF THE UNIVER-
SITY OF MANITOBA to lend or sell copies of this dissertation, to
the NATIONAL LIBRARY OF CANADA to microfilm this
dissertation and to lend or sell copies of the film, and UNIVERSITY
MICROFILMS to publish an abstract of this dissertation.

The author reserves other publication rights, and neither the
dissertation nor extensive extracts from it may be printed or other-
wise reproduced without the author's written permission.

ABSTRACT

Moisture regime and groundwater regime were studied in a sandy soil at Portage la Prairie. The topography of the experimental field was undulating. The groundwater level at the low spots was at a depth of 1.3 m to 1.6 m below the surface and generally contributed beneficially towards the moisture content of the root zone. The groundwater level below 2.0 m had a negligible effect on the moisture regime. Irrigation was essential at the high spots which constituted nearly 80 percent of the area. Random drainage was essential only at the low spots with fine soil texture. Natural drainage of the land was effective in draining away the recharge by precipitation and irrigation. The average slope of the groundwater surface was 0.135 percent and the saturated hydraulic conductivity varied between 11.28 cm/h and 25.80 cm/h.

In an attempt to describe the observed moisture and groundwater regime quantitatively, a simple method was developed to obtain saturated hydraulic conductivity, bubbling pressure and pore-size distribution index. The Green and Ampt model (1911) was used to calculate saturated hydraulic conductivity and average capillary suction from infiltration data. The model of Gardner et al. (1970) and the concept of average capillary pressure at the wetting front put forward by Idike et al. (1977) were used to calculate pore-size distribution index and bubbling pressure. The calculated bubbling pressure was near that of unconsolidated sand, and pore-size distribution index varied from that of unconsolidated sand to that of sandy loam soil as obtained by Laliberte (1966).

ACKNOWLEDGEMENTS

The author wishes to express sincere thanks to Dr. F. F. Penkava; frequent consultations and instructive discussion with him provided valuable guidance throughout this study. Appreciation is due to Dr. G. E. Laliberte whose ideas and encouragement contributed immensely. Thanks are extended to Dr. C. F. Shaykewich for reviewing the thesis as an examination committee member.

I would like to thank Mr. K. Pidhirniak, an undergraduate student, for his assistance in collecting data.

Thanks are also due to Mr. J. G. Putnam and Mr. R. H. Mogan for extending technical services whenever required.

Last but certainly far from least, I am deeply appreciative of my wife, Indu. Without her moral support and encouragement, this study could not have been completed in time.

TABLE OF CONTENTS

CHAPTER		PAGE
	LIST OF TABLES.....	iv
	LIST OF FIGURES.....	vi
	LIST OF SYMBOLS.....	ix
I	INTRODUCTION.....	1
II	REVIEW OF LITERATURE.....	6
	2.1 Infiltration.....	6
	2.1.1 Infiltration Rate.....	6
	2.1.2 Infiltration Equations.....	7
	2.2 Surface Runoff.....	9
	2.3 Redistribution of Moisture.....	10
	2.4 Drainage.....	11
	2.4.1 Drainage Requirements of Crop.....	11
	2.4.2 Design Criteria of Drainage.....	12
	2.5 Properties of Porous Media.....	13
III	THEORETICAL ANALYSIS.....	15
	3.1 Time to the Beginning of Runoff.....	15
	3.2 Infiltration after Runoff Begins.....	18
	3.3 Average Capillary Pressure at the Wetting Front (P_{cav}) and Bubbling Pressure (P_b).....	20
	3.4 Redistribution of Moisture after Precipitation.....	21
IV	MATERIALS AND METHODS.....	26
	4.1 Experimental Site.....	26
	4.2 Measurement of Soil Moisture.....	27
	4.2.1 Selection of Site.....	27
	4.2.2 Site Preparation.....	27
	4.2.3 Neutron Moisture Meter.....	30

TABLE OF CONTENTS - Continued

CHAPTER		PAGE
	4.3 Measurement of Groundwater Level.....	34
	4.4 Measurement of Infiltration.....	34
	4.5 Measurement of Moisture Content after Flooding.....	38
V	RESULTS AND DISCUSSION.....	39
	5.1 Infiltrometer Experiment.....	39
	5.1.1 Effect of Compaction.....	39
	5.1.2 Effect of Soil Texture.....	41
	5.1.3 Representative Infiltration Characteristics.....	41
	5.1.4 Kostiakov Function.....	49
	5.1.5 Green and Ampt Function.....	49
	5.1.6 Use of Kostiakov, and Green and Ampt Functions.....	50
	5.1.7 Significance of Saturated Hydraulic Conductivity (C_s) and Average Capillary Pressure at the Wetting Front (P_{cav})...	50
	5.1.8 Bubbling Pressure and Pore-size Distribution Index.....	51
	5.1.9 Time to the Beginning of Runoff.....	55
	5.2 Groundwater Level Measurement.....	61
	5.2.1 Groundwater Level with Respect to a Reference.....	61
	5.2.2 Groundwater Level with Respect to Ground Surface.....	65
	5.3 Moisture Profiles in the Cousins Field in 1978.....	65
	5.4 Moisture Profiles in the Cousins Field in 1977.....	73
	5.5 Moisture Profiles in the Friesen Field in 1978.....	82
	5.6 Moisture Profiles in the Friesen Field in 1977.....	91
VI	CONCLUSIONS.....	99
VII	RECOMMENDATIONS.....	102
	REFERENCES.....	103

TABLE OF CONTENTS - Continued

CHAPTER	PAGE
APPENDIX A.....	108
Infiltration Data.....	108
APPENDIX B.....	114
Contour Map of the Cousins Field.....	114
APPENDIX C	
Method of Averages.....	115

LIST OF TABLES

TABLE		PAGE
5.1	REPRESENTATIVE INFILTRATION RATE, INFILTRATION DEPTH AND CUMULATIVE INFILTRATION IN SECTION I.....	44
5.2	REPRESENTATIVE INFILTRATION RATE, INFILTRATION DEPTH AND CUMULATIVE INFILTRATION IN SECTION II.....	46
5.3	REPRESENTATIVE INFILTRATION RATE, INFILTRATION DEPTH AND CUMULATIVE INFILTRATION IN SECTION III.....	48
5.4	INFILTRATION RATE AND CUMULATIVE INFILTRATION AT THE END OF FLOODING.....	52
5.5	AVERAGE MOISTURE CONTENT OF THE TRANSMISSION ZONE AFTER THE FLOODING ENDS.....	52
5.6	BUBBLING PRESSURE AND PORE-SIZE DISTRIBUTION INDICES.....	54
5.7	COMPARISON OF BUBBLING PRESSURE AND PORE- SIZE DISTRIBUTION INDEX WITH OTHER RESULTS.....	54
5.8	TOTAL RAINFALL AND MAXIMUM RAINFALL INTENSITIES IN 1977.....	57
5.9	TOTAL RAINFALL AND MAXIMUM RAINFALL INTENSITIES IN 1978.....	58
5.10	TIME TO THE BEGINNING OF RUNOFF IN SECTION I.....	58
5.11	TIME TO THE BEGINNING OF RUNOFF IN SECTION II.....	60
5.12	TIME TO THE BEGINNING OF RUNOFF IN SECTION III....	60
5.13	GROUNDWATER TABLE SLOPES BETWEEN OBSERVATION WELLS.....	64
5.14	REPRESENTATIVE PHYSICAL PROPERTIES OF SOILS (ISRAELSON, 1962).....	67
5.15	AVERAGE MOISTURE CONTENT IN THE COUSINS FIELD IN 1977.....	74
5.16	AVERAGE MOISTURE CONTENT IN THE FRIESEN FIELD IN 1977.....	90

LIST OF TABLES - Continued

TABLE		PAGE
A-1	ELAPSED TIME AND CUMULATIVE INFILTRATION DATA.....	108
A-2	ELAPSED TIME AND CUMULATIVE INFILTRATION DATA.....	108
A-3	ELAPSED TIME AND CUMULATIVE INFILTRATION DATA.....	109
A-4	ELAPSED TIME AND INFILTRATION RATE.....	109
A-5	ELAPSED TIME AND INFILTRATION RATE.....	110
A-6	ELAPSED TIME AND INFILTRATION RATE.....	110
A-7	INITIAL AND FINAL MOISTURE CONTENT DATA OF INFILTRATION EXPERIMENT.....	111
A-8	INITIAL AND FINAL MOISTURE CONTENT DATA OF INFILTRATION EXPERIMENT.....	111
A-9	INITIAL AND FINAL MOISTURE CONTENT DATA OF INFILTRATION EXPERIMENT.....	112
A-10	INITIAL AND FINAL MOISTURE CONTENT DATA OF INFILTRATION EXPERIMENT.....	112
A-11	MOISTURE CONTENT OF THE TRANSMISSION ZONE AFTER THE FLOODING ENDS AT SECTION I AND INITIAL MOISTURE CONTENT.....	113
A-12	MOISTURE CONTENT OF THE TRANSMISSION ZONE ATER THE FLOODING ENDS AT SECTION II AND INITIAL MOISTURE CONTENT.....	113
A-13	MOISTURE CONTENT OF THE TRANSMISSION ZONE AFTER THE FLOODING ENDS AT SECTION III AND INITIAL MOISTURE CONTENT.....	113

LIST OF FIGURES

Figure		Page
3.1	Generalized Soil Moisture Profile during Infiltration at the Moment of Surface Saturation.....	16
3.2	Generalized Soil Moisture Profile during Infiltration after Surface Saturation.....	19
4.1	Locations of Access Tubes in the Cousins Field and Contour Map.....	28
4.2	Locations of Access Tubes in the Friesen Field.....	29
4.3	Photograph of Moisture Gauge Fitted on the Top of Access Tube.....	31
4.4	Photograph of Scaler-ratemeter.....	32
4.5	Photograph of Infiltrometer.....	37
5.1	Infiltration Rate on Furrow and Hill.....	40
5.2	Infiltration Rate in Sandy and Sandy Loam Soils...	42
5.3	Infiltration Rate in Section I.....	43
5.4	Infiltration Rate in Section II.....	45
5.5	Infiltration Rate in Section III.....	47
5.6	Groundwater Level with Respect to a Reference and Rainfall Histogram for 1978.....	62
5.7	Groundwater Level Below the Ground Surface.....	66
5.8	Moisture Profile and Rainfall Histogram at Location Cousins-C1A78 in 1978.....	68
5.9	Moisture Profile and Rainfall Histogram at Location Cousins-C4C78 in 1978.....	69
5.10	Moisture Profile and Rainfall Histogram at Location Cousins-C2B78 in 1978.....	70
5.11	Moisture Profile and Rainfall Histogram at Location Cousins-C3B78 in 1978.....	71

LIST OF FIGURES - Continued

Figure	Page	
5.12	Moisture Profile and Rainfall Histogram at Location Cousins-C1A77 in 1977.....	76
5.13	Moisture Profile and Rainfall Histogram at Location Cousins-C4A77 in 1977.....	77
5.14	Moisture Profile and Rainfall Histogram at Location Cousins-C2B77 in 1977.....	78
5.15	Moisture Profile and Rainfall Histogram at Location Cousins-C2C77 in 1977.....	79
5.16	Moisture Content at 15-cm Depth on Furrow and Rainfall Histogram in the Cousins Field in 1977.....	80
5.17	Moisture Content at 15-cm Depth on Hill and Rainfall Histogram in the Cousins Field in 1977.....	81
5.18	Moisture Profile and Rainfall Histogram at Location Friesen-F3C78 in 1978.....	83
5.19	Moisture Profile and Rainfall Histogram at Location Friesen-F2B78 in 1978.....	84
5.20	Moisture Profile and Rainfall Histogram at Location Friesen-F1B78 in 1978.....	85
5.21	Moisture Profile and Rainfall Histogram at Location Friesen-F1A78 in 1978.....	86
5.22	Moisture Profile and Rainfall Histogram at Location Friesen-F3A78 in 1978.....	87
5.23	Moisture Profile and Rainfall Histogram at Location Friesen-F2C78 in 1978.....	88
5.24	Moisture Profile and Rainfall Histogram at Location Friesen-F3A77 in 1978.....	92
5.25	Moisture Profile and Rainfall Histogram at Location Friesen-F1C77 in 1977.....	93

LIST OF FIGURES - Continued

Figure		Page
5.26	Moisture Profile and Rainfall Histogram at Location Friesen-F2B77 in 1977.....	94
5.27	Moisture Profile and Rainfall Histogram at Location Firesen-F3C77 in 1977.....	95
5.28	Moisture Content at 15-cm Depth on Furrow and Rainfall Histogram in the Friesen Field in 1977.....	96
5.29	Moisture Content at 15-cm Depth on Hill and Rainfall Histogram in the Friesen Field in 1977.....	97
B1	Contour Map of the Cousins Field (E $\frac{1}{2}$ 35-10-8W)....	114

LIST OF SYMBOLS

<u>Symbol</u>	<u>Definition</u>	<u>Dimension</u>
A	Infiltration rate at the end of flooding in Gardner et al. model	LT^{-1}
a	Constant in Kostiakov function	none
b	Constant in Kostiakov function	none
C_w	Effective hydraulic conductivity	LT^{-1}
C_s	Saturated hydraulic conductivity	LT^{-1}
D	Constant in the method of averages	L^2
E	Constant in the method of averages	L
F	Cumulative infiltration at anytime	L
F_s	Infiltrated depth up to saturation	L
f_p	Infiltration rate in Green and Ampt equation	LT^{-1}
H	Matric potential	L
h	Head of water above the soil surface	L
I	Rainfall intensity	LT^{-1}
IMD	Initial moisture deficit	none
k_r	Relative permeability	none
k_s	Permeability at saturation	L^2
k_w	Effective permeability	L^2
L	Depth of the moisture profile above the wetting front	L
L_s	Equivalent depth of the moisture profile at surface saturation	L
P_c	Capillary pressure - the difference in pressure across the interface between the wetting fluid and the non-wetting fluid	FL^{-2}

LIST OF SYMBOLS - Continued

<u>Symbol</u>	<u>Definition</u>	<u>Dimension</u>
P_b	Bubbling pressure - approximately the minimum capillary pressure on the drainage cycle at which the non-wetting fluid is continuous	FL^{-2}
P_{cav}	Average capillary pressure at the wetting front - the area under the curve drawn between capillary pressure and relative permeability	FL^{-1}
q	Flux - flow per unit area per unit time	LT^{-1}
S	Saturation	none
S_i	Initial saturation	none
S_{ei}	Effective saturation at initial moisture content	none
S_{ef}	Effective saturation at final moisture content	none
S_r	Residual saturation	none
t	Time	T
Y	Cumulative infiltration	L
Z	Depth	L
α	Constant in Kostiakov function	none
ϵ	Constant in Gardner et al. model	none
θ_s	Volumetric moisture content	none
θ_i	Volumetric moisture content at saturation	none
θ	Volumetric moisture content at initial moisture content	none
λ	Pore-size distribution index, $-d(\log S)/d(\log P_c)$	none
ρ	Density of water	$FL^{-4}T^{-2}$
g	Acceleration due to gravity	LT^{-2}

CHAPTER I

INTRODUCTION

Development of the world's agricultural production potential is a challenge that must be met by mankind to keep pace with the increasing world population and its need for an adequate supply of food and fibre. The emphasis must be laid on the efficient use of the resources, the most important being land and water.

To achieve maximum yield, the optimum soil moisture content is one of the dominant factors. The sources of moisture are precipitation, irrigation and groundwater, if the groundwater is near the surface. Moisture is lost from the soil by deep percolation and evapotranspiration. Their combined effects govern the moisture regime of the soil. The moisture regime should provide optimum moisture throughout the growing period of a crop.

In achieving improved efficiency of land use, one can not always depend upon precipitation as the only source of moisture throughout the growing period. Deficient moisture at any growing stage can be injurious to the crop and can severely limit the yield. Irrigation, therefore, may be required throughout the growing period or for a part of it. In either case, investment in an irrigation system has to be made and it must be determined whether the investment will succeed or be lost. The land may be ruined if natural drainage is not adequate to drain away the excess irrigation water which leaves the root zone. The problem is aggravated by the presence of an excess

of salt in the soil as leaching of these salts will require additional irrigation water and good drainage. If the groundwater rises near to the surface a soil with good production potential can be reclaimed by providing artificial drainage. Artificial drainage is expensive and may not be justified if the capital investment is too high to be recovered in a reasonably short period. Also, the depth to which the groundwater table can be lowered is limited by impervious strata below the surface. If the groundwater can not be lowered with artificial drainage, sufficiently to allow the deep-rooting crops to grow, such artificial drainage will not succeed because with limited root growth deep-rooting crops are not economical.

In the Portage la Prairie area irrigation is often practiced on land with a shallow groundwater table. An impervious stratum is present 3 m to 5 m below the surface. Therefore, there is a high possibility of loss of investment on an irrigation system. Harmful long-term effects on the suitability of land for agriculture can also be expected. To answer some of the questions connected with permanent irrigation agriculture on the soil, classified as Almasippi series by the Manitoba Soil Survey, the present study has been conducted.

The observation of moisture content at a number of locations in two fields at depths from 15 cm to 110 cm provided information on the present state of the moisture regime as influenced by precipitation, irrigation, groundwater, deep percolation and evapotranspiration. An analysis of the irrigation and drainage requirements was undertaken based on a study of the soil moisture regime. In one of

the two experimental fields, it was found that a high groundwater table at a depth of about 1.5 m was generally contributing beneficially towards the moisture content of the root zone and no irrigation was required. At places where the groundwater table was more than 2.0 m deep, irrigation was required and, in the absence of irrigation, the crop permanently wilted.

To determine the extent of natural drainage and the feasibility of artificial drainage, a study of the groundwater regime and the determination of saturated hydraulic conductivity were required. The groundwater regime was monitored in three observation wells. The slope of the groundwater table was 0.135 percent on the average which was considered quite high. The saturated hydraulic conductivity was determined by applying the model of Mein and Larson (1971) to the infiltration characteristics of the soil and was found to vary between 11.28 cm/h to 25.80 cm/h. The relatively steep slope of the groundwater table and the high saturated hydraulic conductivity showed that natural drainage was effective. This observation was substantiated by the groundwater regime which showed that almost the whole of the recharge by precipitation and irrigation was drained naturally.

The texture of the soil in the field varied from place to place. This resulted in large variations in infiltration characteristics. The representative infiltration characteristics for three sections of the field were determined. A design infiltration equation was selected using data from the sections of the field based upon the criterion of zero runoff in the section of the field

having a relatively low rate of infiltration.

To determine the moisture regime quantitatively, it is necessary to know the unsaturated hydraulic conductivity-moisture content relationship, bubbling pressure, pore-size distribution index and residual saturation. Precise determination of these parameters requires long experiments in the laboratory. The conditions similar to the laboratory are not met and, hence, approximations are involved. On the other hand, in this study in an attempt to explain the observed moisture regime quantitatively, a simple method for determining the parameters of porous media in a field was developed. An assumption was made that the residual saturation is negligibly small, which is very nearly true for sandy soils. The redistribution model developed by Gardner et al. (1970) and the concept of average capillary suction at the wetting front put forward by Idike et al. (1977) have been used to determine the porous media parameters.

The topography of the field was undulating. Surface runoff on such a field could erode the upper productive layer of the soil and accumulate water at the low spots, thereby increasing the drainage requirement. Potential surface runoff was calculated from the Green and Ampt (1911) equation as modified by Mein and Larson (1971).

On the basis of these considerations the objectives of this study were defined as follows:

1. To determine a design infiltration equation for the soil.
2. To determine saturated hydraulic conductivity, the unsat-

urated hydraulic conductivity-moisture content relationship, pore-size distribution index and bubbling pressure.

3. To determine time to the beginning of runoff for various combinations of initial moisture content and precipitation intensity.
4. To study moisture content profiles from depths of 15 cm to 110 cm.
5. To determine the groundwater regime of the soil.
6. To determine draingage and irrigation requirements.

CHAPTER II

REVIEW OF LITERATURE

2.1 Infiltration

2.1.1 Infiltration Rate

Infiltration rate was first called infiltration capacity by Horton (1940) and defined as the maximum rate at which a given soil in a given condition can absorb rain as it falls. The term "infiltration capacity" has been an object of some controversy (Richards, 1952). The term infiltration rate has been accepted as more suitable.

Infiltration rate varies with time until a certain minimum infiltration rate, called the basic infiltration rate, is reached. Flooding of an initially dry soil results in an initially very high rate of infiltration, due to a very steep gradient of moisture content acting in a thin surface layer with high conductivity and diffusivity of saturation. This rate steadily declines as the development of the moisture profile reduces the gradient of moisture content at the surface. In fact, the flow of water is in response to the hydraulic gradient set up by the moisture gradient.

The infiltration rate (Childs, 1967) should be differentiated from the hydraulic conductivity, which is only one factor entering into the process of infiltration. It may be regarded as a consequence of hydraulic conductivity and of potential gradient at the surface, in accordance with Darcy's law or alternately as the rate

of increase of the total amount of water stored in the soil profile.

2.1.2 Infiltration Equations

A rational infiltration equation may be defined as one which can be derived directly from fundamental principles, which fits all experimental data and which represents the physical conditions correctly throughout the entire range of their occurrence and hence is valid outside the range of experimental observations. The Kostiakov (1932) and Horton (1940) equations are the best known infiltration equations which have been popular because of their simplicity and capacity to fit most infiltration rate data. However, both equations contain parameters which are difficult to predict because they have no physical significance.

A more recent empirical equation given by Holtan (1961) expresses the infiltration rate not as a function of time but of unoccupied pore space in the soil. A model of this type is convenient for a watershed model, but the determination of the so-called "control depth" introduces an uncertainty. This equation takes into account the storage recovery, vegetative cover, soil characteristics, soil moisture content and ponding effect when necessary.

Philip (1957) derived an infiltration equation with predictable parameters. Unfortunately, computing these parameters is difficult (Whisler and Bower, 1970) and their values are more commonly obtained by fitting. A further difficulty in the use of this equation for sprinkler irrigation is the assumption of an excess of water supply at the surface.

Green and Ampt (1911) derived an equation to describe vertical downward movement of water in a soil with the assumption that water was ponded on the surface. Morel-Seytoux and Khanji (1974) derived an equation of infiltration which was essentially the same as the Green and Ampt equation but without many of its restrictions. This equation is based upon the assumption that water profiles can be represented as a step function. In the strictest sense, the step function profiles will only occur in a porous medium having primary porosity and pores similar in shape and identical in size. While this is an obvious idealization, it does, nevertheless, allow for the interconnected flow through the porous medium, so that the assumption of non-interconnected parallel capillary tubes is not required. However, for the more common porous medium that departs from such idealism by having pores of more than one size, the step function profiles will be qualitatively inaccurate for time near zero. In such instances, the water content at the soil surface is at first a finitely increasing function of time (Rubin and Steinhardt, 1963; Rubin, 1967; Childs, 1967; Braester, 1973), rather than an instantaneous jump from one position to the other. Once the surface ponding has begun, it seems reasonable to expect that the step function will be followed at least to some fair degree. In the continuous ponding studies of Youngs (1957) in which excellent step-function profiles were found for a glass-bead medium, even his more general medium (slate dust) exhibited profiles that could be reasonably approximated as step functions. This was also found for field soils (Nielsen et al.,

1962; Jackson, 1963) ranging from sandy loam through loam, silt loam and silt clay.

Even if there is some qualitative inaccuracy in the assumption of a step function at times near zero, it does not necessarily follow that the profile at time near zero is, therefore, rendered inaccurate, particularly for evaluating infiltration flux and cumulative infiltration.

2.2 Surface Runoff

Utilizing the concepts of flow similar to those of Green and Ampt (1911) Mein and Larson (1971) developed an equation describing the volume of water infiltrating prior to surface saturation. They considered constant application rates. The model is important in the sense that it uses parameters having physical significance and describes the process itself. All the parameters are measurable and none is dependent on field data for evaluation by fitting. However, the model does not provide a direct way of introducing variations in vegetative cover. The model also assumes constant rainfall intensity. Idike et al. (1977) found that prediction of infiltration by the Mein and Larson model was generally good during the latter portion and middle portion of the run. The Holtan (1961) model generally under-predicted the infiltration during initial stages of the runs and generally under-predicted the time to the beginning of runoff. The Mein and Larson model predicted fairly accurately in both instances. Chu (1977) has shown that the same relationship is equally valid for time-varying rate of rainfall.

2.3 Redistribution of Moisture

Of the various flow processes involved in the field water cycle, the post-infiltration redistribution of soil moisture, often referred to as internal drainage (Gardner et al., 1970) is one of the least understood. The process is important in the sense that it determines the amount of water retained at various times at different depths in the soil profile and can affect the water consumption of plants. This is also important because of its effect on infiltration.

The presumed water content at which internal drainage becomes negligible within a few days or ceases entirely, termed the 'field capacity', had long been accepted as an actual physical property, characteristic of and constant for each soil. Though the field capacity concept was originally derived from crude measurements of water content in the field, some workers have sought to explain this concept in terms of a static equilibrium value or a discontinuity in the capillary water (Kohnke, 1968).

In recent years with the development of theory and more precise experimental techniques in the study of unsaturated flow processes, the field capacity concept as originally defined has been recognized as arbitrary and is considered by some that it may have done more harm than good (Richards and Moore, 1952). The experimental work of Youngs (1958 a, 1958 b) with synthetic porous materials, and the numerical analysis of Rubin (1967), and Staple (1969) showed that redistribution in the absence of a water table is a continuous process and one that is influenced by the hysteretic properties of the soil.

Several infiltration models and a few redistribution models have been proposed and used. These models are either based on the Richards unsaturated flow equation or empirical relationships between infiltration rate and time. Models based on the Richards equation are more desirable because they use measured, physical parameters rather than empirical "constants" and, in general, are more accurate. They are, however, difficult to use. Since the Richards equation does not have a general analytical solution, it must be solved numerically. Such solutions are complex, use a lot of computer time and require more detailed input data.

Gardner et al. (1970) developed a redistribution model by simplifying the Richards equation by applying certain assumptions based on actual observations. The model is relatively simple. James (1976) used this model to describe the moisture profiles and showed a good agreement of calculated and observed values.

2.4 Drainage

2.4.1 Drainage Requirements of Crop

The purposes of the drainage engineer are best served if the data are available for every stage of every crop telling how much flooding the crop could stand under all circumstances. Hoveland and Webster (1965), for example, have found that among several clovers, ball and white clover were the most resistant to flooding damage, and that these two clovers could be flooded three days out of every ten for a three-month period without suffering reduction in yield. Experimental verification made by Williamson (1964) showed

that in the absence of salt problems, most annual crops can grow and produce well even if only the top 30 cm of soil are well drained.

When water stands in the low areas of a field for a period of time after a rain and the plants in the area die, two things are obvious. The drainage is inadequate and the crop suffocates due to the deficiency of oxygen at the plant roots. To properly evaluate the adequacy of drainage in such situations requires that the aeration status of the soil during the stress period be measured (Erickson et al., 1964).

2.4.2 Design Criteria of Drainage

The properties of soils required for the design of a drainage system are: hydraulic conductivity, drainable porosity, texture and structure. Hydraulic conductivity has been used most extensively in the design equations of the drainage system. The other three quantities are indirect measures of the ability of soils to transmit water. They are not directly usable in design equations, but in some cases may be correlated with hydraulic conductivity.

In the last two decades considerable interest has developed in evaluating the hydraulic conductivity of soils. Bouwer (1961, 1962, 1964) has developed a double-tube method for the in-place measurement of the saturated hydraulic conductivity of soils in the absence of a water table. The soil is saturated through the tubes placed in the soil at depth of measurement and the flow from one tube to the other is rated to obtain the conductivity. Collis-George (1964) devised a two-well method for measuring hydraulic conductivity in discrete soil layers. Dendy and Asmusson (1963)

used small well points to determine the hydraulic conductivity. Snell and Van Schilfqaarde (1964) developed a four-well method for measuring the conductivity of soil in place, and Fang Ching (1965) and Thomas (1965) tested the method in the field. In the Snell four-well method, one of the wells supplies water, one receives water and two act as piezometers. Smiles and Young (1965) developed and tested in a sand tank a multiple-well method in which alternate wells received a supply of water. They compared, using the same sand tank, several field methods for measuring hydraulic conductivity.

2.5 Properties of Porous Media

A good deal of work has been done to describe unsaturated flow in terms of parameters which have physical significance. These parameters are pore-size distribution index, bubbling pressure, tortuosity, effective porosity, hydraulic radius, and residual saturation. All of them except tortuosity can be determined in the laboratory (Laliberte, 1966; Corey, 1977). The tortuosity is determined indirectly. Burdine (1952) employed the concept of hydraulic radius to develop a relationship of relative permeability with residual saturation, saturation and capillary pressure. This relationship was verified by Corey (1954). Brooks and Corey (1966) suggested an empirical relationship of effective saturation with capillary pressure and a constant, characteristic of the soil, called the pore-size distribution index. Laliberte (1966) made a study of this constant for a number of soils. The Brooks and Corey equation is valid for capillary pressure greater than bubbling

pressure. For the range of capillary pressure less than bubbling pressure, empirical relationships have been suggested by Laliberte (1969) and Su and Brooks (1975). White et al. (1972) have also presented a semi-analytical relationship for the entire range. Kozeny (1927) and later Carman (1937) and Fair and Hatch (1933) developed an equation for the velocity of a wetting fluid through a fully saturated media, in which hydraulic conductivity was related to porosity, shape factor and tortuosity. This equation is known as the Kozeny-Carman equation. Brooks and Corey (1966) developed simple relationships among relative permeability, bubbling pressure, capillary pressure and pore-size distribution index. The relationships were experimentally verified by Brooks and Corey (1966).

CHAPTER III

THEORETICAL ANALYSIS

3.1 Time to the Beginning of Runoff

The description in this section has been taken from the paper by Mein and Larson (1973).

During rainfall the moisture content at the surface keeps on increasing until surface saturation is reached. At the moment of surface saturation, hydraulic conductivity and moisture content at the surface are known. Therefore, by applying Darcy's law, useful relationships can be developed.

The moisture content profile at the moment of surface saturation is approximately as shown in Figure 3.1. The area above the new moisture profile, F_s , is the amount of infiltration up to the time of surface saturation. The shaded area is drawn equal to this area. A saturation zone of equivalent depth L_s has been substituted for the actual moisture profile. The two areas are by definition equal and given by:

$$F_s = \text{IMD} \times L_s \quad (3.1)$$

IMD is initial moisture deficit and is equal to $\theta_s - \theta_i$,

where: θ_s is the volumetric moisture content at saturation and,

θ_i is the initial volumetric moisture content.

In finite-difference form, Darcy's law can be written as:

$$q = -C(\theta) \frac{[H_2 - H_1]}{[Z_2 - Z_1]} \quad (3.2)$$

LEGEND

- θ_i = Initial Volumetric Moisture Content
- θ_s = Volumetric Moisture Content at Saturation
- F_s = Infiltrated Depth up to Saturation
- L_s = Equivalent Length

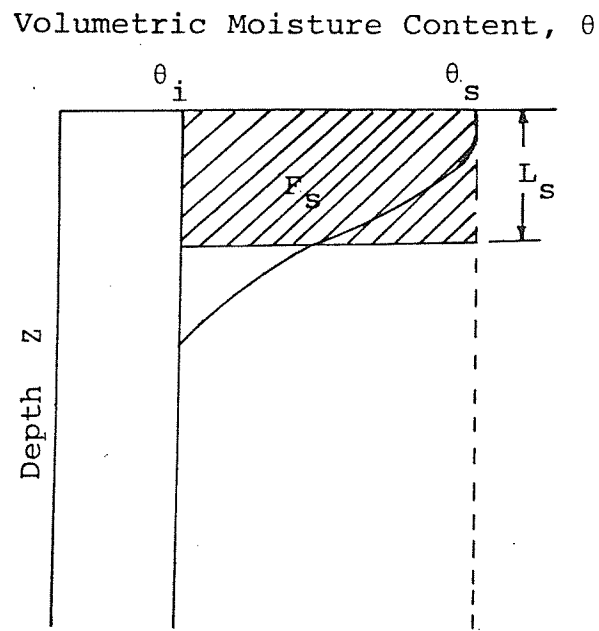


Figure 3.1 Generalized Soil Moisture Profile during Infiltration at the Moment of Surface Saturation.

where: q = flux,

$C(\theta)$ = hydraulic conductivity,

H = total potential, and

Z = distance below the surface.

The subscripts 1 and 2 refer to the surface and the wetting front, respectively.

$$Z_2 - Z_1 = L_s \quad (3.3)$$

and, when there is no flooding,

$$H_1 = 0 \quad (3.4)$$

$$H_2 = -(L_s + P_{cav}) \quad (3.5)$$

where: P_{cav} = average capillary pressure at the wetting front.

At this moment of surface saturation the infiltration rate is still equal to the rainfall intensity I , so that,

$$q = I \quad (3.6)$$

The hydraulic conductivity can be assumed to be equal to the saturated hydraulic conductivity C_s . Making these substitutions in (3.2), we obtain

$$I = C_s \frac{P_{cav} + L_s}{L_s} \quad (3.7)$$

and by combining (3.1) and (3.7),

$$F_s = \frac{P_{cav} \times IMD}{\left[\frac{I}{C_s} - 1\right]} \quad (3.8)$$

Equation (3.8) is applicable for $I > C_s$. F_s gives the cumulative infiltration prior to the runoff. For a uniform rainfall intensity time to the beginning of runoff is given by

$$T = \frac{F_s}{I} \quad (3.9)$$

3.2 Infiltration after Runoff Begins

Some time after the surface has become saturated, the moisture profile can be represented by Figure 3.2. Applying Darcy's law to the situation of Figure 3.2, and substituting flow rate equal to the infiltration capacity, we obtain,

$$f_p = C_s \frac{[P_{cav} + L_s + L]}{[L_s + L]} \quad (3.10)$$

f_p = infiltration capacity

Infiltration rate is now equal to the infiltration capacity.

$$L_s = \frac{F_s}{IMD} \quad \text{and}$$

$$L = \frac{[F - F_s]}{IMD}, \quad \text{where:}$$

F = cumulative infiltration at any time, and

F_s = cumulative infiltration at saturation

Hence $L_s + L = \frac{F}{IMD}$, and equation (3.10) becomes

$$f_p = C_s \left[1 + \frac{P_{cav} \times IMD}{F} \right] \quad (3.11)$$

Equation (3.11) gives infiltration rate after runoff begins. For ponded infiltration, equation (3.11) becomes

$$f_p = C_s \left[1 + \frac{(P_{cav} + h)IMD}{F} \right], \quad \text{where:} \quad (3.12)$$

h = head above the soil surface.

LEGEND

- θ_i = Initial Volumetric Moisture Content
- θ_s = Volumetric Moisture Content at Saturation
- F = Infiltrated Depth at any Time
- F_s = Infiltrated Depth up to Saturation
- L_s = Equivalent Depth

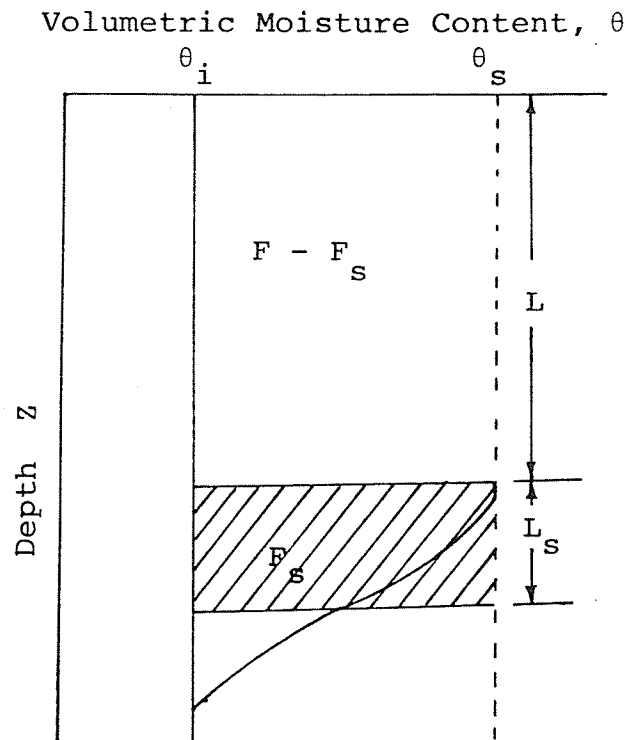


Figure 3.2 Generalized Soil Moisture Profile during Infiltration after Surface Saturation

3.3 Average Capillary Pressure at the Wetting Front (P_{cav}) and Bubbling Pressure (P_b)

P_{cav} is defined as the weighted value of capillary pressure expressed as a function of relative permeability.

Mathematically,

$$P_{cav} = \frac{\int_0^{1.0} P_c d(Kr)}{1 - Kri}, \text{ where:} \quad (3.13)$$

Kr = relative permeability

Kri = relative permeability at initial moisture content

To evaluate the integral in equation (3.13) P_c and Kr are defined in terms of effective saturation S_e by applying Corey's (1954) equation and Brooks and Corey's (1966) equation.

Corey's equation is

$$Kr = S_e^\epsilon, \text{ where} \quad (3.14)$$

ϵ = constant, a characteristic of soil

Differentiating (3.14)

$$d(Kr) = \epsilon S_e^{\epsilon-1} (ds_e) \quad (3.15)$$

Brooks and Corey's equation is:

$$S_e = \left(\frac{P_b}{P_c}\right)^\lambda \quad (3.16)$$

Equation (3.16) is valid for $P_c \geq P_b$, and

λ = pore-size distribution index, a characteristic of the soil

Rearranging (3.16), we obtain

$$P_c = \frac{P_b}{(S_e)^{\frac{1}{\lambda}}} \quad (3.17)$$

In addition, λ and ϵ are related by the equation

$$\epsilon = \frac{2 + 3\lambda}{\lambda} \quad (3.18)$$

Substituting equations (3.14), (3.15), (3.17) and (3.18) into equation (3.13), we obtain

$$P_{cav} = \left[\frac{2 + 3\lambda}{\lambda} \right] \left[\frac{P_b}{1 - S_{ei}^\epsilon} \right] \int_{S_{ei}}^{1.0} (S_e)^{\frac{1+2\lambda}{\lambda}} d(S_e) \quad (3.19)$$

Performing the integration in equation (3.19), we obtain

$$P_{cav} = P_b \cdot \left[\frac{2 + 3\lambda}{1 + 3\lambda} \right] \frac{\left[1 - (S_{ei})^{\frac{1+3\lambda}{\lambda}} \right]}{\left[1 - (S_{ei})^{\frac{2+3\lambda}{\lambda}} \right]} \quad (3.20)$$

$$P_b = P_{cav} \cdot \left[\frac{1 + 3\lambda}{2 + 3\lambda} \right] \frac{\left[1 - (S_{ei})^{\frac{2+3\lambda}{\lambda}} \right]}{\left[1 - (S_{ei})^{\frac{1+3\lambda}{\lambda}} \right]} \quad (3.21)$$

S_{ei} = effective saturation at initial moisture content

3.4 Redistribution of Moisture after Precipitation

The description given in this section is a modified form of the model developed by Gardner et al. (1970).

If the infiltration proceeds for a sufficiently long time a constant infiltration rate is eventually achieved. When this occurs the hydraulic gradient in the upper portion of a uniform soil profile is unity and the infiltration rate is equal to the hydraulic conductivity of the soil. The equation describing this process is:

$$\frac{\partial \theta}{\partial t} = -\frac{\partial}{\partial Z} \left[C \left(\frac{H}{Z} + 1 \right) \right] \quad (3.22)$$

θ = volumetric moisture content

t = time

Z = depth below the soil surface

C = hydraulic conductivity

H = matric potential

The integration of equation (3.22) with respect to Z between the limits $Z = 0$ (the soil surface) and some depth Z gives

$$\int_0^Z \left(\frac{\partial \theta}{\partial t}\right) dZ = - \left[C \left(\frac{dH}{dZ} + 1\right) \right]_0^Z \quad (3.23)$$

The Gardner et al. (1970) explained that left hand side of equation (3.23) represents the rate of drainage out of the portion of the soil profile above the depth Z . The right hand side of equation (3.23) when evaluated at $Z = 0$ represents the flux q_0 into the profile at the surface and when evaluated at Z represents the flux q_z out of the profile at that depth. This can be written:

$$\int_0^Z \left(\frac{\partial \theta}{\partial t}\right) dZ = - \frac{dw}{dt} = q_z - q_0 \quad (3.24)$$

w = volume of water per unit area of the initially wetted zone

For the redistribution problem considered here the flux at the surface q_0 is set equal to zero.

If infiltration had continued so that a constant infiltration rate was achieved, the matrix gradient would be negligible above the wetting front in comparison to the gravitational gradient. Experience has shown that this situation persists during the redistribution process except at the soil surface. Experimental observations have also shown that the entire profile above the initial wetting front tends to drain at a uniform rate independent of depth. On the basis of these observations equation (3.22) can be approximated by the simpler expression:

$$\left(\frac{d\theta}{dt}\right)Z = -C(\theta, Z) = -C_w \quad (3.25)$$

C_w = effective hydraulic conductivity

The effective hydraulic conductivity is related to the effective saturation as follows:

$$C_w = C_s S_e^\epsilon \quad (3.26)$$

C_s = saturated hydraulic conductivity

ϵ = constant, a characteristic of soil

S_e = effective saturation

The effective saturation is related to the residual saturation as

$$S_e = \frac{S - S_r}{1 - S_r} \quad (3.27)$$

Rearranging equation (3.27)

$$S = S_e(1 - S_r) + S_r \quad (3.28)$$

But $\theta = \phi S$

where ϕ = porosity

Substituting this expression in (3.28) results in

$$\theta = \phi[S_e(1 - S_r) + S_r] \quad (3.29)$$

Differentiating equation (3.29) with respect to t, we get

$$\frac{d\theta}{dt} = \phi(1 - S_r)\frac{dS_e}{dt} \quad (3.30)$$

If θ_i is the moisture content before the flooding, θ_f is the moisture content after the flooding ends and F is the cumulative infiltration, then the depth Z to which the wetting front penetrates is given by

$$Z = \frac{F}{\theta_f - \theta_i}$$

Substituting $\theta_f = \phi[S_{ef}(1 - S_r) + S_r]$

and $\theta_i = \phi[S_{ei}(1 - S_r) + S_r]$

We get

$$Z = \frac{F}{\phi[1 - S_r][S_{ef} - S_{ei}]} \quad (3.31)$$

Substituting the values of C_w , $\frac{d\theta}{dt}$ and Z from equations (3.26), (3.30) and (3.31), respectively in equation (3.25), we obtain

$$\left[\frac{F}{S_{ef} - S_{ei}} \right] \frac{dS_e}{dt} = -C_s S_e^\epsilon \quad (3.32)$$

Rearranging equation (3.32), we obtain

$$\left[\frac{F}{S_{ef} - S_{ei}} \right] S_e^{-\epsilon} dS_e = -C_s dt \quad (3.33)$$

Integrating equation (3.33), we obtain

$$\left[\frac{F}{S_{ef} - S_{ei}} \right] \left[\frac{S_e^{-\epsilon+1} - S_{ef}^{-\epsilon+1}}{-\epsilon + 1} \right] = -C_s t \quad (3.34)$$

Rearranging equation (3.34), we obtain

$$\left[\left(\frac{S_{ef}}{S_e} \right)^{\epsilon-1} - 1 \right] = \frac{S_{ef}^{\epsilon-1} \cdot C_s \cdot t [\epsilon - 1] [S_{ef} - S_{ei}]}{F} \quad (3.35)$$

Rearranging again equation (3.35), we obtain

$$\left(\frac{S_{ef}}{S_e} \right)^{\epsilon-1} = \frac{F + C_s \cdot t \cdot S_{ef}^\epsilon \left[1 - \frac{S_{ei}}{S_{ef}} \right] [\epsilon - 1]}{F} \quad (3.36)$$

Rearranging again equation (3.36) and substituting

$C_s S_{ef}^\epsilon = A$, we obtain

$$\frac{S_e}{S_{ef}} = \left[\frac{F}{F + A \cdot t[\epsilon - 1] \left[1 - \frac{S_{ei}}{S_{ef}} \right]} \right]^{\frac{1}{\epsilon - 1}} \quad (3.37)$$

S_e = effective saturation at any time t after the flooding ends

A = infiltration rate at the end of flooding

CHAPTER IV

MATERIALS AND METHODS

4.1 Experimental Site

The experiments were conducted on two fields, named the Cousins field and Friesen field, located on E $\frac{1}{2}$ -35-10-8W and NW $\frac{1}{4}$ -18-11-7W, respectively. The geological history of both fields is similar. The surficial deposits consist of a 7.5-m-thick sand layer at the base of which, sand and gravel deposits appear to be fairly common. The surficial deposits are underlain by a 30-m-thick clay layer, that in turn is underlain by glacial till.

Three main groundwater flow systems appear to exist in the area. They are shallow, intermediate and regional flow systems. Only the shallow groundwater system has been considered in the present study. The shallow groundwater system is above the clay layer and in the surficial layer. It is recharged locally by precipitation and most likely flows towards the Assiniboine River. The water in this system is fresh.

Soil texture in the Cousins field varies from sandy to loamy sand. At a few places, it is sandy loam. The upper 90-cm layer of the soil is mainly sand. From 90 cm downwards to the clay layer, the soil texture is loamy sand.

Soil texture in the Friesen field varies from sand to loamy sand in the upper 90-cm layer. Below 90 cm and up to the clay layer, the texture is clay loam. Bulk density in both fields varies from 1.40

to 1.45. The porosity varies from 0.40 to 0.45.

Topography of the fields is undulating, as is clear from the contour map of Cousins field in Figure B1 in Appendix B. The tacheometric method was used to prepare the map. The places with relatively low elevations were called low spots and the ones with relatively high elevations were called high spots. The maximum difference in the elevations of the low and high spots was 1.6 m.

A potato crop was grown in the Cousins field and corn in the Friesen field. Irrigation was applied with a central pivot irrigation unit. The irrigation water was conveyed from the Assiniboine River by an underground pipe line system.

4.2 Measurement of Soil Moisture

4.2.1 Selection of Site

The moisture content was measured at a number of locations in both of the fields. The criteria for selecting a location were: topography, texture and structure of the soil. The observations were taken in the growing period of the crops for two consecutive years, 1977 and 1978. In 1977, four locations were selected in each field. In 1978, four locations in the Cousins field and six locations in Friesen's field were selected. The moisture content was recorded every second or third day. Figures 4.1 and 4.2 show the locations in the Cousins field and the Friesen field, respectively.

4.2.2 Site Preparation

With the help of a post-hole auger a hole of 7.56-cm diameter

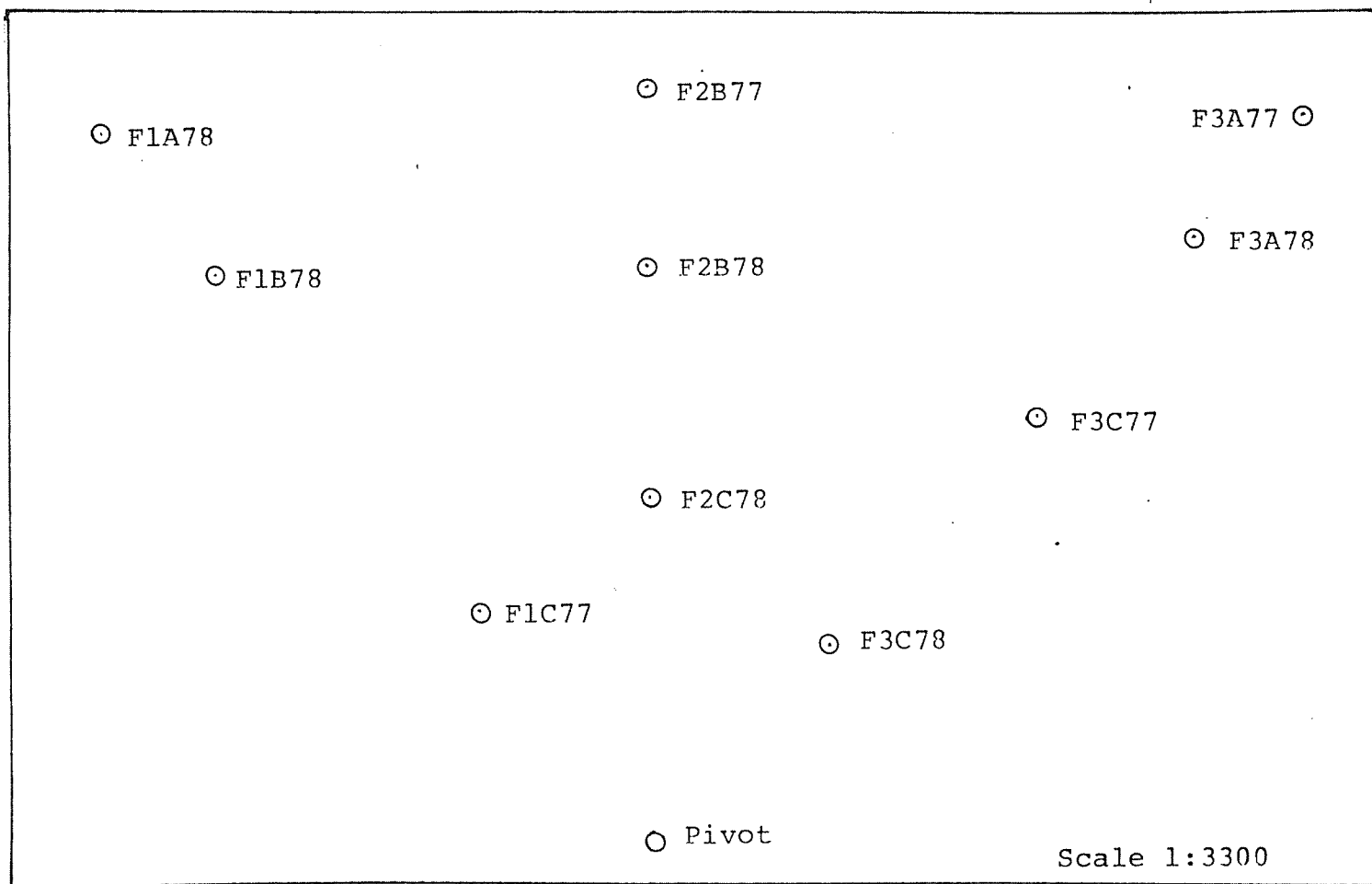


Figure 4.2 Locations of Access Tubes in the Friesens Field

extending downward to 120 cm was bored at each location. Aluminum irrigation pipe, having an outer diameter of 5.08 cm and an inner diameter of 4.83 cm was placed in the hole to serve as an access tube for the moisture and density measuring unit. The lower end of the access tube was plugged to prevent the groundwater from entering into it. Soil was poured all around the access tube and compacted to prevent an air gap between the soil and the access tube. A heap of the soil was made around the access tube to prevent the ponding of water near it and to prevent the rainfall or irrigation water from entering into the soil along the walls of the access tube. The access tube was covered at the top with a can to prevent the rainfall and irrigation water from entering the access tube.

4.2.3 Neutron Moisture Meter

The moisture content was recorded at 30-cm, 60-cm, 90-cm and 110-cm depths with the help of a neutron moisture meter. At the 15-cm depth it was measured by the thermogravimetric method.

The neutron moisture meter consists of a depth moisture gauge and a scaler-ratemeter. Figure 4.3 shows the moisture gauge fitted on the top of an access tube. Figure 4.4 shows the scaler rate meter. The moisture gauge was a Troxler unit, model 1255. The scaler-ratemeter was Troxler unit, model 2651. The neutron moisture meter works on the principle that fast-moving neutrons emitted by a radioactive source are moderated by the hydrogen in soil moisture. The moderated neutrons, called thermal neutrons are detected by a detector. The count of these neutrons is read from the scaler rate meter. The



Figure 4.3 Photograph of Moisture Gauge Fitted on the Top of Access Tube



Figure 4.4 Photograph of Scaler-ratemeter

radioactive source in the model 1255 is 100 millicurie Americium-241-Beryllium. The source is triple-sealed.

In principle, the zone of influence of a neutron probe is infinite; in practice, it is limited. There is an effective space zone within which 90 to 95 percent of the detected neutron interaction occurs. For pure water the calculated zone diameter is 30.5 cm; for material at 40 percent volumetric moisture content, 40.6 cm; for 10 percent volumetric moisture content, 63.5 cm. Studies made at the Troxler Laboratories indicate that the zone of influence for pure water is 10.8 cm. Also, the zone of measurement is less than the zone of influence.

Due to the decay of the radioactive source and change in daily temperature, the number of the neutrons emitted changes. To account for this, instead of relating the observed count directly to the moisture content the ratio of the observed count to the standard count is related to the moisture content. The standard count is taken by placing the probe on the levelled surface away from any organic source. The standard count was taken before and after the observations and the average of these two was used in calculations. For the observations of moisture content a one-minute count was selected. The other counts available were 0.25 min, 0.50 min, and 2.00 min. For the standard count, four one-minute counts are taken automatically, summed, divided by four and displayed as the average one-minute count. The volumetric moisture content is taken from the tables corresponding to the ratio of the observed count and

the standard count. The tables have been provided by Troxler Laboratories.

4.3 Measurement of Groundwater Level

Three observation wells were located in the Cousins field as shown in Figure B1 in Appendix B. Three observation wells were considered sufficient to draw equipotential lines because of fairly uniform impermeable layer below the groundwater. At wells I and II, the level was measured manually and the observations were taken every week. At well III, a recorder (Stevens Recorder, Model 68, Type F, Leupold S. Stevens, Inc., Beaverton, Oregon, U.S.A.) was used. Using the top of the water hydrant as a reference, the groundwater level was calculated and plotted in Figure 5.6. The groundwater level below the surface was calculated and plotted in Figure 5.7. The average groundwater level at each well was approximated from Figure 5.6. The average level was used to draw the equipotential lines on Figure B1 in Appendix B.

4.4 Measurement of Infiltration

Three methods of estimating infiltration characteristics have been recognized. They are: use of cylinder infiltrometers, measurement of subsidence of free water in a large basin, and estimation of accumulated infiltration from the water front advance data. The use of a cylinder infiltrometer has been made as this is simple and the most common method.

Infiltration characteristics with an infiltrometer are determined by ponding water in a metal cylinder installed on the field

surface and observing the rate at which the water level is lowered in the cylinder. In the earlier studies (Folk, 1970) only a single cylinder was used and many of the data indicated a high degree of variability. The variability was mainly due to the uncontrolled lateral movement of water from the cylinder. After the initiation of infiltration, while the wetting front is in the cylinder, the water subsidence rate corresponds to the infiltration rate. When the wetting front passes below the cylinder, a divergence of flow will occur. The lateral movement of water from cylinders is minimized by ponding water in a guard cylinder or buffer area around the cylinder.

Infiltration rates observed by cylinder infiltrometers are influenced by the cylinder diameter, thickness of the cylinder, bevelling of the cylinder bottom, the method of driving the cylinder into the soil and the installation depth. The infiltrometer method used previously by Folk (1970) consisted of replenishing the infiltrated water in the inner cylinder by adding water from a measuring cylinder and noting the amount of water added as the total infiltration. The rate of infiltration of sandy soils is high compared to clay. The addition of water is required frequently. The frequent measurement of water into a cylinder adds to the experimental errors and also it disturbs the soil surface each time the water is poured. Sealing of the pores by the disturbed soil particles results into a change in the infiltration characteristics. Therefore, taking into consideration all of this, an infiltrometer suitable for the field conditions was designed and developed in the laboratory.

Figure 4.5 shows the infiltrometer. It consists of a cylindrical water tank, 60 cm in height, connected to a float valve through a flexible plastic tubing. The water tank provides a continuous supply to the inner cylinder. The float valve keeps the water level constant throughout the experiment. Water in the outer cylinder is poured manually. The outer cylinder is 39 cm in diameter and the inner cylinder is 28 cm in diameter. The height of both cylinders is 30 cm. The diameter of the supply cylinder is 28 cm. Therefore, the depth of water depleted from the supply tank corresponds directly to the infiltration depth in the inner cylinder. The level of water in the supply tank is noted from the piezometer connected to it. The surface of the soil is not disturbed because the supply of water is continuous. The tops of the inner cylinder and supply tank were covered so that evaporation would be minimum. Both cylinders were marked so that they could be pushed into the soil to a depth of 19 cm in all the experiments and, thus, the variability due to the depth of the cylinders into the soil was avoided. The cylinders were pushed into the soil by hammering on the middle of a wooden plank placed on the top of the cylinders. The same procedure was followed in all the experiments.

To start the experiment, the inner and outer cylinders were pushed into the soil. A piece of cloth was placed on the soil surface. The float valve maintained a 5-cm depth of water in the inner cylinder; therefore, an equivalent depth of water was poured simultaneously into the outer cylinder so that initial depth of the water was 5 cm. After certain intervals of time, the level in the

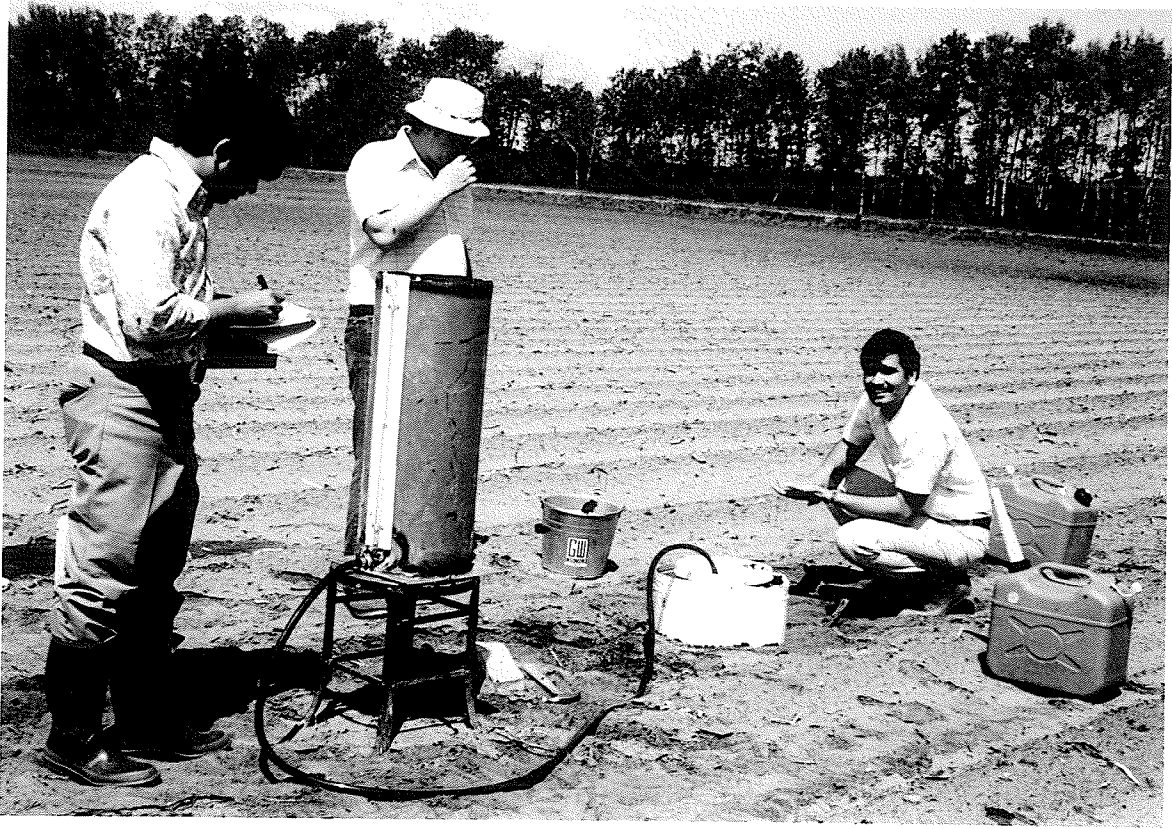


Figure 4.5 Photograph of Infiltrimeter

supply tank was noted. From time to time water was added into the outer cylinder to keep the depth of water nearly constant. The experiment was stopped when a constant rate of infiltration was achieved. Immediately the cylinders were pulled out and water from the soil surface was drained to the sides. Soil samples, for the thermogravimetric method of soil moisture measurement, were taken at the 15-cm, 30-cm, 45-cm and 60-cm depths with a soil sampling tube. Initial moisture content was measured at the same depth at a place near the infiltrometer experiment. A number of experiments were performed in the Cousins field.

4.5 Measurement of Moisture Content after Flooding

At the end of the infiltrometer experiments, soil samples from the region of the inner cylinder were taken from the 7.5-cm depth to the 30-cm depth with the help of a soil sampling tube. The moisture content was determined by the thermogravimetric method. The region of inner and outer cylinder was covered with a piece of cloth to minimize evaporation. The samples were taken at the same site after elapsed times of one hour, two hours, three hours, six hours, ten hours and twenty four hours.

CHAPTER V

RESULTS AND DISCUSSION

5.1 Infiltrometer Experiment

The cumulative infiltration data have been presented in Tables A-1 to A-3 in Appendix A. The calculated infiltration rates have been presented in Tables A-4 to A-6 in Appendix A. The moisture content before and after the infiltrometer experiment has been presented in Tables A-7 to A-10 in Appendix A. The data have also been plotted for the discussion.

5.1.1 Effect of Compaction

The infiltration rates observed on a furrow and a hill have been presented in Figures 5.1(a) and 5.1(b), respectively. The furrow had been compacted by the wheels of machinery. The hill was uncompacted and the soil was pulverized. The compaction affected the initial and the basic infiltration rates. The infiltration rate after 5 minutes was 0.08 cm/min in the furrows and 0.32 cm/min on the hill. The basic infiltration rate was 0.03 cm/min in the furrow and 0.14 cm/min on the hill. Therefore, both initial and the final infiltration rates on the hill were approximately four times greater than those in the furrows. If the irrigation application rate is designed on the basis of infiltration characteristics of the hill, surface runoff in the furrows may take place and the runoff water may accumulate in the low spots resulting in non-uniform moisture distribution and increased drainage requirements.

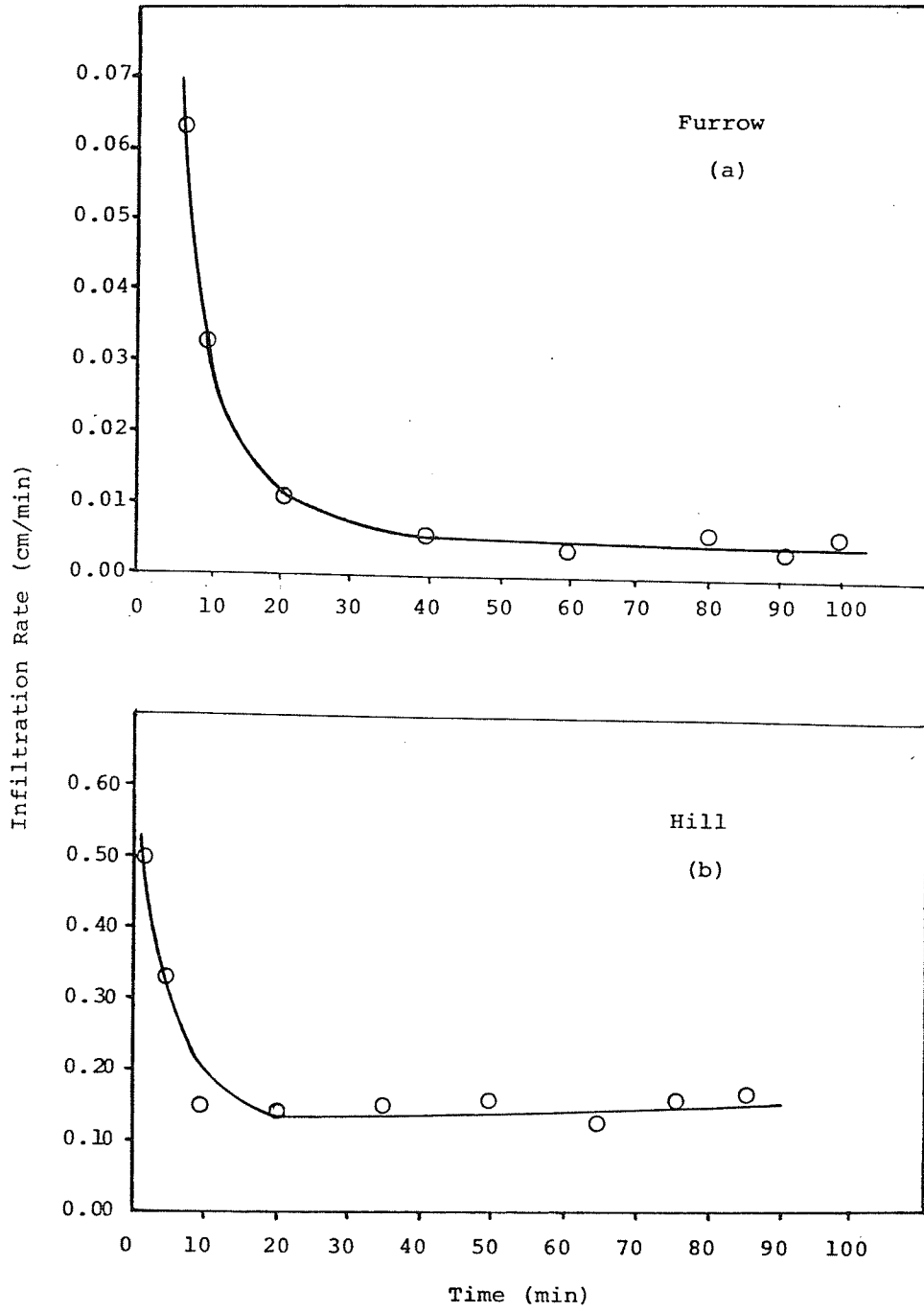


Figure 5.1 Infiltration Rate on Furrow and Hill

5.1.2 Effect of Soil Texture

The soil texture affects basic infiltration rate, initial infiltration rate and time in which the basic infiltration rate is reached. Figure 5.2 shows the infiltration rate in sandy and sandy loam soils. The infiltration rate after 5 minutes was 0.34 cm/min in sandy soil and 0.11 cm/min in sandy loam soil. The basic infiltration rate was 0.22 cm/min in sandy soil and 0.02 cm/min in sandy loam soil. The infiltration rate becomes constant in 30 minutes in sandy soil and in 60 minutes in sandy loam soil.

If such a variation in soil texture is found under the same irrigation unit, consideration must be given to the characteristics of both soil textures. Irrigation rate should not cause surface runoff in the sandy loam soil.

5.1.3 Representative Infiltration Characteristics

Based upon the results of the infiltrometer experiment, the field can be divided into three sections. The first section had a basic infiltration rate between 0.45 cm/min and 0.56 cm/min. The second section had a basic infiltration rate between 0.23 cm/min and 0.26 cm/min. The third section had a basic infiltration rate between 0.10 cm/min and 0.15 cm/min. The data of Sections I, II and III have been plotted in Figures 5.3, 5.4 and 5.5, respectively. In each figure, an average curve was drawn through the plotted points as a representative infiltration curve. The infiltration rates were taken from these curves and have been presented in Tables 5.1, 5.2 and 5.3 for Sections I, II and III, respectively. The representative

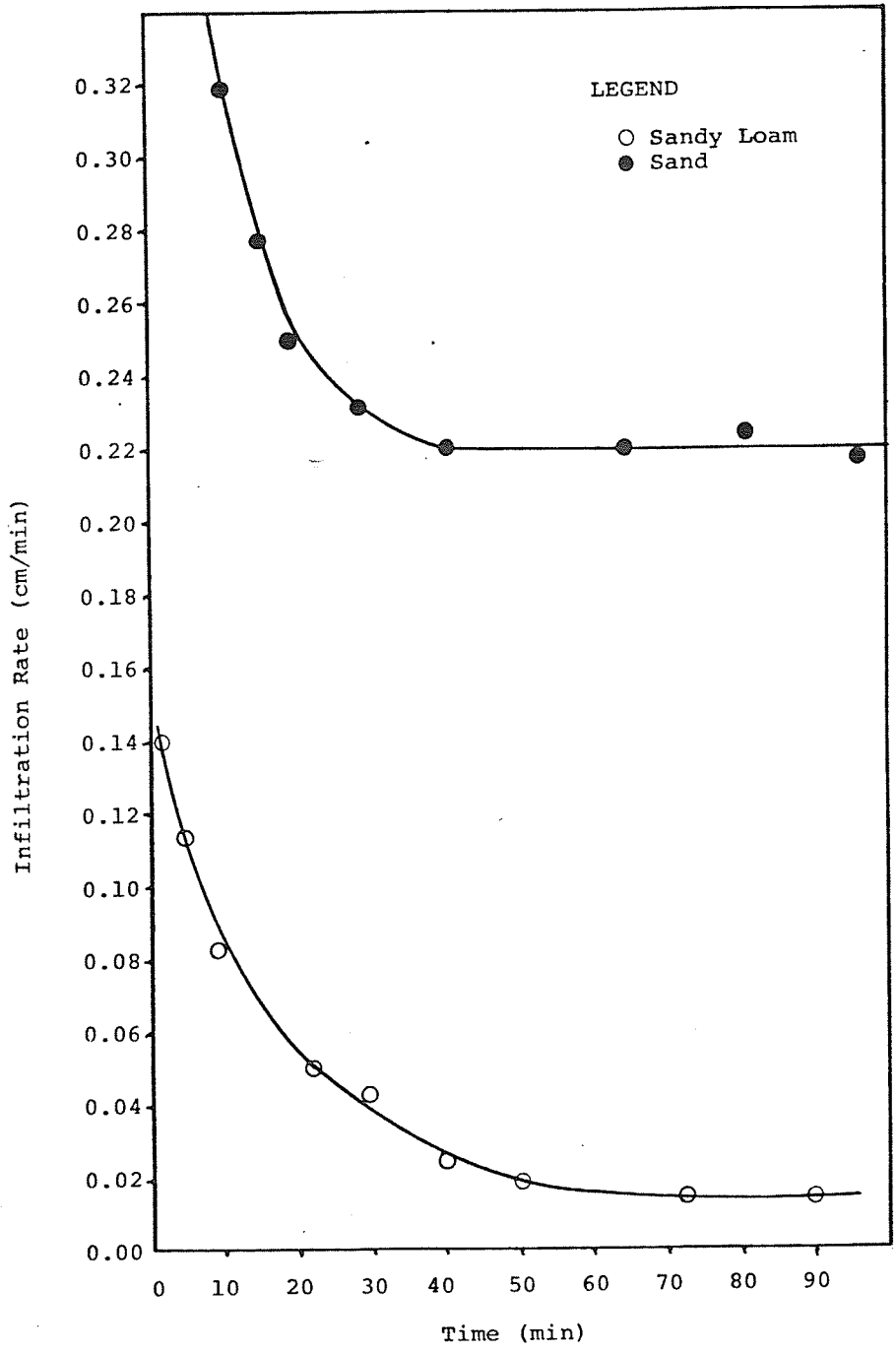


Figure 5.2 Infiltration Rate in Sandy and Sandy Loam Soils



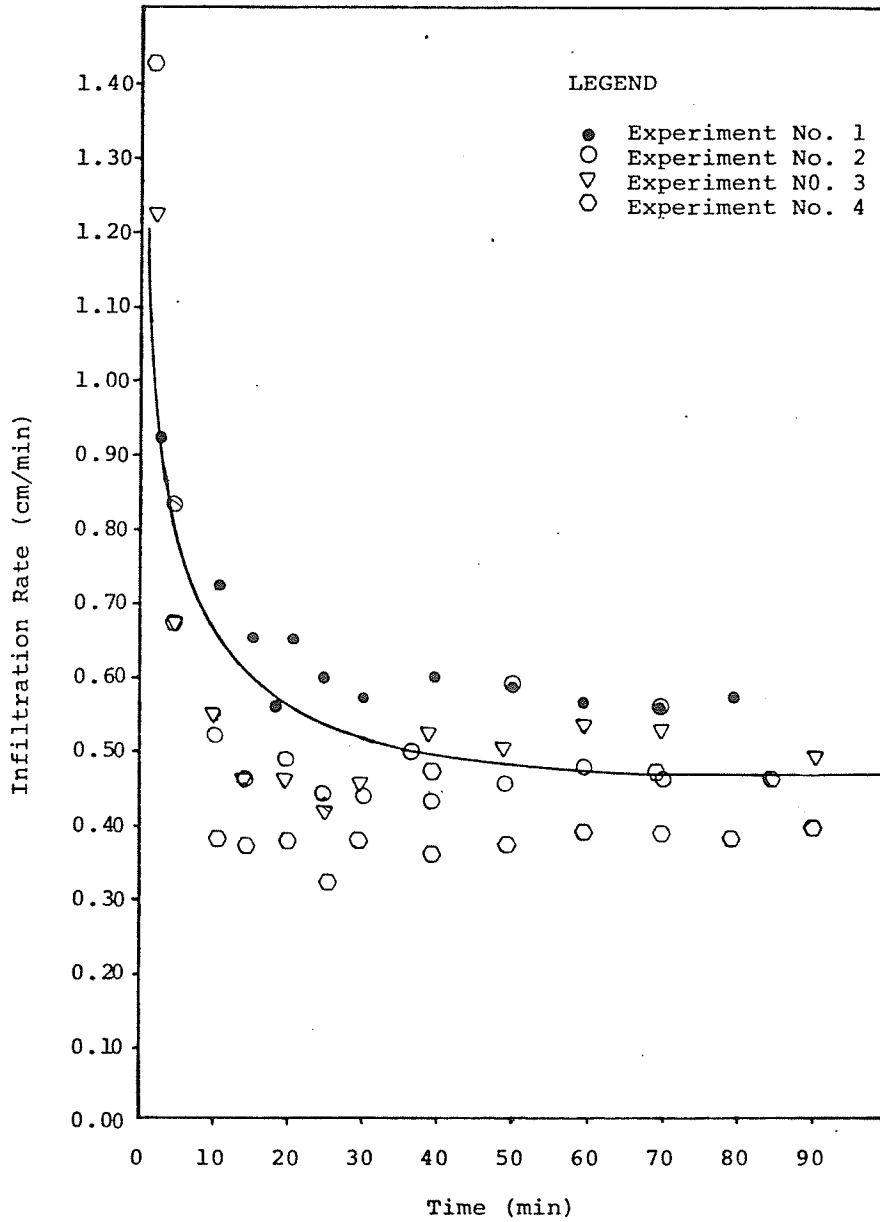


Figure 5.3 Infiltration Rate in Section I

TABLE 5.1 REPRESENTATIVE INFILTRATION RATE, INFILTRATION DEPTH AND CUMULATIVE INFILTRATION IN SECTION I*

Time (min)	Infiltration Rate (cm/min)	Infiltration Depth (cm)	Cumulative Infiltration (cm)
0	-	-	-
2	0.94	1.88	1.88
5	0.78	2.34	4.22
10	0.66	3.30	7.52
20	0.55	5.50	13.02
30	0.51	5.10	18.12
40	0.49	4.90	23.02
50	0.48	4.80	27.82
60	0.47	4.70	32.52
70	0.46	4.65	37.17
80	0.46	4.60	41.82
90	0.46	4.60	46.42
100	0.46	4.60	51.02
110	0.46	4.60	55.62

*constants of infiltration equation $y = at^\alpha + b$
a = 1.376
b = -0.469
 $\alpha = 0.769$

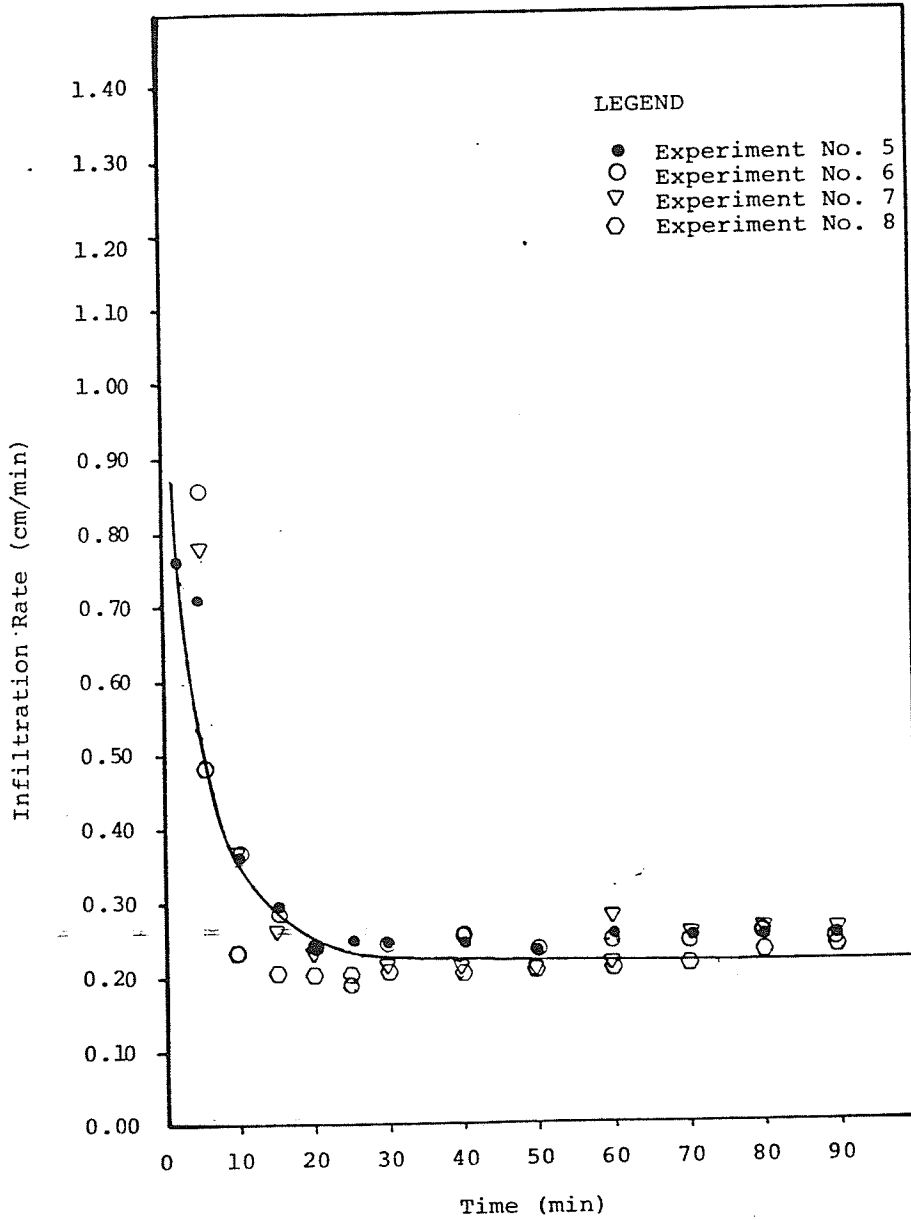


Figure 5.4 Infiltration Rate in Section II

TABLE 5.2 REPRESENTATIVE INFILTRATION RATE, INFILTRATION DEPTH AND CUMULATIVE INFILTRATION IN SECTION II*

Time (min)	Infiltration Rate (cm/min)	Infiltration Depth (cm)	Cumulative Infiltration (cm)
0	-	-	-
2	0.80	1.60	1.60
5	0.53	1.69	3.29
10	0.34	1.70	4.99
20	0.24	2.40	7.39
30	0.22	2.20	9.59
40	0.22	2.20	11.79
50	0.22	2.20	13.99
60	0.22	2.20	16.19
70	0.22	2.20	18.39
80	0.22	2.20	20.59
90	0.22	2.20	22.79
100	0.22	2.20	24.99
110	0.22	2.20	27.19

* constants of infiltration equation $y = at^\alpha + b$

a = 1.055

b = -0.094

α = 0.683

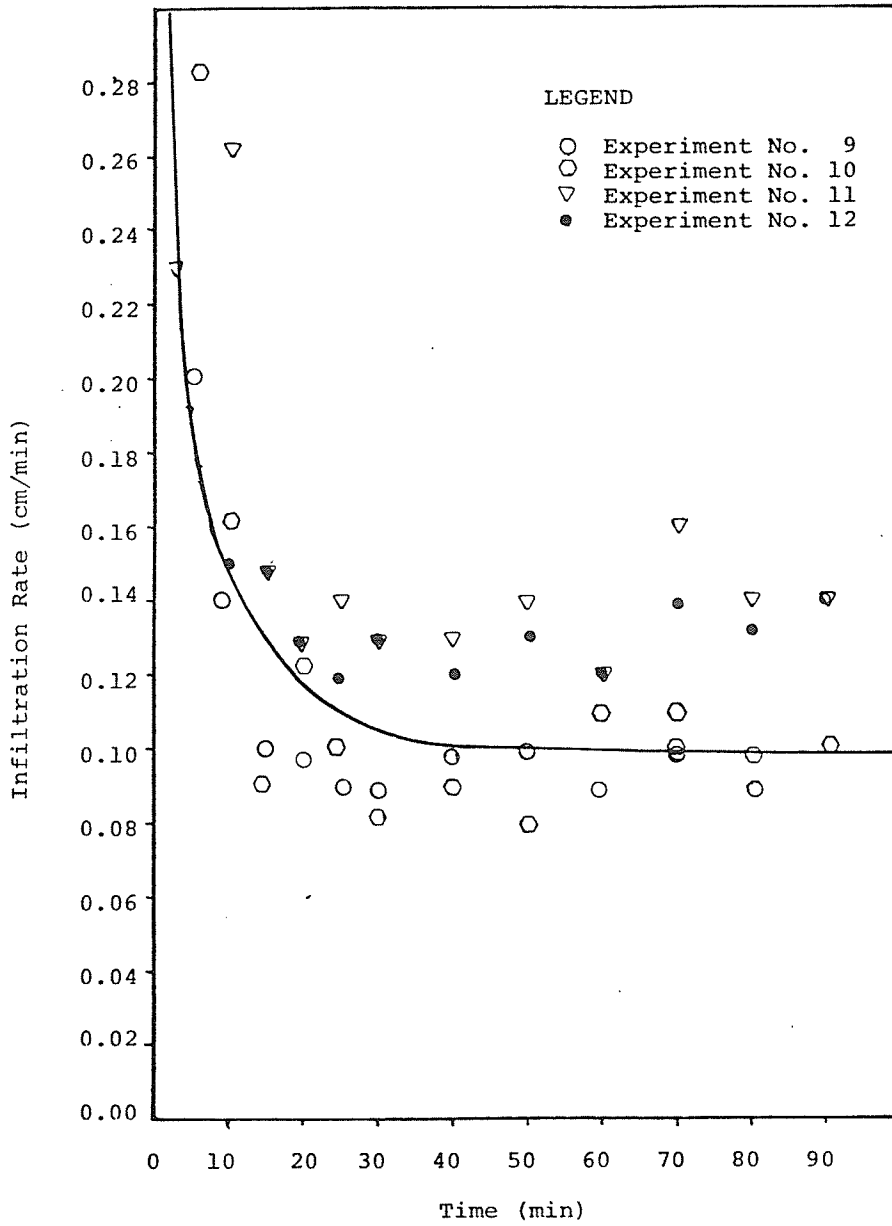


Figure 5.5 Infiltration Rate in Section III

TABLE 5.3 REPRESENTATIVE INFILTRATION RATE, INFILTRATION DEPTH AND CUMULATIVE INFILTRATION IN SECTION III

Time (min)	Infiltration Rate (cm/min)	Infiltration Depth (cm)	Cumulative Infiltration (cm)
0	-	-	-
2	0.72	1.44	1.44
5	0.18	0.54	1.98
10	0.14	0.70	2.68
20	0.10	1.00	3.68
30	0.10	1.00	4.68
40	0.10	1.00	5.68
50	0.10	1.00	6.68
60	0.10	1.00	7.68
70	0.10	1.00	8.68
80	0.10	1.00	9.68
90	0.10	1.00	10.68
100	0.10	1.00	11.68
110	0.10	1.00	12.68

*constants of infiltration equation $y = at^\alpha + b$
a = 0.620
b = -1.209
 $\alpha = 0.656$

basic infiltration rates were 0.47 cm/min, 0.22 cm/min and 0.10 cm/min in sections I, II and III, respectively.

5.1.4 Kostiakov Function

The Kostiakov function

$$y = at^{\alpha} + b$$

was fitted to each set of the representative data. The data were plotted on logarithmic scale to obtain a straight-line function. The constant α was determined from the slope of this line. The remaining two constants a and b were calculated by substituting the data points in the function. The constant a varied from 0.620 to 1.376. The constant b varied from -0.094 to -1.209 and constant α varied from 0.656 to 0.769. These constants are in agreement with those obtained by Folk (1970).

5.1.5 Green and Ampt Function

The Green and Ampt function

$$f(p) = C_s \left[1 + \frac{(P_{cav} + h) \text{ IMD}}{F} \right]$$

was fitted to each set of the representative data. The known variables of the function were infiltration rate, cumulative infiltration, head of water above the soil surface and initial moisture deficit. The saturated hydraulic conductivity and average capillary pressure head at the wetting front were calculated by the method of averages which has been explained in Appendix C. The calculated values will be reported in Section 5.17.

5.1.6 Use of Kostiakov, and Green and Ampt Functions

The Kostiakov function is simple. It directly gives cumulative infiltration and infiltration rate for any elapsed time. The Green and Ampt function is involved and does not give cumulative infiltration directly. But the Kostiakov function is applicable when the initial moisture content is in the range at which the data are collected. In the present study the data were collected at the initial moisture content at which irrigation was applied. Therefore, a design infiltration equation for use in connection with irrigation was selected from the three Kostiakov equations of the field.

The Green and Ampt function was used to calculate saturated hydraulic conductivity C_s and average capillary pressure at the wetting front P_{cav} . The average capillary pressure was used to determine bubbling pressure P_b and to predict time to the beginning of runoff.

5.1.7 Significance of Saturated Hydraulic Conductivity (C_s) and Average Capillary Pressure at the Wetting Front (P_{cav})

The calculated saturated hydraulic conductivity values were 25.80 cm/h, 11.28 cm/h and 3.92 cm/h for Sections I, II and III, respectively. Approximately 80 percent of the field was represented by Section II. According to the Manitoba Soil Survey report (Michalyna and Smith, 1972), the value of saturated hydraulic conductivity for Almasippi series soils varies from 7.12 cm/h to 12.45 cm/h.

The calculated values of capillary pressure at the wetting front (P_{cav}) were 9.60 mb, 9.84 mb and 13.24 mb for Sections I, II and III, respectively. The physical significance of P_{cav} is that it controls the initial infiltration rate, whereas the basic infiltration

rate is controlled by the saturated hydraulic conductivity of the upper soil layer. The basic infiltration rate was 0.46 cm/min in Section I and 0.22 cm/min in Section II which was approximately one half that of Section I. The initial infiltration rate was 0.94 cm/min in Section I and 0.89 cm/min in Section II. The initial infiltration rates were not very much different. This can be explained with the help of the parameters P_{cav} and C_s . Initially when the wetting front was in the upper soil layer, the only head which could have caused variation was P_{cav} and that was nearly the same in both sections. Hence, initial rates of infiltration were nearly the same. As the process of infiltration continued, the surface layer became saturated. Then the infiltration rate was controlled by the saturated hydraulic conductivity of the surface layer which was different in the two sections and, hence, the basic infiltration rates were different.

5.1.8 Bubbling Pressure and Pore-size Distribution Index

The infiltration rate and the cumulative infiltration at the end of flooding have been presented in Table 5.4. The moisture content before and after the infiltration was measured to the 30-cm depth. The data have been presented in Tables A-11, A-12 and A-13 for Sections I, II and III, respectively. The average moisture content of the transmission zone (0 to 30 cm) after the flooding ends has been presented in Table 5.5. Residual saturation S_r was taken as 0.1 from the results obtained by Van Schaik and Laliberte (1968). Using equation (3.38) the parameter ϵ was calculated by trial and error method. The parameters λ and P_b were calculated from equations (3.18) and (3.21), respectively. The bubbling pressure and pore-size distribution indices for the three sections of the field have been presented in Table 5.6.

TABLE 5.4 INFILTRATION RATE AND CUMULATIVE INFILTRATION AT THE END OF FLOODING

Section	Infiltration Rate (cm/min)	Cumulative Infiltration (cm)
I	0.40	48.30
II	0.23	28.10
III	0.10	17.20

TABLE 5.5 AVERAGE MOISTURE CONTENT OF THE TRANSMISSION ZONE AFTER THE FLOODING ENDS

Elapsed Time (h)	Moisture Content, Dry Weight Basis		
	Section I	Section II	Section III
0	28.0	27.0	28.0
1	21.9	19.1	23.8
2	18.9	16.4	21.0
3	17.1	14.8	19.3
6	14.0	12.4	16.5
10	12.0	10.8	14.5
24	9.5	8.7	11.9

Using equation 3.18, equations 5.1, 5.2 and 5.3 were derived to describe the relationship between capillary pressure and saturation for each section of the field, as follows

Section I

$$P_c = 9.60 \left[\frac{S - 0.1}{0.9} \right]^{\frac{1}{5.71}} \quad (5.1)$$

Section II

$$P_c = 9.84 \left[\frac{S - 0.1}{0.9} \right]^{\frac{1}{3.33}} \quad (5.2)$$

Section III

$$P_c = 13.24 \left[\frac{S - 0.1}{0.9} \right]^{\frac{1}{2.22}} \quad (5.3)$$

P_c = capillary pressure (mb)

S = saturation

Using equation (3.20), equations (5.4), (5.5) and (5.6) were developed for average capillary pressure at the wetting front, for each section of the field, as follows

Section I

$$P_{cav} = 10.13 \left[\frac{1 - (S_{ei})^{3.17}}{1 - (S_{ei})^{3.35}} \right] \quad (5.4)$$

Section II

$$P_{cav} = 10.73 \left[\frac{1 - (S_{ei})^{3.30}}{1 - (S_{ei})^{3.60}} \right] \quad (5.5)$$

Section III

$$P_{cav} = 14.96 \left[\frac{1 - (S_{ei})^{3.45}}{1 - (S_{ei})^{3.90}} \right] \quad (5.6)$$

TABLE 5.6 BUBBLING PRESSURE AND PORE-SIZE DISTRIBUTION INDICES

Section	λ	ϵ	P_b (mb)
I	5.71	3.35	9.60
II	3.34	3.60	9.84
III	2.20	3.90	13.24

TABLE 5.7 COMPARISON OF BUBBLING PRESSURE AND PORE-SIZE DISTRIBUTION INDEX WITH OTHER RESULTS

Soil Type	Porosity	λ	P_b (mb)	Source of the Results
Unconsolidated Sand	0.435	4.38	17.7	LaLiberte (1966)
	0.445	4.16	14.7	
Sandy Soil	0.450	5.71	9.60	Present Study
	0.450	3.34	9.84	
Loamy Sand	0.450	2.20	13.24	
Sandy Loam	0.458	1.76	55.6	LaLiberte (1966)
	0.449	1.70	58.7	

In each case P_{cav} is in mb. Using equation (3.26), equations (5.7), (5.8) and (5.9) were developed to determine effective hydraulic conductivity - saturation relationship for each section of the field, as follows:

Section I

$$C_w = 25.80 \left[\frac{S - 0.1}{0.9} \right]^{3.35} \quad (5.7)$$

Section II

$$C_w = 11.28 \left[\frac{S - 0.1}{0.9} \right]^{3.60} \quad (5.8)$$

Section III

$$C_w = 3.92 \left[\frac{S - 0.1}{0.9} \right]^{3.90} \quad (5.9)$$

C_w is in ch/h

The porous media parameters obtained in this study have been compared with those obtained by Laliberte (1966) in Table 5.7. It is found that the bubbling pressure is close to that for unconsolidated sand. The pore size distribution index varied from that for unconsolidated sand to that for sandy loam soil. The method of obtaining the porous media parameters developed in the present study should be verified in the laboratory under controlled conditions.

5.1.9 Time to the Beginning of Runoff

Runoff can start at the beginning of rainfall if the intensity of rainfall is higher than the initial rate of infiltration. Usually the rainfall intensity is lower than the initial rate of infiltration. Runoff starts when the rainfall continues for a time long enough that

the basic infiltration rate is reached and when this rate is smaller than the rainfall intensity. The time to the beginning of runoff depends upon the initial moisture content and such soil parameters as the capillary pressure at the wetting front and saturated hydraulic conductivity.

Using equations (3.8), (3.9) and (3.10), equations (5.10), (5.11) and (5.12) were developed to determine time to the beginning of runoff for different initial moisture content for each section of the field, as follows:

Section I

$$T = \frac{10.33[1 - (S_{ei})^{3.17}]}{I \left[\frac{I}{25.80} - 1 \right] [1 - (S_{ei})^{3.35}]} \quad (5.10)$$

Section II

$$T = \frac{10.94[1 - (S_{ei})^{3.30}]}{I \left[\frac{I}{11.28} - 1 \right] [1 - (S_{ei})^{3.60}]} \quad (5.11)$$

Section III

$$T = \frac{15.25[1 - (S_{ei})^{3.45}]}{I \left[\frac{I}{3.92} - 1 \right] [1 - (S_{ei})^{3.90}]} \quad (5.12)$$

T = time (min)

I = rainfall intensity (cm/h)

Tables 5.8 and 5.9 show maximum rainfall intensities and total rainfall on the days of heavy rainfall for the years 1977 and 1978, respectively. The maximum intensities were 23 mm/h and 37 mm/h in 1977 and 1978, respectively.

Table 5.10 shows that the minimum rainfall intensity causing runoff is 260 mm/h and which should continue for 135.4 minutes to

TABLE 5.8 TOTAL RAINFALL AND MAXIMUM RAINFALL INTENSITIES IN 1977*

Date	Total Rainfall (mm)	Maximum Rainfall Intensity (mm/h)
4 May	31.7	8.7
5 May	8.1	2.2
8 May	31.7	22.7
19 May	6.5	6.3
28 May	7.8	7.8
12 June	20.9	2.5
17 June	31.2	6.0
9 July	10.5	10.2
11 July	10.7	1.6
13 July	21.2	9.9
30 July	32.0	7.3
9 Sept.	9.1	9.1
5 Sept.	17.2	5.8
8 Sept.	34.0	8.6
9 Sept.	12.8	7.8

* Only rainfalls more than 6 mm have been listed

TABLE 5.9 TOTAL RAINFALL AND MAXIMUM RAINFALL INTENSITIES IN 1978*

Date	Total Rainfall (mm)	Maximum Rainfall Intensity (mm/h)
4 July	10.0	4.8
7 July	11.8	2.4
24 July	2.0	2.0
28 July	4.6	1.8
25 Aug.	4.0	3.8
27 Aug.	36.8	36.8

* Only rainfalls more than 2 mm have been listed

TABLE 5.10 TIME TO THE BEGINNING OF RUNOFF IN SECTION I*

Initial Moisture Content, Volume basis %	Time to Runoff (min)				
	Rainfall Intensity (mm/h)*				
	260	270	280	290	300
10	1074.6	172.4	90.8	60.2	44.3
20	762.0	122.3	64.3	42.7	31.4
30	449.5	72.1	37.9	25.2	18.6
40	135.4	23.4	12.3	8.2	6.0

* Runoff will occur instantaneously on saturated soil if the rainfall intensity is greater than 258 mm/h.

cause runoff at an initial moisture content at 40 percent. If the soil is saturated, runoff will occur instantaneously for a rainfall intensity greater than 258 mm/h (the saturated hydraulic conductivity), which is much higher than the maximum rainfall intensities found in 1977 and 1978. Hence, runoff is unlikely to occur in Section I as indicated by the record of 1977 and 1978.

Table 5.11 shows that the minimum rainfall intensity causing runoff in Section II, at an initial moisture content of 40 percent, is 120 mm/h which should continue for 41.7 minutes. If the soil is saturated, runoff will occur instantaneously for a rainfall intensity greater than 113 mm/h (the saturated hydraulic conductivity). It shows that runoff in Section II is also unlikely.

Table 5.12 shows that minimum rainfall intensity causing runoff in Section III is 50 mm/h which should continue for 29.3 minutes to cause runoff at an initial moisture content of 40 percent. If the soil is saturated, runoff will occur instantaneously for a rainfall greater than 39 mm/h (the saturated hydraulic conductivity). The maximum intensity being 37 mm/h, chances of runoff are also improbable in Section III. Since a large part of the field was represented by Section I and Section II, it can be concluded, on the basis of rainfall data of two years, that runoff in the field is unlikely. On the basis of the calculated time to the beginning of runoff, the infiltration equation of Section II can be selected as the design infiltration equation. This will ensure no runoff in Sections I and II. Runoff in Section III will occur. But Section III represents only about 5 percent of the total area.

TABLE 5.11 TIME TO THE BEGINNING OF RUNOFF IN SECTION II*

Initial Moisture Content, Volume basis %	Time of Runoff (min)				
	Rainfall Intensity (mm/h)				
	120	180	240	300	360
10	309.1	21.5	8.5	4.6	2.9
20	217.9	15.2	6.0	3.3	2.1
30	127.5	8.9	3.5	1.9	1.2
40	41.2	2.9	1.1	0.6	0.4

*Runoff will occur instantaneously on saturated soil if the rainfall intensity is greater than 113 mm/h.

TABLE 5.12 TIME TO THE BEGINNING OF RUNOFF IN SECTION III*

Initial Moisture Content, Volume basis %	Time of Runoff (min)				
	Rainfall Intensity (mm/h)				
	50	90	130	170	210
10	227.2	27.2	10.6	5.6	3.5
20	159.9	19.2	7.4	3.9	2.4
30	92.7	11.1	4.3	2.3	1.4
40	29.3	3.5	1.4	0.7	0.4

*Runoff will occur instantaneously on saturated soil if the rainfall intensity is greater than 39 mm/h.

5.2 Groundwater Level Measurement

5.2.1 Groundwater Level With Respect to a Reference

Figure 5.6 shows the groundwater level with respect to the top of the water hydrant at the end of the underground irrigation pipeline. The rise in level from 14 April to 17 May was very quick. This rise was due to the contribution by the thawing snow on the surface of the soil. The curve for well III shows the exact nature of the groundwater fluctuations because a continuous record of the level was available. The curve for well III shows that the level rose at a decreasing rate until 17 May and then became constant. This marked the end of contribution by the snow. The initial levels on 14 April were 97.43 m, 97.40 m and 97.27 m in wells, I, II and III, respectively. The total rise in groundwater levels due to snow were 60 cm, 20 cm and 31 cm in wells I, II and III, respectively.

From 17 May to 30 May, groundwater levels rose due to 52 mm rainfall by 13 cm, 10 cm and 7 cm in wells I, II and III, respectively. The levels in well II and III became equal. At this time, the hydraulic gradient between wells I and II was 0.250 percent and between wells I and III, it was 0.320 percent. Under these hydraulic gradients water was flowing towards wells II and III. Due to this flow the level in well I dropped by 17 cm by 24 June. The levels in wells II and III also dropped due to the water flow away from them. By 16 June, they were 5 cm lower. The rainfall totalling 28 mm raised the level in well between 16 June and 19 June. The rise of water level in well I started right after the rainfall while in well II the response was felt only after three days.

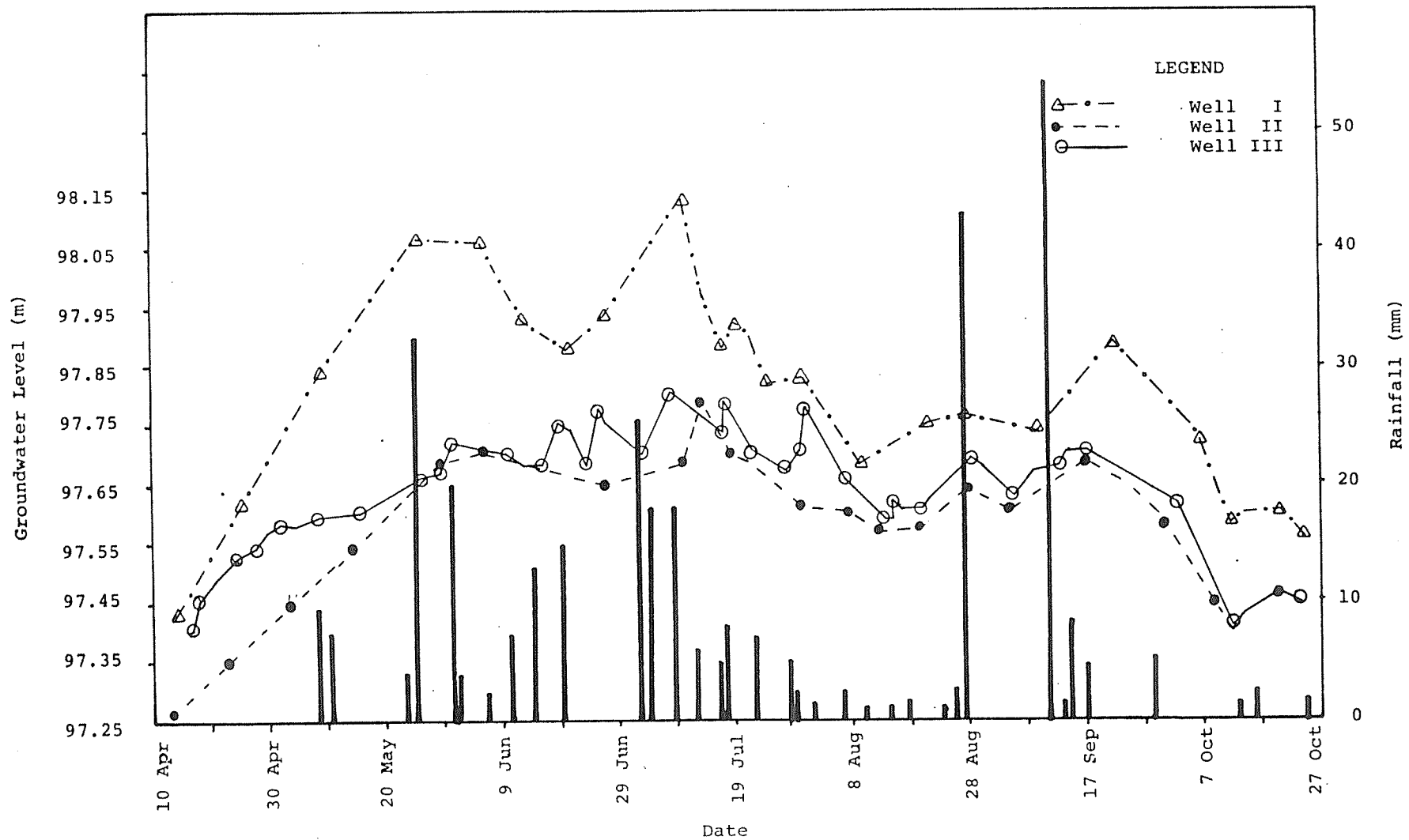


Figure 5.6 Groundwater Level With Respect to a Reference and Rainfall Histogram for 1978

From 2 July to 16 July there was a total rainfall of 62 mm and the water level raised by 10 cm in wells I and III and by 13 cm in well II. From 6 July to 18 August the level in each well dropped. During this period there was 41 mm rainfall but it was spread over many days. Evapotranspiration was high during July and August which should result in a fall of the water table. Therefore, the level did not change substantially due to the combined influence of rainfall and evapotranspiration during this period.

On 28 August, there was a heavy rain of 43 mm following which the groundwater level rose. Due to concentrated rainfall, deep percolation was high and resulted in the rise of groundwater level. Another concentrated rainfall caused a sharp rise in the groundwater levels by 13 cm, 8 cm and 8 cm in wells I, II and III, respectively. Table 5.13 shows the groundwater slopes between the observation wells. It shows that the flow was mainly from well I towards wells II and III. This direction of the flow indicates that the flow is towards the Assiniboine River.

From April to October, the level in well I fluctuated between 98.14 m and 97.44 m. The maximum rise was 70 cm. In the same period, the level in well II fluctuated between 97.27 m and 97.79 m. The maximum rise was 52 cm. The level in well III fluctuated between 97.40 m and 97.80 m. The maximum rise was 40 cm.

The total rainfall during 1977 was 384 mm and it did not result in any permanent rise in the groundwater level. The water from snowmelt was also drained naturally. The average slope of groundwater table was 0.135 percent. The saturated hydraulic

TABLE 5.13 GROUNDWATER TABLE SLOPES BETWEEN OBSERVATION WELLS*

Wells	Groundwater Slopes at the Points of Inflection (%)								Average
	10 Apr	30 May	19 Jun	9 Jul	28 Sep	5 Sep	17 Sep	10 Oct	
I - II	0.090	0.250	0.128	0.281	0.600	0.800	0.123	0.109	0.135
I - III	0.024	0.320	0.095	0.206	0.056	0.095	0.143	0.143	0.140
II - III	0.085	0.000	0.058	0.078	0.019	0.013	0.013	0.000	0.033

*Distance between wells

I - II 163.8 m
 I - III 153.3 m
 II - III 120.0 m

conductivity, ranging between 113 mm/h and 258 mm/h, was quite high. These two factors assure that permanent irrigation agriculture is possible under the local soil and groundwater conditions.

5.2.2 Groundwater Level with Respect to Ground Surface

The groundwater level with respect to the ground surface has been presented in Figure 5.7. During the growing period of the crop, that is from 30 May to 30 September, the groundwater levels were 1.35 m, 1.80 m, and 1.45 m, on the average, in wells I, II and III, respectively. The level in well I fluctuated between 1.13 m and 1.52 m. The level in well II fluctuated between 1.62 m and 1.90 m. The level in well III fluctuated between 1.22 m and 1.40 m.

The high groundwater table up to 1.60 m below the surface resulted in substantial upward flow of water. The groundwater table below 1.60 m resulted in very small upward flow of water.

5.3 Moisture Profiles in the Cousins Field in 1978

Figures 5.8, 5.9, 5.10 and 5.11 show the moisture profiles and rainfall histogram at locations C1A78, C4C78, C2B78 and C3B78, respectively. Table 5.14 (Israelson, 1962) shows representative physical properties of different soils. Field capacity and permanent wilting point have been considered from this table for the discussion of results.

Locations C1A78 and C4C78 were in the low spots. At C1A78, the volumetric moisture content at the 60-cm, 90-cm and 110-cm depths remained above 40.0 percent, whereas, it remained above 32.5 percent

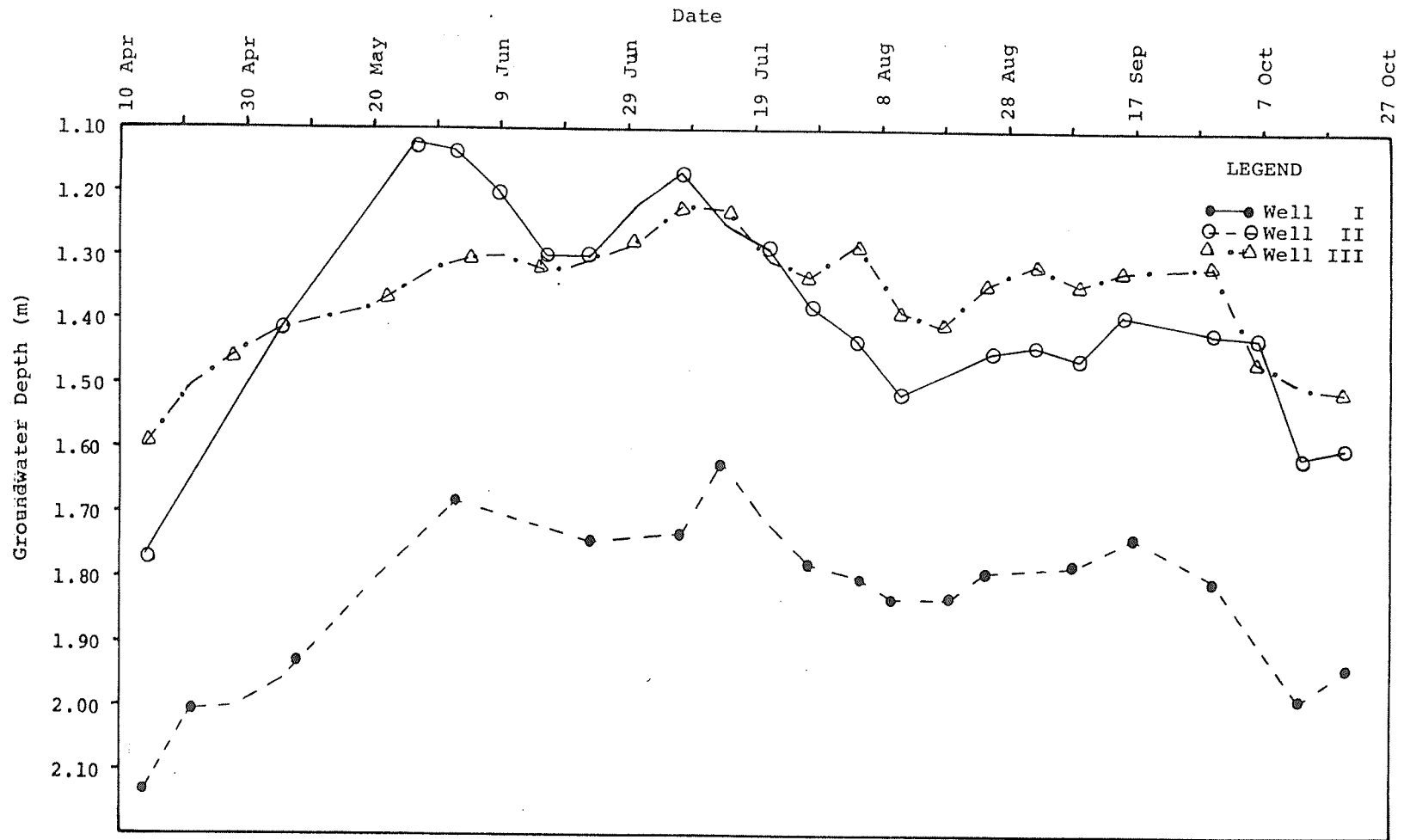


Figure 5.7 Groundwater Level Below the Ground Surface

TABLE 5.14 REPRESENTATIVE PHYSICAL PROPERTIES OF SOILS (ISRAELSON, 1962)

Soil Texture	Infiltration ¹ and Permeability Inches/hour	Total Pore Space %	Apparent Specific Gravity	Field Capacity %	Permanent Wilting %	Total Available Moisture ²		
						Dry Weight Basis %	Volume Basis %	Inches per Foot
Sandy	2 (1-10)	38 (32-42)	1.65 (1.55-1.80)	9 (6-12)	4 (2-6)	5 (4-6)	8 (6-10)	1.0 (0.8-1.2)
Sandy Loam	1 (0.5-3)	43 (40-47)	1.50 (1.40-1.60)	14 (10-18)	6 (4-8)	8 (6-10)	12 (9-15)	1.4 (1.1-1.8)
Loam	0.5 (0.3-0.8)	47 (43-49)	1.40 (1.35-1.50)	22 (18-26)	10 (8-12)	12 (10-14)	17 (14-20)	2.0 (1.7-2.3)
Clay Loam	0.3 (0.1-0.6)	49 (47-51)	1.35 (1.30-1.40)	27 (23-31)	13 (11-15)	14 (12-16)	19 (16-22)	2.3 (2.0-2.6)
Silty Clay	0.1 (0.01-0.2)	51 (49-53)	1.30 (1.25-1.35)	31 (27-35)	15 (13-17)	16 (14-18)	21 (18-23)	2.5 (2.2-2.8)
Clay	0.2 (0.05-0.4)	53 (51-55)	1.25 (1.20-1.30)	35 (31-39)	17 (15-19)	18 (16-20)	23 (20-25)	2.7 (2.4-3.0)

¹Intake rates vary greatly with soil structure and structural stability, even beyond the normal ranges shown above.

²Readily available moisture is approximately 75% of the total available moisture. [Normal ranges are shown in parentheses.]

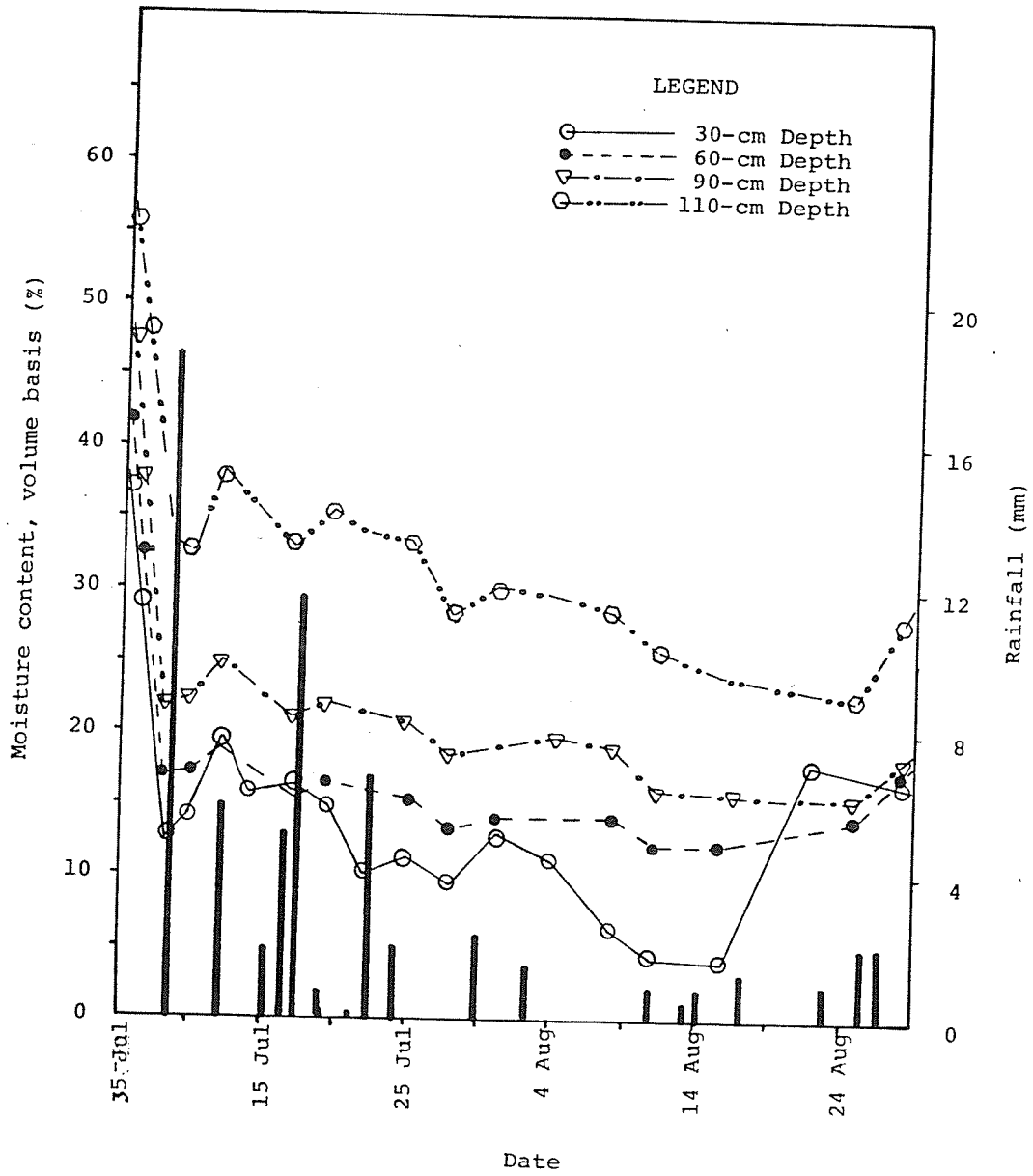


Figure 5.10 Moisture Profile and Rainfall Histogram at Location Cousins-C2B78 in 1978

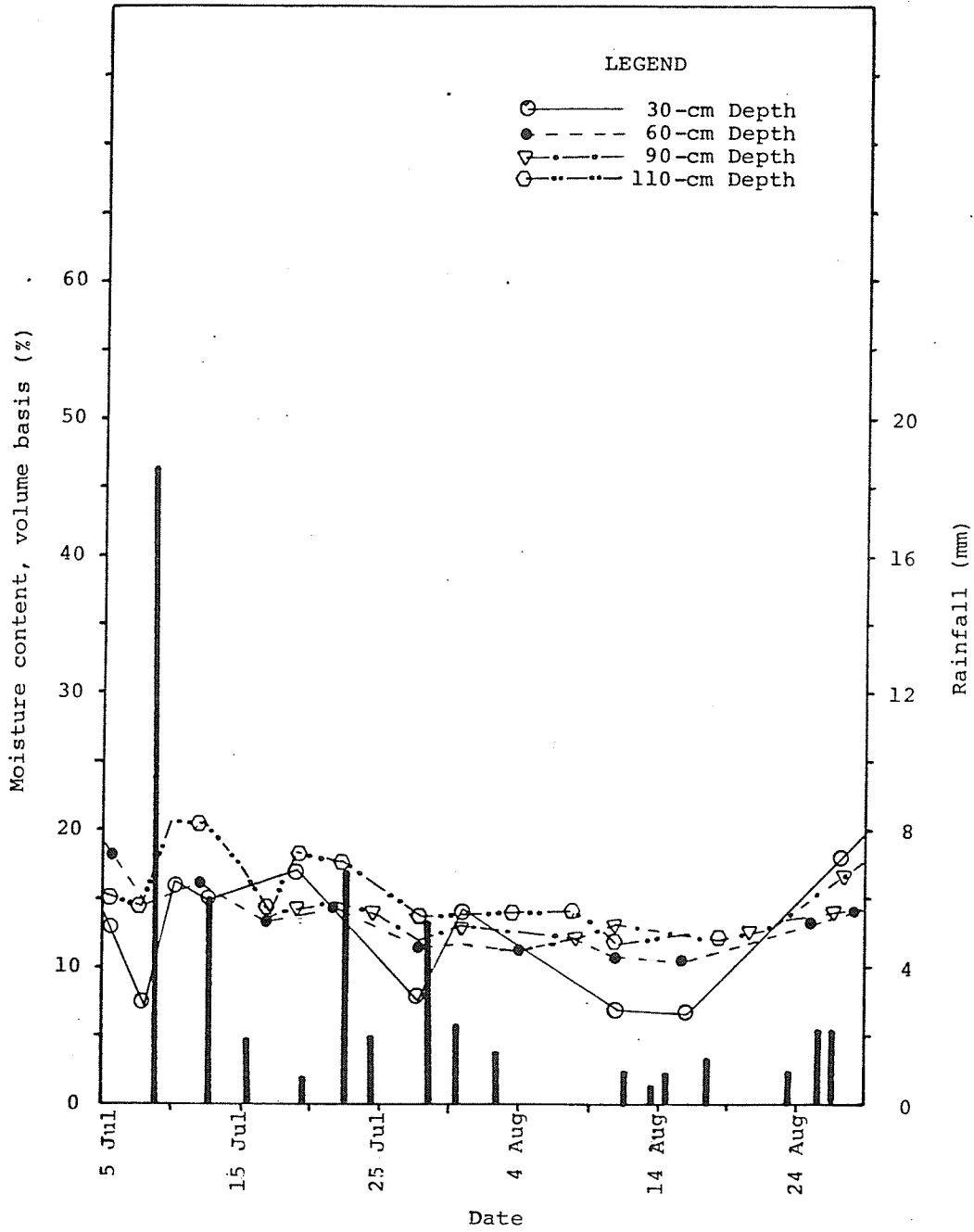


Figure 5.11 Moisture Profile and Rainfall Histogram at Location Cousins-C3B78 in 1978

at C4C78. The difference in moisture content can be attributed to the difference in soil properties and the upward flow from the groundwater. But the soil properties at these depths were similar at both locations.

Upward flow from the groundwater depends upon its depth below the soil surface, the hydraulic gradient set up by dry soil at the surface and the soil properties. The hydraulic gradient at C4C78 was higher than at C1A78 because of low moisture content at the 30-cm depth at C4C78 and the upward flow should be, therefore, larger at C4C78. But the groundwater depth was 1.62 m at C4C78 and only 1.45 m at C1A78 and because of that the flow should be smaller at C4C78. Figures 5.8 and 5.9 show that the influence of depth prevailed. This indicates that the depth of groundwater has a stronger effect than the hydraulic gradient.

There was a significant difference in the moisture content at the 30-cm depth at these locations. At C4C78, the moisture content remained between 17.5 percent and 30.0 percent for most of the period, whereas, it remained between 40.0 percent and 45.0 percent at C1A78. This difference is attributed to the difference in soil texture of the 30-cm layer in addition to the effect of groundwater. The soil texture was sandy loam at C1A78 and sandy at C4C78. In the middle of August, the rainfall was limited and no irrigation was applied, but the moisture content remained above 17.5 percent at C4C78 and above 38.0 percent at C1A78.

Locations C2B78 and C3B78 were in the high spots. The groundwater was 1.98 m below the surface at C2B78 and 2.10 m below the

surface at C3B78. The soil texture at both locations was similar. It was sandy loam at 110 cm depth and sand at the other monitored depths. Figure 5.10 shows that the upward flow from groundwater was influencing the moisture content at the 110-cm and 90-cm depths, as they retain moisture content above the field capacity. As the ground water level fell in the month of July and August, the influence of the groundwater declined as indicated by the reduced moisture content at the 110-cm depth. Figure 5.11 shows that the groundwater had no effect on the moisture regime at C3B78. Here, the moisture content at the 60-cm, 90-cm and 110-cm depths fluctuated very near the field capacity.

During the middle of August, the moisture content at the 30-cm depth decreased below the permanent wilting point at C2B78 and was equal to the permanent wilting point at C3B78. The rainfall was limited and irrigation was not applied. The plants suffered from prolonged wilting.

Irrigation was required at the high spots and no irrigation was required at the low spots to maintain proper moisture content. Table 5.15 shows the average moisture content taken from the discussed figures. It shows that 80 percent of the field required irrigation during the months of July and August.

5.4 Moisture Profiles in the Cousins Field in 1977

Figures 5.12, 5.13, 5.14 and 5.15 show the moisture profiles at locations C1A77, C4A77, C2B77 and C2C77, respectively. Figures 5.16 and 5.17 show the moisture content at the 15-cm depth on the

TABLE 5.15 AVERAGE MOISTURE CONTENT IN THE COUSINS FIELD IN 1977

Location	Percent of Total Area	Average Moisture Content, Volume Basis (%)								Plant Growth	
		July				August					
		30 cm	60 cm	90 cm	110 cm	30 cm	60 cm	90 cm	110 cm		
High Spot	C2B77	15.0	12.5	15.0	20.2	37.5	7.5	12.5	16.0	25.0	Fair
	C3B77	65.0	13.0	13.0	13.0	17.0	10.0	12.5	12.5	13.0	Poor
Low Spot	C1A77	5.0	42.5	45.0	50.0	52.5	42.5	42.5	42.5	52.5	Good
	C4C77	15.0	25.0	37.5	42.5	47.5	20.0	35.0	42.5	47.5	Good

furrow and hill, respectively.

Locations C1A77 and C4A77 were in the high spots. The moisture content at the 30-cm, 60-cm, 90-cm and 110-cm depths varied between 12 percent and 20 percent at both locations, except at the 110-cm depth at C1A77, where it was near 25 percent in the months of July and August. From 8 July to 13 July frequent rainfall resulted in a sharp rise in moisture content at all the depths. Deep percolation depleted the moisture content from the upper layers and added to the lower layer as is clear from Figure 5.13. Had the rainfall been evenly distributed over a period of time, the deep percolation losses would have been smaller. Therefore, the distribution of the rainfall is as important as the amount of the rainfall. Heavy rainfall of 32 mm on 30 July did not increase the moisture content. This was because the top 15-cm layer was very dry before the rainfall. Figures, 5.16 and 5.17 show that the moisture content, then was below the permanent wilting point, being 2.0 percent to 6.0 percent. This shows the effect of the initial moisture content. In August, the evapotranspiration was high. The sequence of small rainfalls kept the moisture content near field capacity. The moisture content at the 15-cm depth had more effect on the crop than at any other depth. In the last week of July, the moisture content at the 15-cm depth, which was below the permanent wilting point, caused damage to the crop, even when the moisture content at all the other depths was above the field capacity. Irrigation was required during this period.

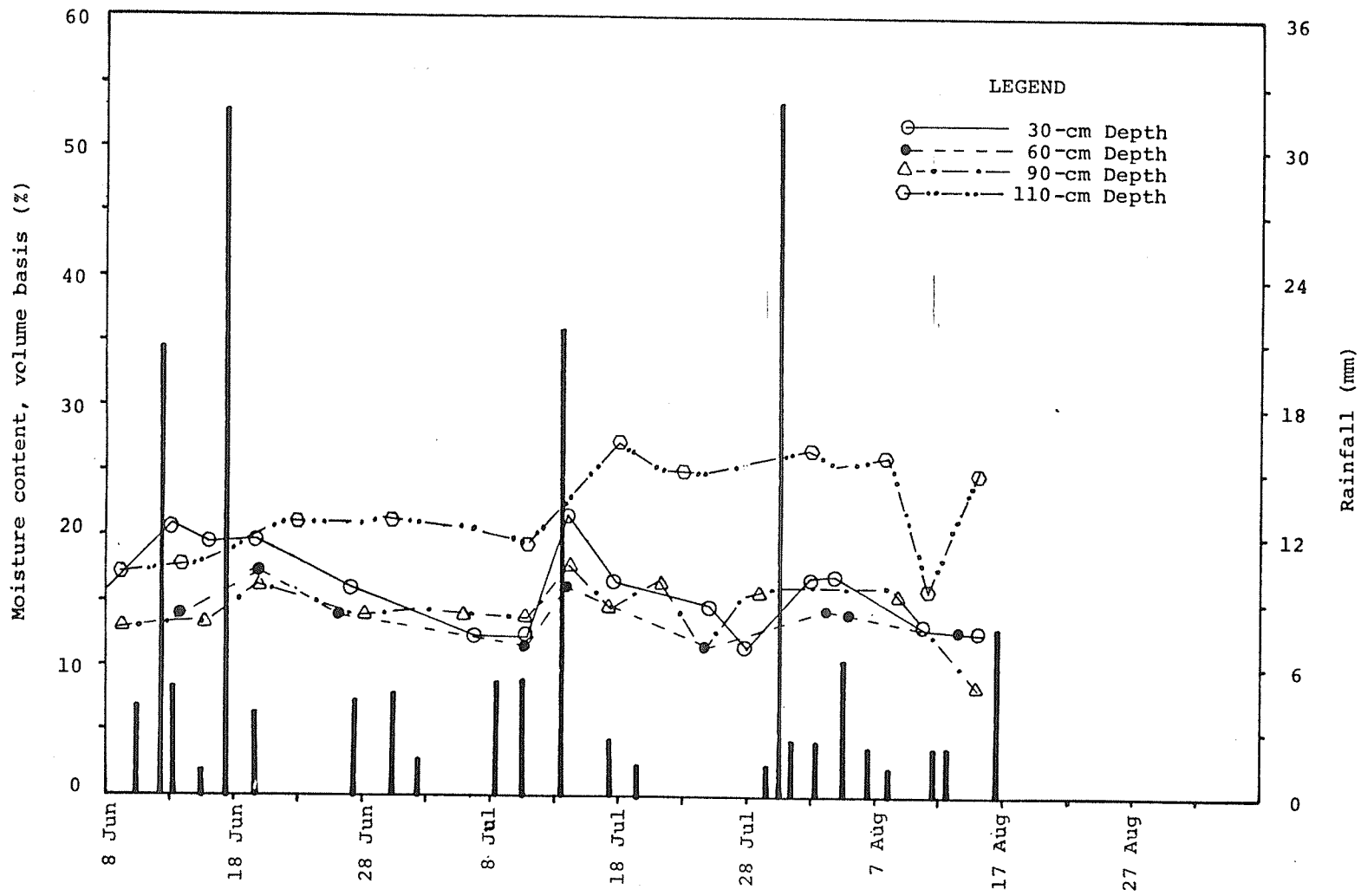


Figure 5.12 Moisture Profile and Rainfall Histogram at Location Cousins-ClA77 in 1977

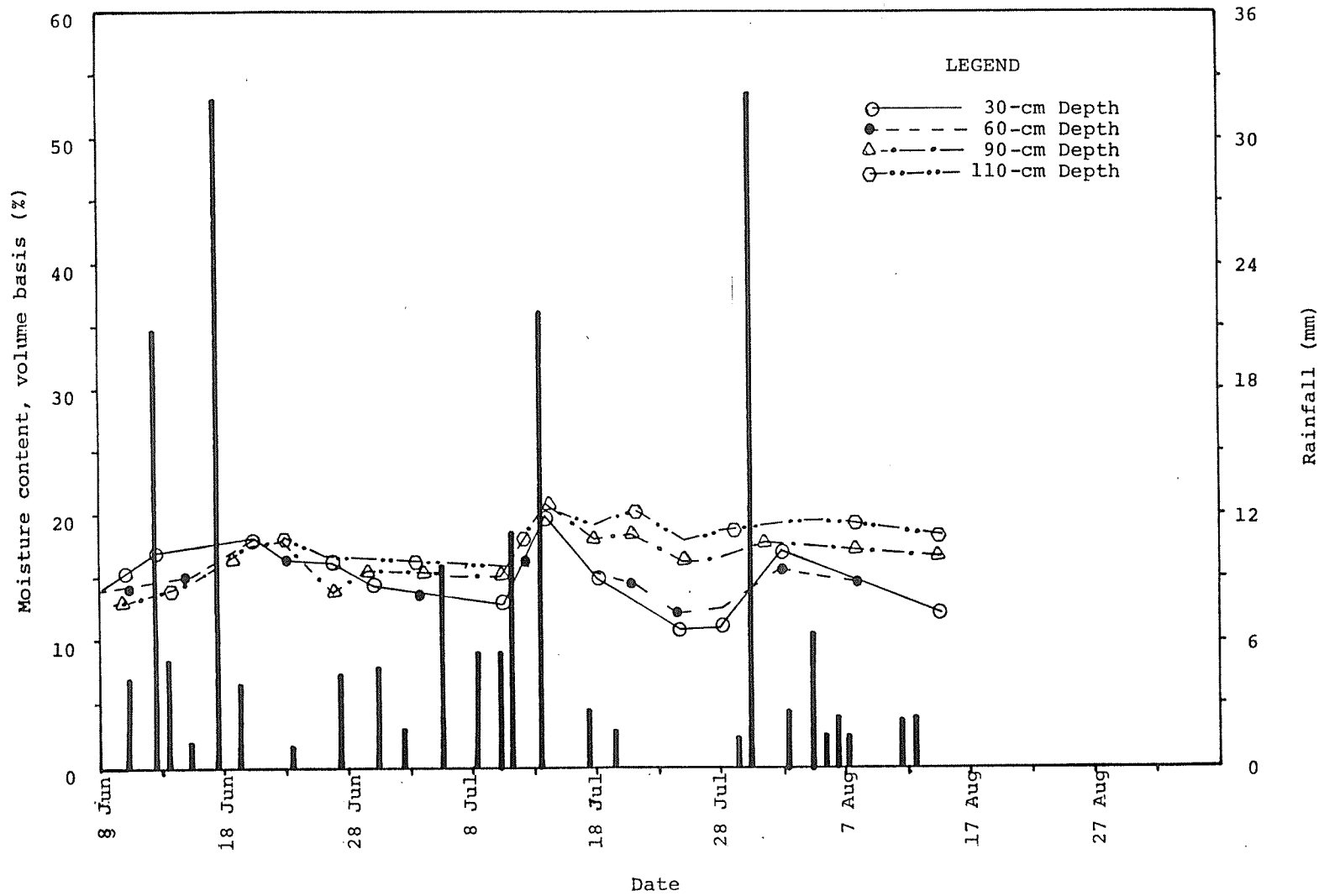


Figure 5.13 Moisture Profile and Rainfall Histogram at Location Cousins-C4A77 in 1977

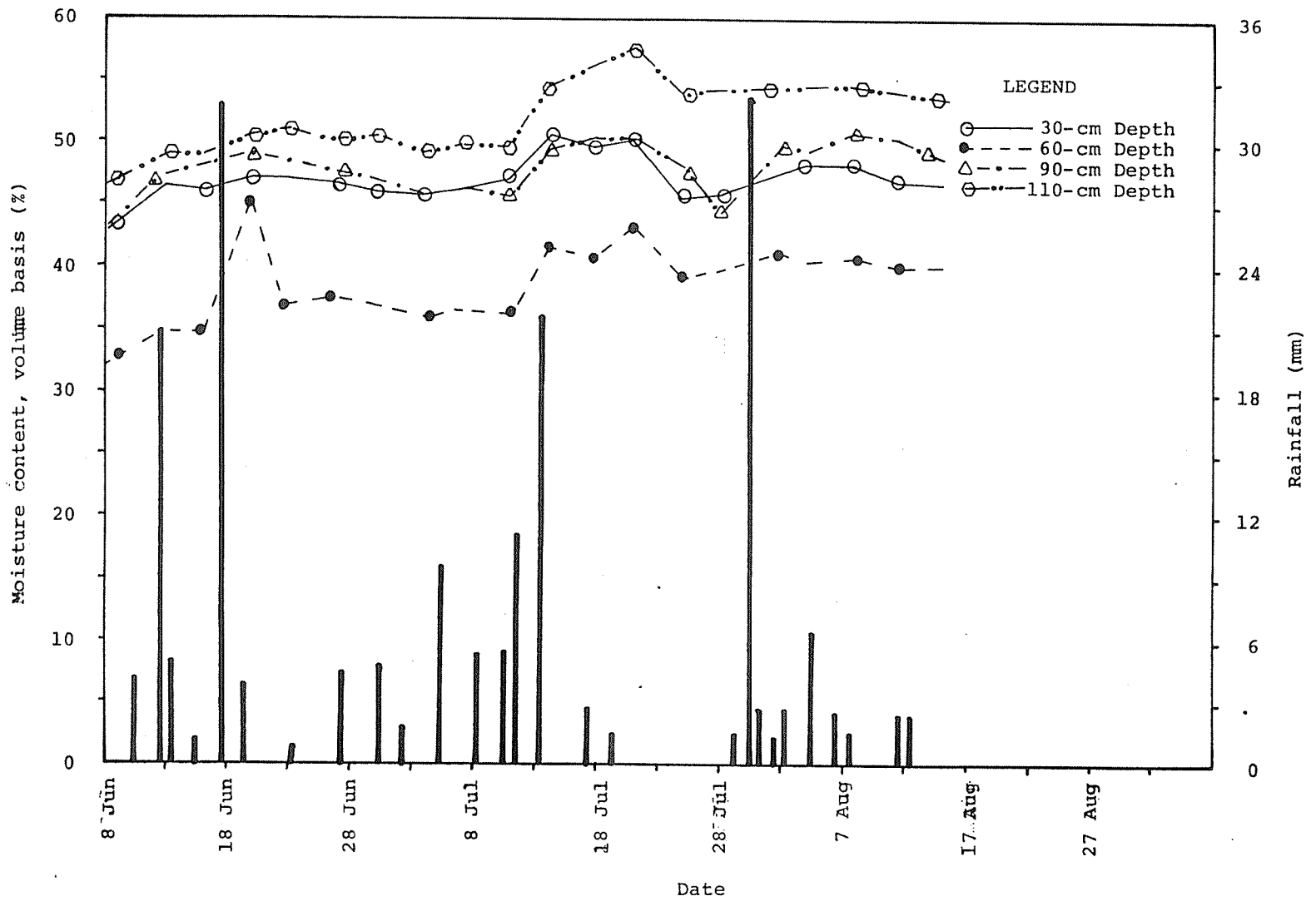


Figure 5.14 Moisture Profile and Rainfall Histogram at Location Cousins-C2B77 in 1977

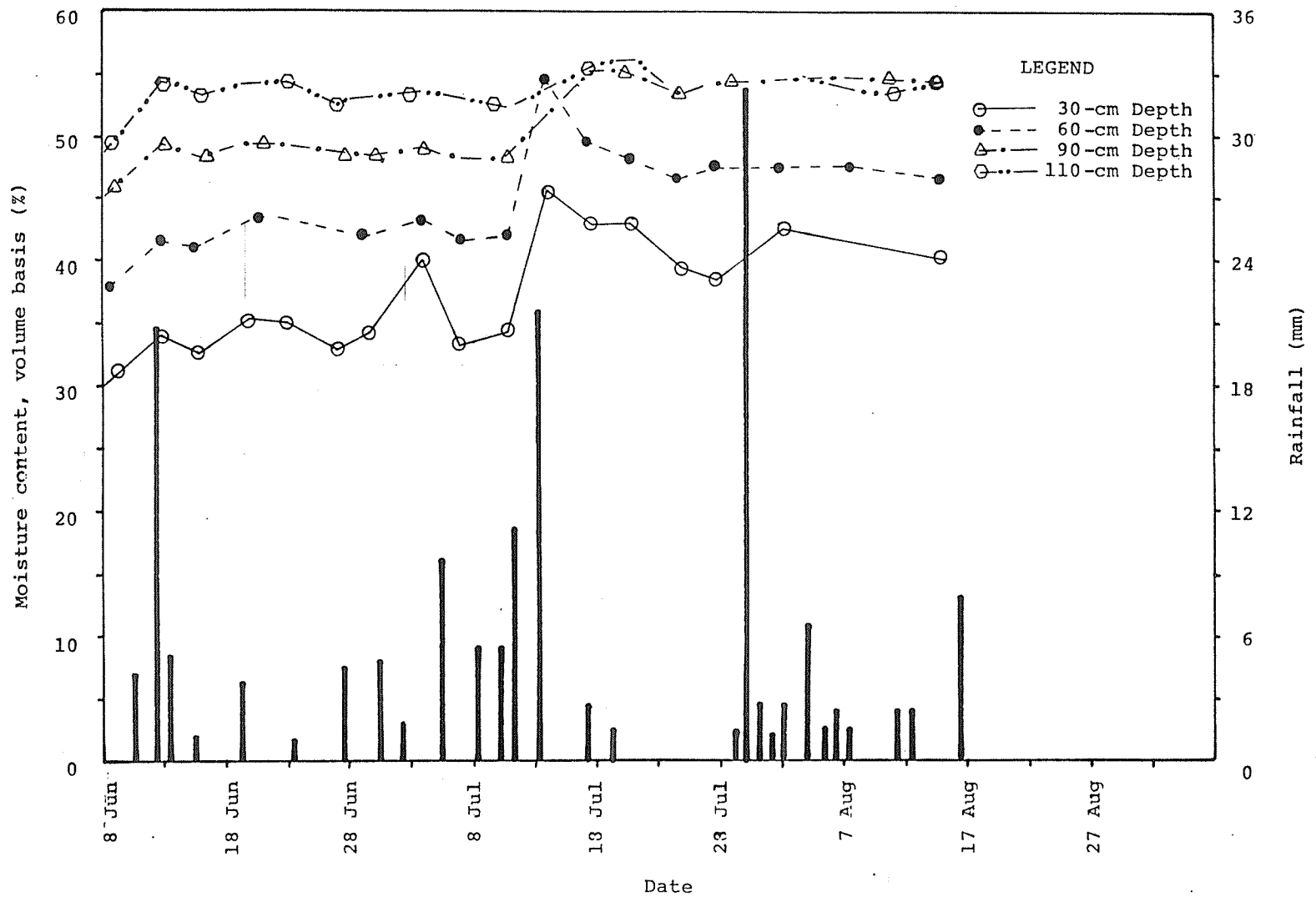


Figure 5.15 Moisture Profile and Rainfall Histogram at Location Cousins-C2C77 in 1977

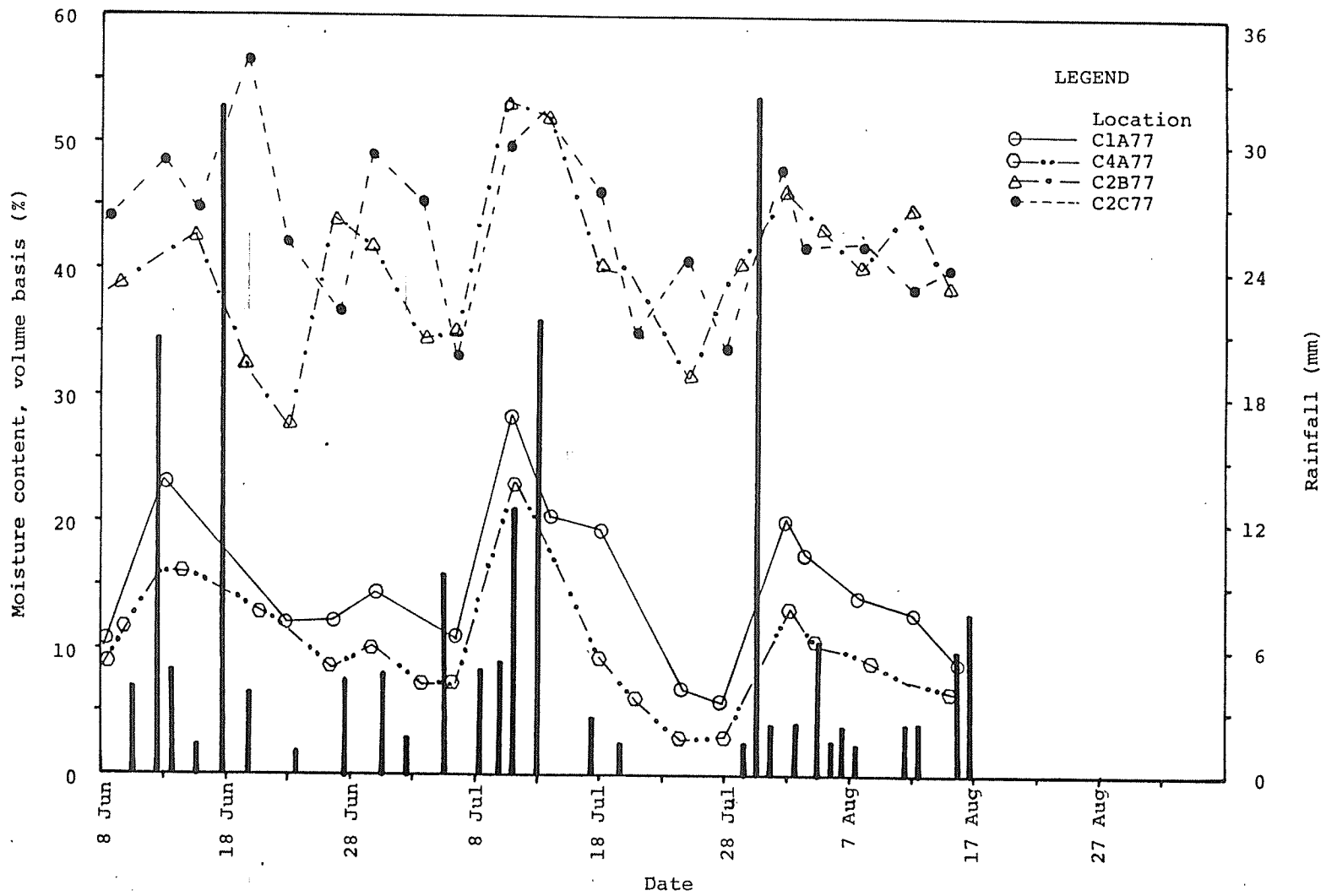


Figure 5.16 Moisture Content at 15-cm Depth on Furrow and Rainfall Histogram in the Cousins Field in 1977

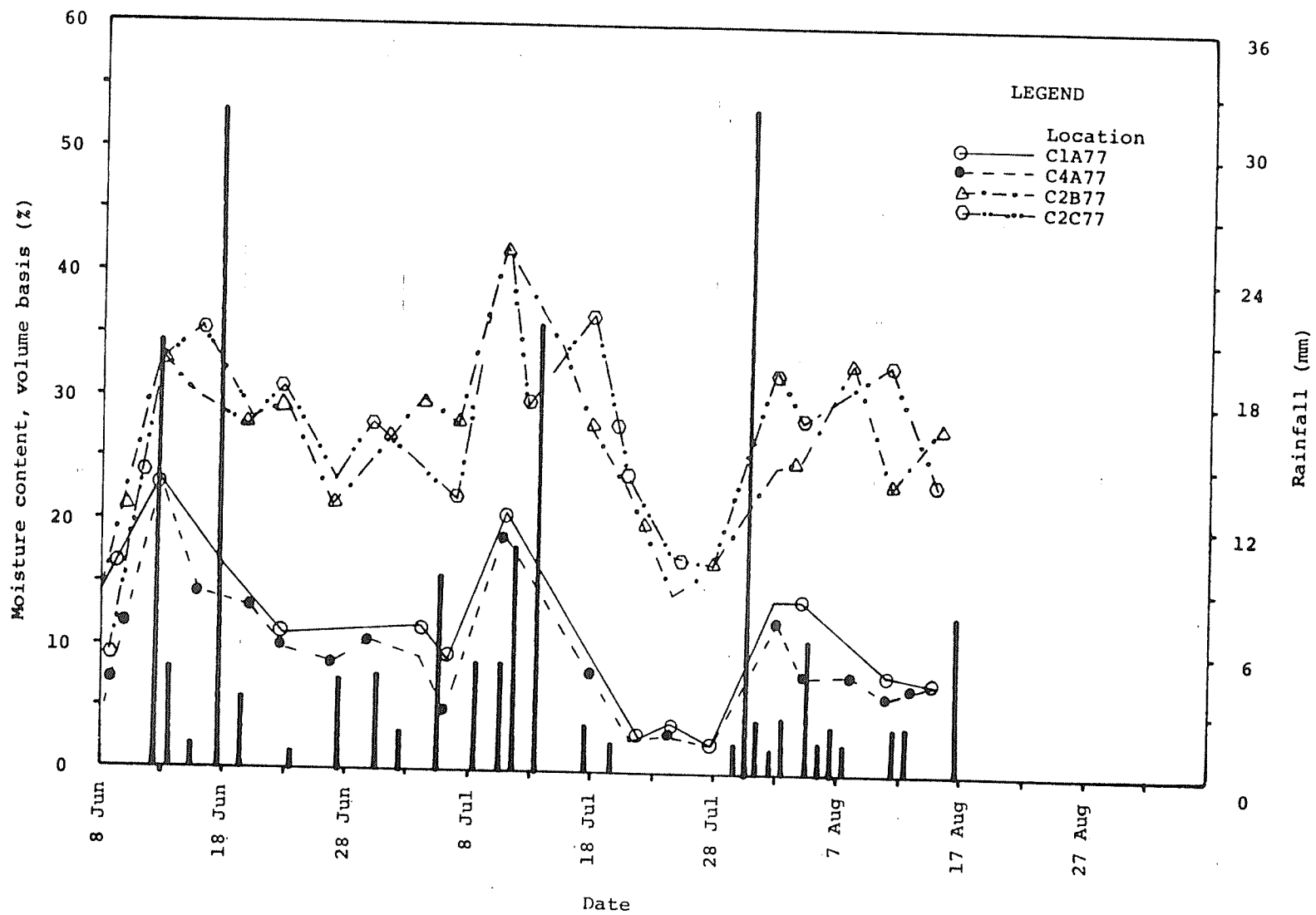


Figure 5.17 Moisture Content at 15-cm Depth on Hill and Rainfall Histogram in the Cousins Field in 1977

Locations C2C77 and C2B77 were in the low spots. The moisture profiles at both the locations are very similar. Here too, the frequent rainfall from 8 July to 13 July caused a sharp rise in the moisture content at all depths. The moisture content was above 30.0 percent throughout the growing period. At the 15-cm depth the moisture content was 25.0 percent on the average. This high moisture content was harmful for the crop. These spots required drainage.

5.5 Moisture Profiles in the Friesen Field in 1978

The moisture profiles at locations F1A78, F3A78, F1B78, F2B78, F3C78 and F2C78 have been presented in Figures 5.18 to 5.23.

At all the six locations, the moisture content at the 110-cm depth remained above 40.0 percent. During the month of July, it fluctuated between 50.0 percent and 60.0 percent and during the month of August between 40.0 percent and 50.0 percent. At F3C78 (Figure 5.18) it remained 55.0 percent on the average. The variations of the moisture content at this depth were due to the fluctuations in the groundwater level.

The pattern of the moisture content at the 90-cm depth was similar to that at the 110-cm depth. But at F3A78 (Figure 5.22), it was well below that at the 110-cm depth. This location was in the high spot in the field. The difference in the moisture content of the 90-cm and 110-cm depths was caused by the deep groundwater table at this location, which resulted in less upward flow as compared to that at the other locations. The crop was better at this location as compared to the other five locations.

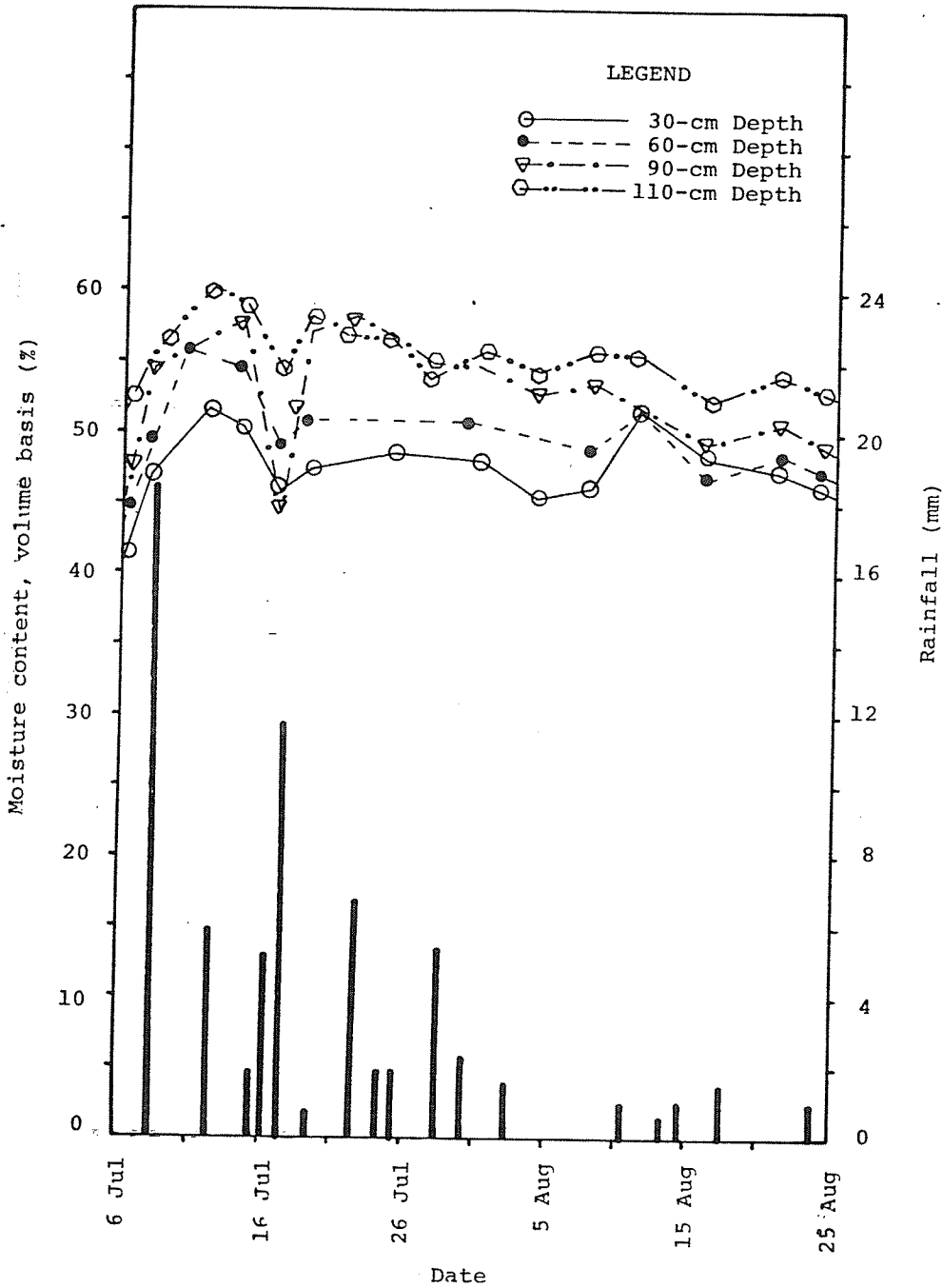


Figure 5.18 Moisture Profile and Rainfall Histogram at Location Friesen-F3C78 in 1978

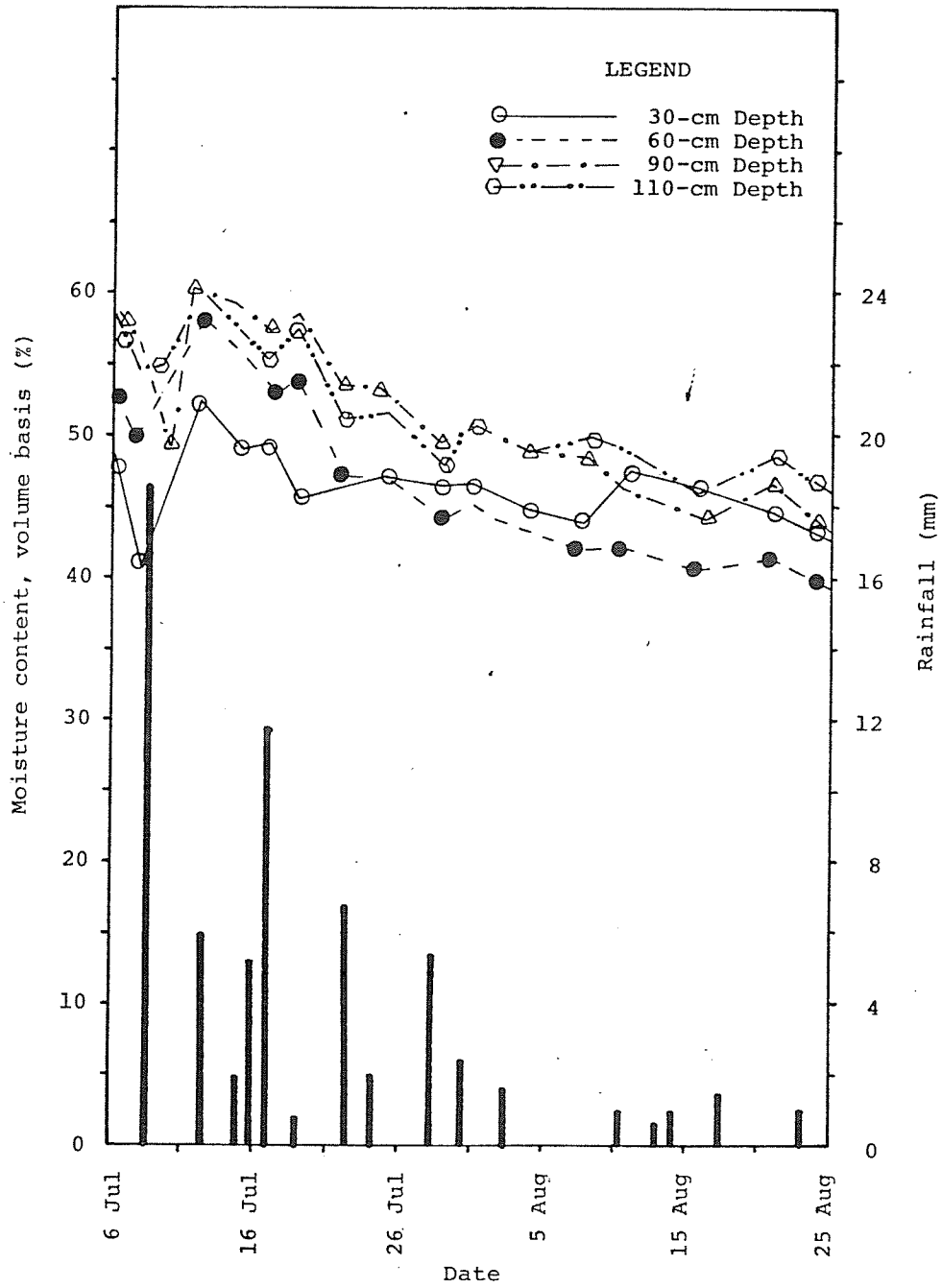


Figure 5.19 Moisture Profile and Rainfall Histogram at Location Friesen-F2B78 in 1978.

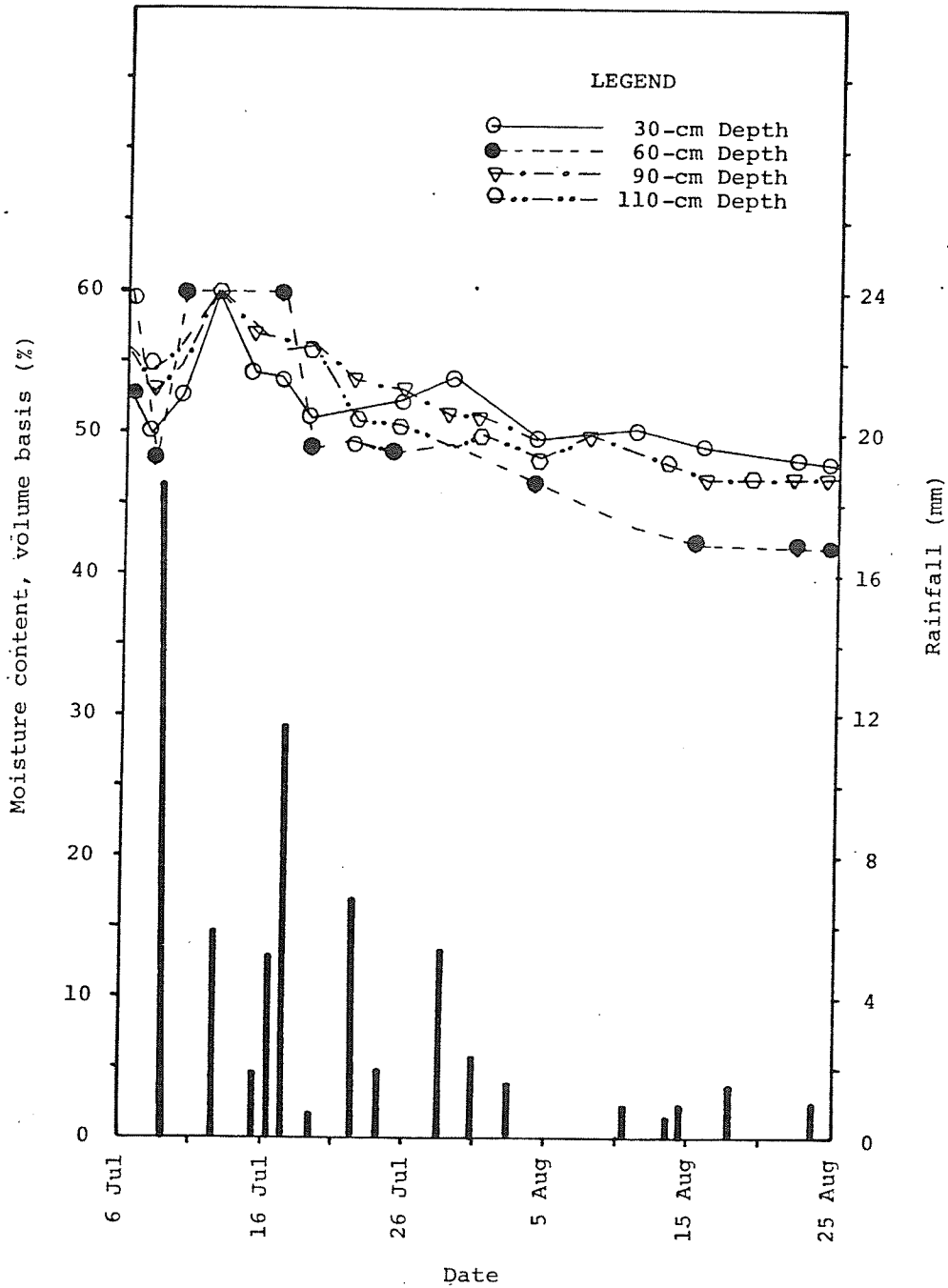


Figure 5.20 Moisture Profile and Rainfall Histogram at Location Friesen-F1B78 in 1978.

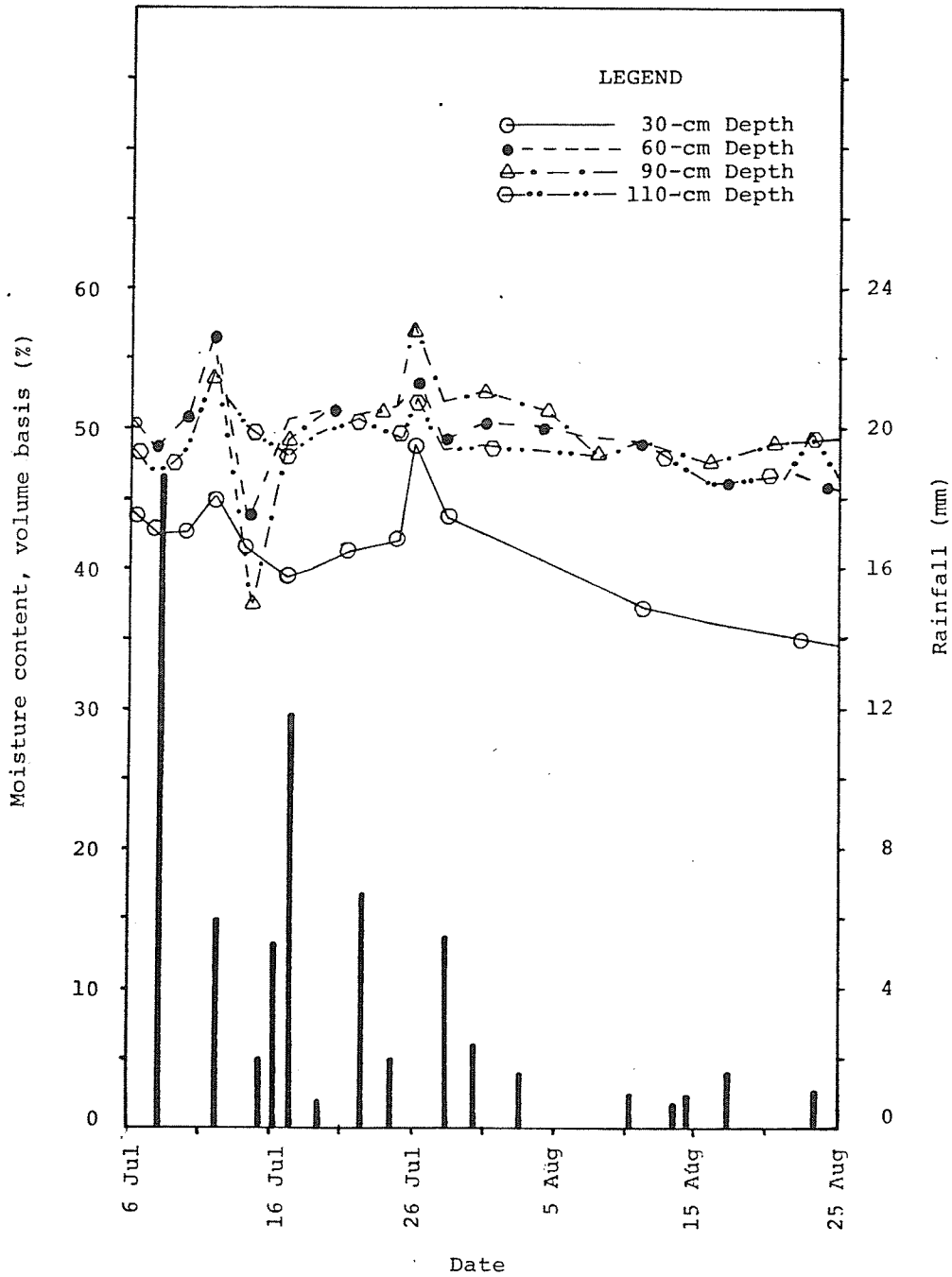


Figure 5.21 Moisture Profile and Rainfall Histogram at Location Friesen-FLA78 in 1978

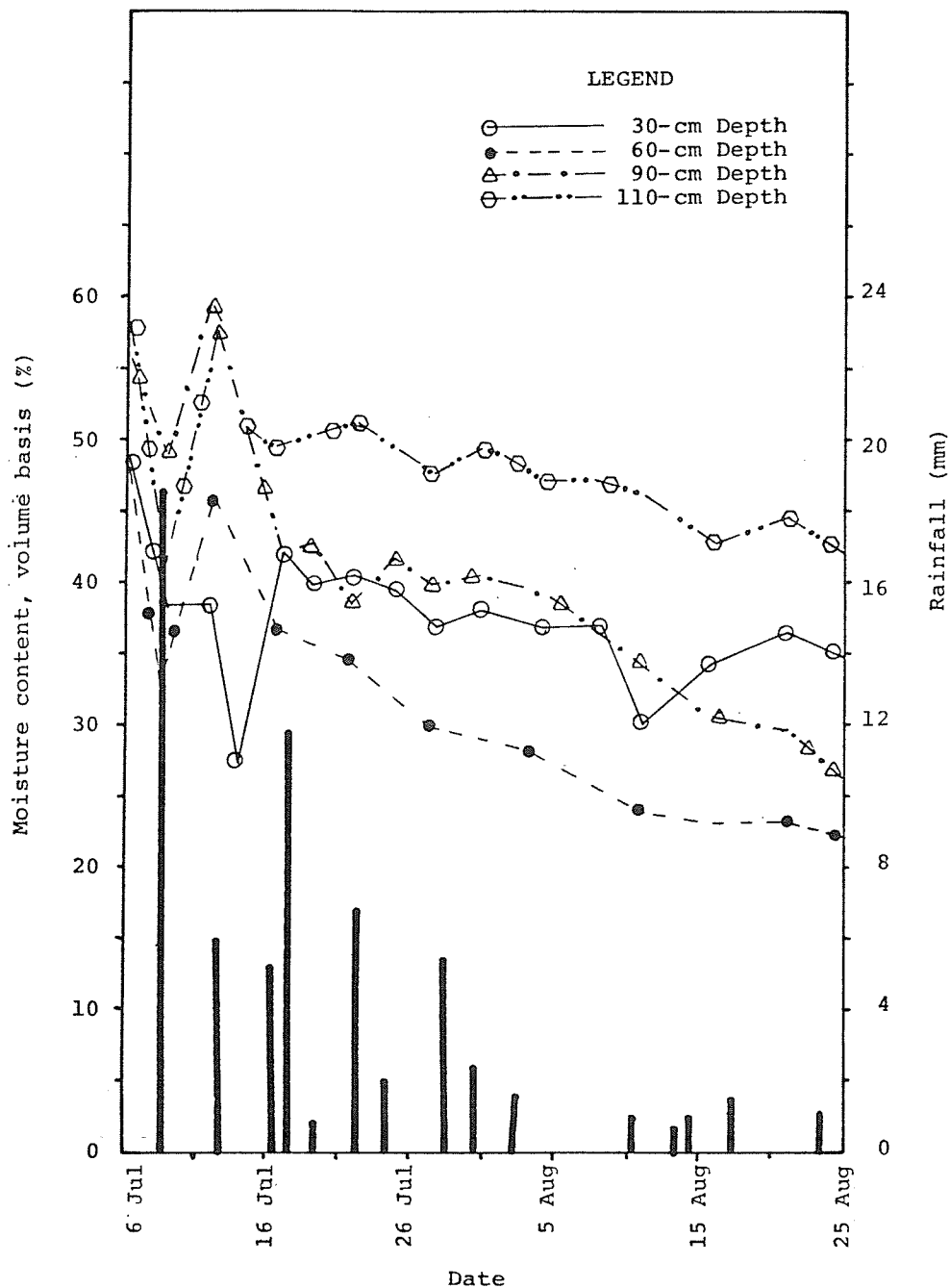


Figure 5.22 Moisture Profile and Rainfall Histogram at Location Friesen-F3A78 in 1978.

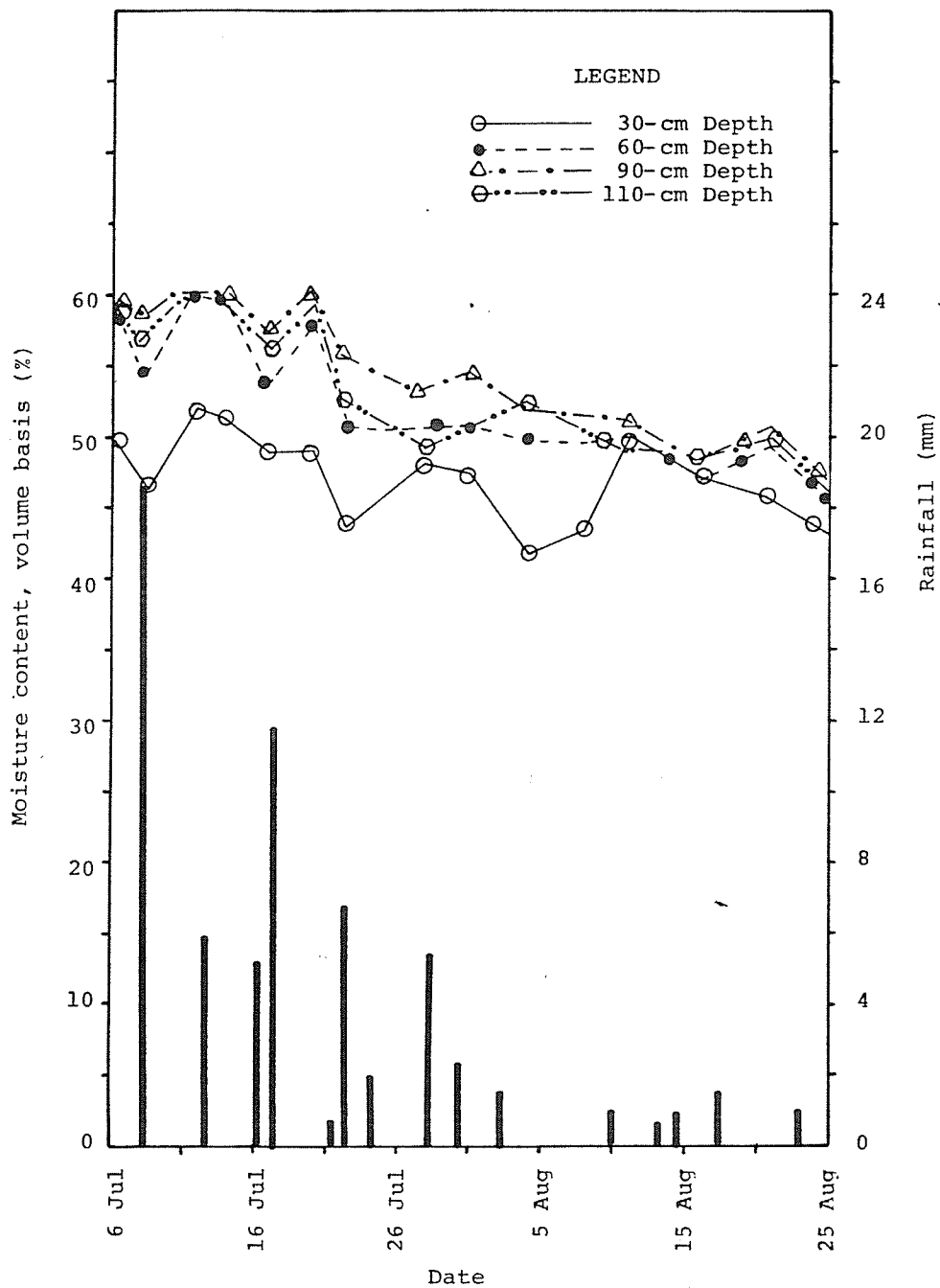


Figure 5.23 Moisture Profile and Rainfall Histogram at Location Friesen-F2C78 in 1978

The moisture content at the 60-cm depth at five locations was above 40.0 percent. At F2B78 (Figure 5.19), it was between 45.0 and 60.0 percent in the month of July and between 45.0 and 50.0 percent in the month of August. This spot was a low spot and the texture of the soil was clay instead of sandy loam, as it was at the other locations. At F3A78 (Figure 5.22), the pattern was different. The moisture content varied between 30.0 percent and 45.0 percent in July, and 22.5 percent and 30.0 percent in August. The August moisture content was favourable to the crop as indicated by the fast growth of the crop.

The moisture content at the 30.0 cm depth at F1B78 and F2B78, (Figures 5.20 and 5.19, respectively) was higher than the moisture content at the 60-cm depth. Usually the moisture content at the 30-cm depth is lower than the moisture content at the 60-cm depth. This condition prevailed due to the sandy loam texture of the 30-cm layer and sandy texture of the 60-cm layer. There was ponding of the rainfall water on the surface, the rate of infiltration being very low. A similar situation existed at F3A78 (Figure 5.22). The moisture content at the 30-cm depth at F3C78, F2B78 and F1B78 (Figures 5.18, 5.19 and 5.20, respectively) remained above 45.0 percent but was below that of the 60-cm depth. At F3A78 (Figure 5.22), it fluctuated between 35.0 percent and 48.0 percent.

Table 5.16 shows the average moisture content taken from the figures discussed. The moisture content was above 40.0 percent at all depths in a large part of the field. This was due to the high groundwater table. At the low spots it was only 75 cm below the

TABLE 5.16 AVERAGE MOISTURE CONTENT IN THE FRIESEN FIELD IN 1978

Location	Average Moisture Content, Volume Basis (%)							
	July				August			
	30 cm	60 cm	90 cm	110 cm	30 cm	60 cm	90 cm	110 cm
F1A78	42.5	50.0	50.0	50.0	37.5	47.5	47.5	47.5
F1B78	50.0	52.5	52.5	52.0	50.0	44.0	47.5	47.5
F2B78	47.5	53.0	55.0	55.0	45.0	42.5	45.0	47.8
F3C78	47.5	52.5	52.5	57.5	47.5	50.0	52.5	54.0
F2C78	47.5	55.0	55.0	55.0	47.5	50.0	50.0	50.0
F3A78	37.5	35.0	40.0	50.0	35.0	25.0	35.0	40.0

surface. The low spots as well as the high spots required drainage.

5.6 Moisture Profiles in the Friesen Field in 1977

The moisture profiles at locations F3A77, F1C77, F2B77 and F3C77 have been presented in Figures 5.24, 5.25, 5.26 and 5.27, respectively.

Locations F3A77 and F2B77 were in the high spots. The moisture content at F3A77, at the 30-cm and 60-cm depths fluctuated between 17.0 percent and 22.0 percent, which was favourable for the crop. At the 90-cm depth, it was near 30.0 percent and at the 110-cm depth, it was near 42.0 percent. The high moisture content at the 90-cm and 110-cm depths did not affect the crop. The moisture content at F2B77 was 5.0 percent more at each depth as compared to that at F3A77. This difference is attributed to the difference in texture.

Locations F1C77 and F3C77 were the low spots. At F1C77 the moisture content remained above 45.0 percent at all the depths. At F3C77 the moisture content at the 30-cm depth decreased from 48.0 percent at 31.0 percent in response to the evapotranspiration and deep percolation. This difference in the moisture content at the two low spots is attributed to the difference in texture, which was sandy at F3C77 and sandy loam at F1C77.

Figures 5.28 and 5.29 show the moisture content at the 15-cm depth on the furrow and the hill, respectively. The moisture content at the high spots on the ridge at F3A77 was at wilting point, on the average. At F2B77 also, it was at the wilting point for a

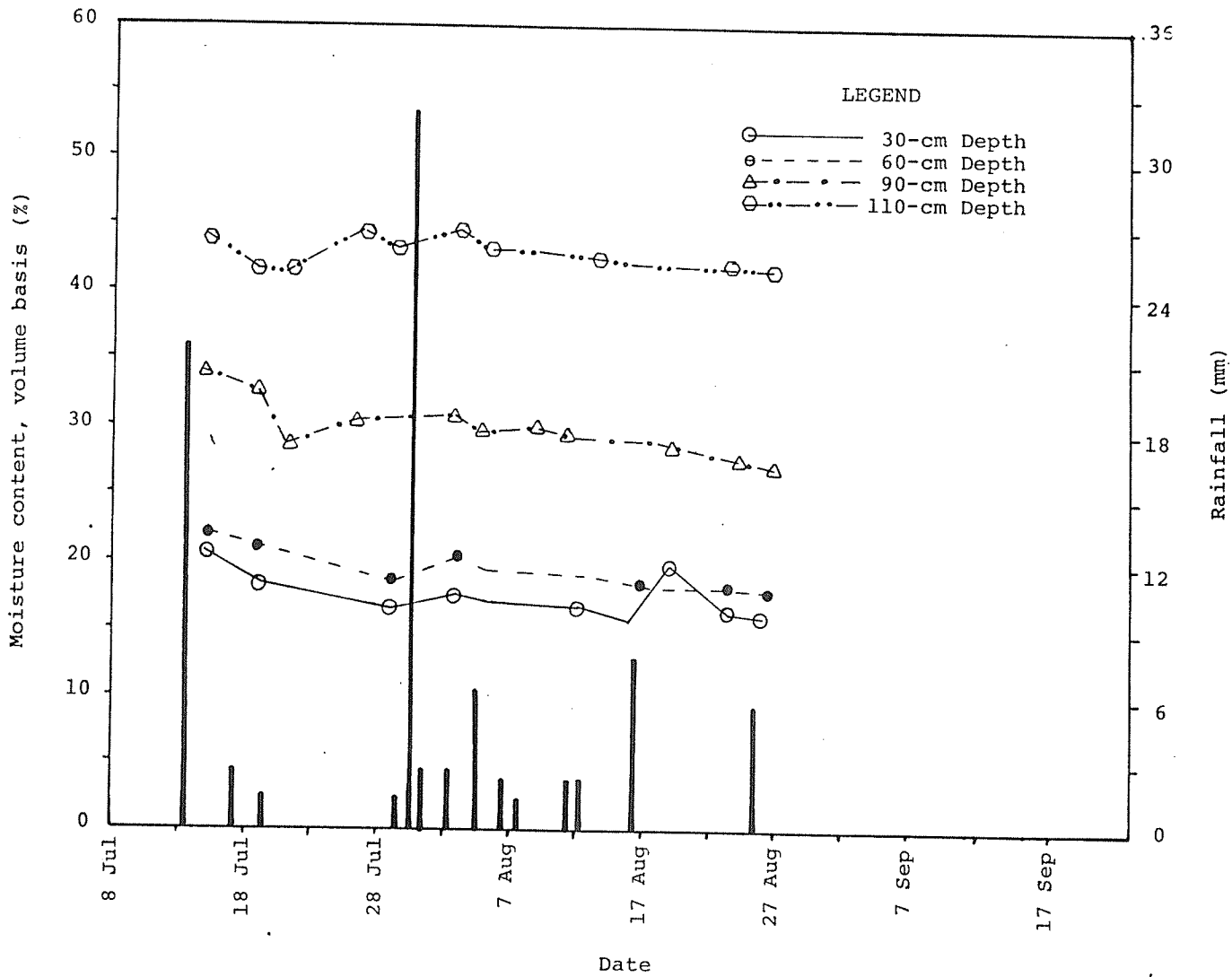


Figure 5.24 Moisture Profile and Rainfall Histogram at Location Friesen-F3A77 in 1977

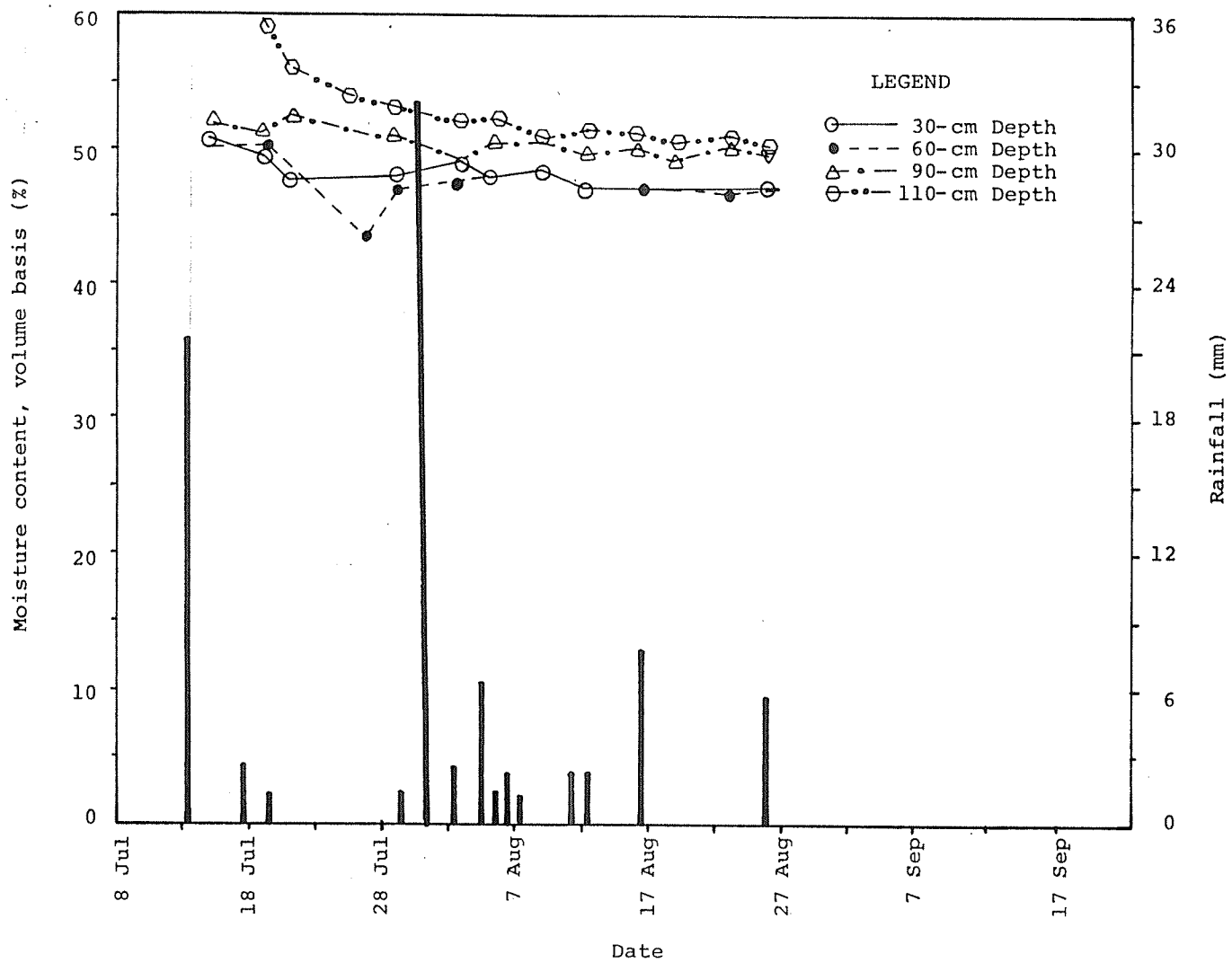


Figure 5.25 Moisture Profile and Rainfall Histogram at Location Friesen-FlA77 in 1977

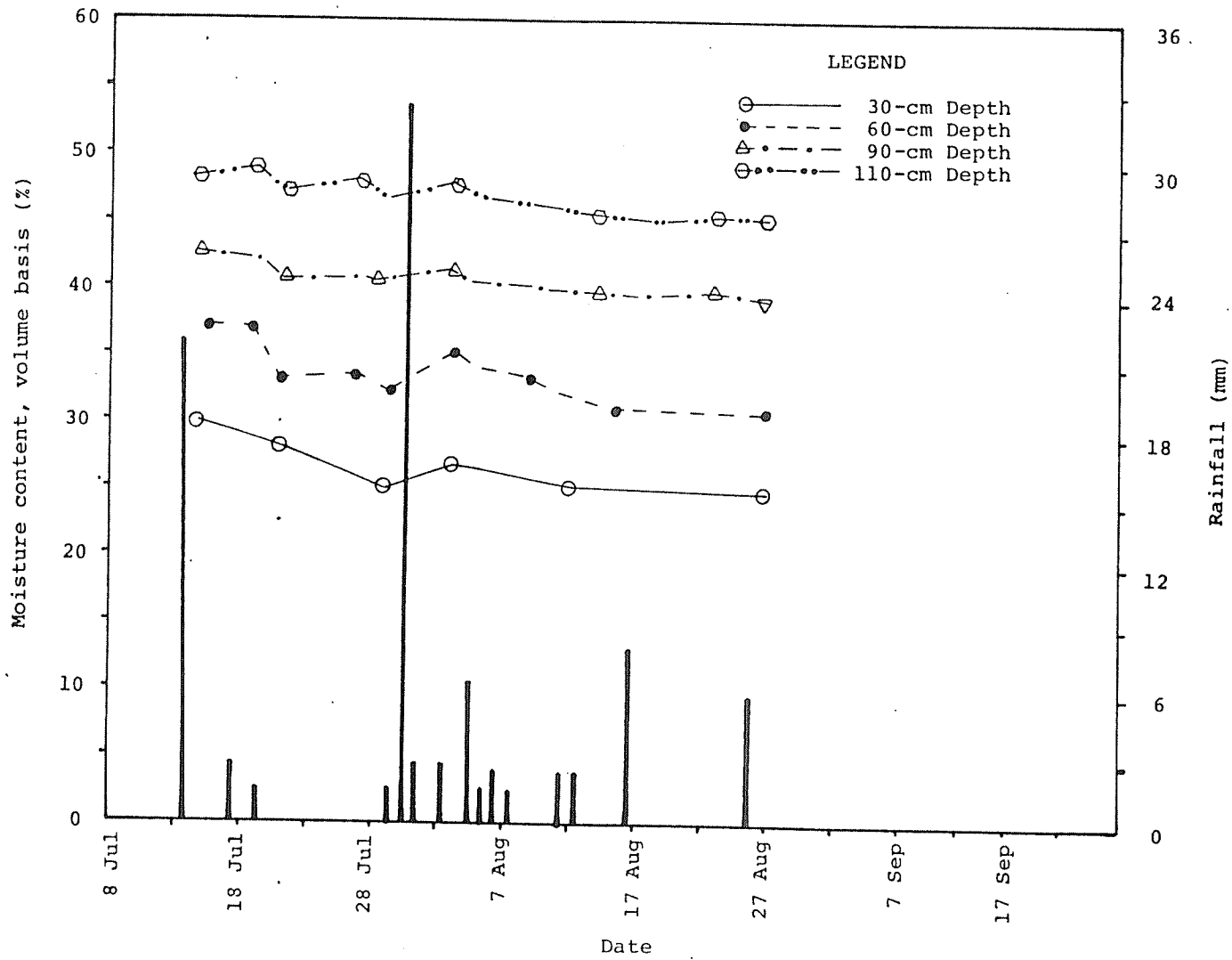


Figure 5.26 Moisture Profile and Rainfall Histogram at Location Friesen-F2B77 in 1977

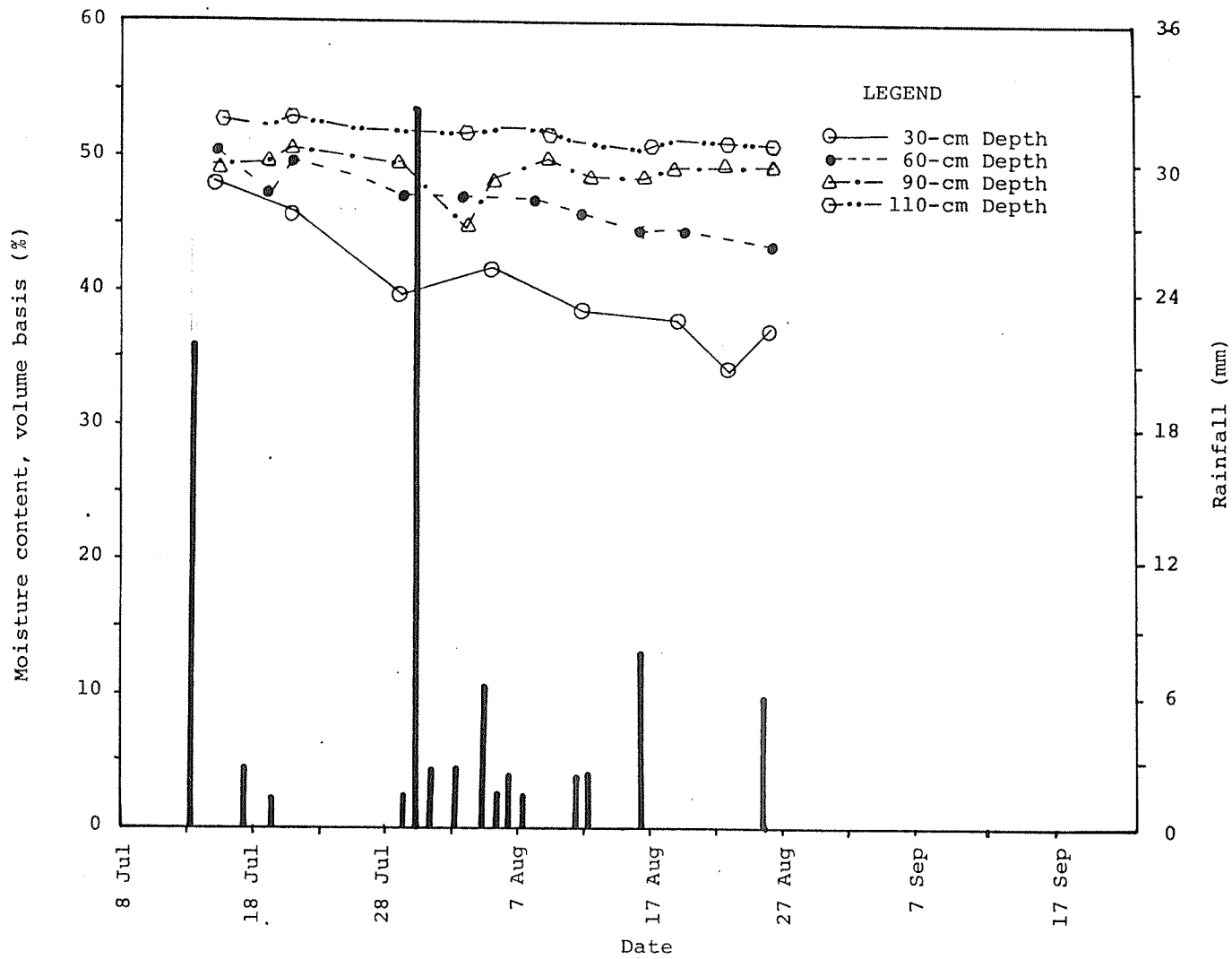


Figure 5.27 Moisture Profile and Rainfall Histogram at Location Friesen-F3C77 in 1977

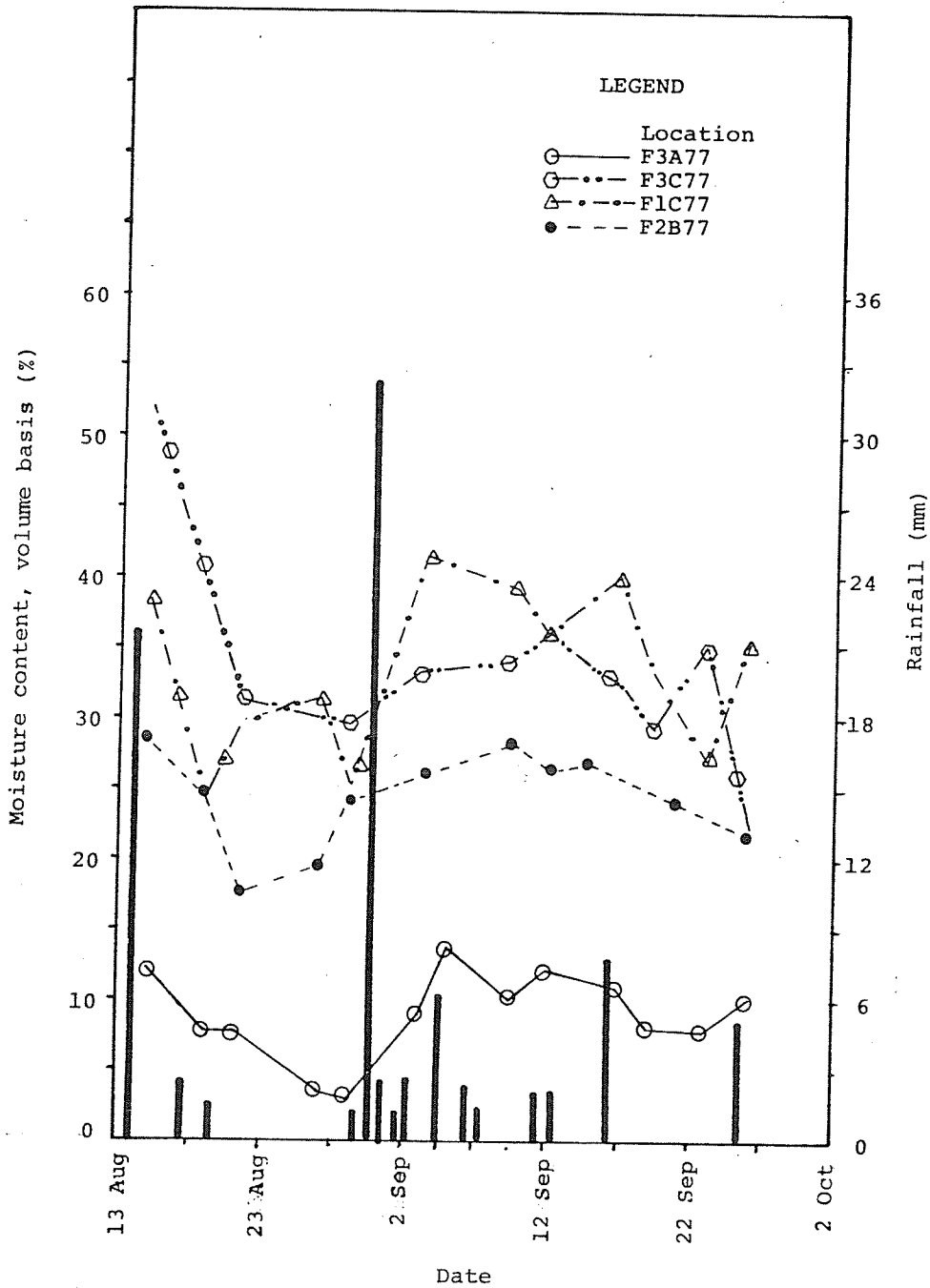


Figure 5.28 Moisture Content at 15-cm Depth on Furrow and Rainfall Histogram in the Friesen Field in 1977

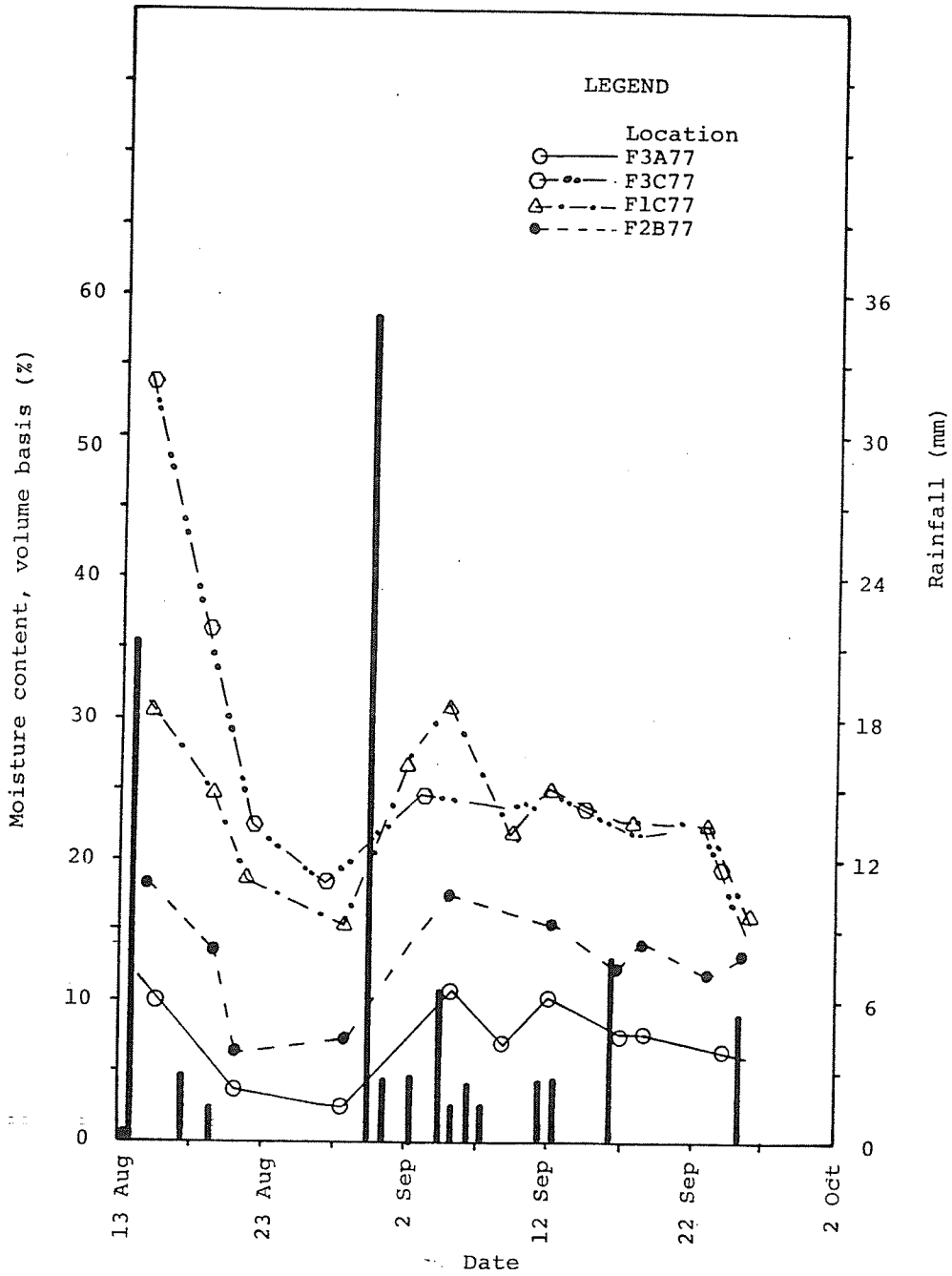


Figure 5.29 Moisture Content at 15 cm Depth on Hill and Rainfall Histogram in the Friesen Field in 1977

period of one week. The roots of the plants did not develop more deeply due to the high moisture content at the lower layers and at the upper layers, the moisture content was not optimum. This affected the crop development. At the low spots the moisture content at the 15-cm depth was above 25.0 percent. Some air spaces available at this depth allowed the growth of the plants, but the crop was very poor. A similar pattern of the moisture content was observed in the furrow except that it was higher by 10.0 percent at F2B77 as compared to that on the ridge at the same location.

Drainage is required at the low spots. If irrigation were provided at the high spots, drainage would also be required.

The moisture content on volume basis was found to be as high as 60 percent in both the years 1977 and 1978. The porosity of the soil was 0.45. This is an impossible situation. The sources of error may be improper packing of the soil around the access tubes and incorrect calibration. Therefore, the moisture content data are not reliable for determining the average values of moisture content. Their main utility is for purposes of relative comparison.

CHAPTER VI

CONCLUSIONS

The conclusions resulting from this study are as follows

1. A design infiltration equation for the Cousins field is:
$$y = 1.055t^{0.683} - 0.094$$

y = cumulative infiltration (cm)
 t = elapsed time (min).
2. Saturated hydraulic conductivity of the soil in the Cousins field varied from 11.28 cm/h to 25.80 cm/h for nearly 95 percent of the area and was 3.92 cm/h for the remaining area.
3. The results of this study showed that the bubbling pressure was close to that for unconsolidated sand as obtained by Laliberte (1966). The pore-size distribution index varied from that of unconsolidated sand to that of sandy loam soil as obtained by the same author.
4. Runoff is unlikely to occur on the Cousins field.
5. The equations derived for average capillary pressure at the wetting front are useful in determining the time of runoff for any initial moisture content and, hence, there is no limitation of the assumption of dry soil.
6. The moisture content at eighty percent saturation or even more below the 30-cm depth, did not have a harmful effect on the crop, provided that the moisture content at the 15-cm depth was near field capacity.

7. There was a significant effect of the groundwater on the moisture regime. A difference of 40 cm in the groundwater level affected the moisture regime substantially.
8. The slope of the groundwater table was 0.135 percent on the average.
9. Flow of the groundwater is towards the Assiniboine River.
10. The large slope of the groundwater table and the high saturated hydraulic conductivity showed that the natural drainage was effective. Almost the whole of the recharge by precipitation was drained naturally.
11. The rise in the groundwater level due to snowfall was from 20 cm to 60 cm. Precipitation in the form of snowfall affected the groundwater regime more than rainfall or irrigation. Therefore, snowfall in any year affects the groundwater regime which in turn affects the moisture regime.
12. More frequent rains resulted in less deep percolation and, hence, less rise in groundwater level as compared to rains of the same amount occurring in a short duration. Therefore, amount as well as duration of the rainfall is important in determining the moisture and groundwater regime.
13. In the Cousins field, irrigation during the months of July and August is essential. In the absence of irrigation, the yield of the crop will be severely affected.
14. The low spots in the Cousins field having a sandy-textured soil do not require drainage, but drainage is required on those low spots having fine-textured soils.

15. Both drainage and irrigation are required at the Friesen field.

CHAPTER VII

RECOMMENDATIONS

The following recommendations for further studies are made.

1. The method of determining the properties of porous media by applying the model of Gardner et al. (1970), and the concept of average capillary pressure should be supported by laboratory studies.
2. The direction of groundwater flow is known; additional observation wells should be placed "downstream" outside the irrigation field to determine the effect of irrigation on adjacent land.
3. Special wells or pits should be installed to monitor the movement and quality of groundwater from the surface to the water table.
4. Effects of irrigation on the groundwater should be studied independently from rainfall.

REFERENCES

REFERENCES

1. Bouwer, H. (1961). A double-tube method for measuring hydraulic conductivity of soil in situ above a water table. *Soil Sci. Soc. Amer. Proc.*, 25: 334-339.
2. Bouwer, H. (1962). Field determination of hydraulic conductivity above a water table with a double tube method. *Soil Sci. Soc. Amer. Proc.*, 26: 330-335.
3. Bouwer, H. (1964). Measuring horizontal and vertical hydraulic conductivity of soil with the double-tube method. *Soil Sci. Soc. Amer. Proc.*, 28: 19-23.
4. Braester, C. (1973). Linearized solution of infiltration at constant rate. *Ecological Studies 4, Physical Aspects of Soil Water and Salts in Ecosystems*, pp. 59-63. Springer-Verlag, Heidelberg.
5. Brooks, R. H. and A. T. Corey (1966). Properties of porous media affecting fluid flow. *J. Irrig. and Drain. Div., Proc. ASCE*, IR-2, Vol. 92, 61-88.
6. Burdine, N. T. (1952). Relative permeability calculations from pore size distribution data. *Petroleum Transactions, Amer. Inst. Mining Metallurgical Engrs.*, 198: 71-78.
7. Carman, P. C. (1937). Fluid flow through a granular bed. *Trans. Inst. Chem. Eng., London*, Vol. 75, 150-156.
8. Childs, E. C. (1967). The physical basis of soil water phenomena, pp. 274-294. *John Wiley & Sons, Inc., New York and London.*
9. Chu, S. T. (1977). Modeling infiltration during a variable rain. *ASAE paper No. 77-2063, St. Joseph, Michigan.*
10. Collis-George, Neville and A. N. Evans (1964). A two-well method of determining the hydraulic conductivity of discrete layers in layered saturated soils in the field. *Australian J. of Soil Res.*, 2: 8-19.
11. Corey, A. T. (1954). The interrelation between gas and oil relative permeabilities. *Producer's Monthly*, Vol. 19, No. 1, November.
12. Corey, A. T. (1977). Mechanics of heterogeneous fluids in porous media. pp. 72-129. *Lithocrafters, Ann Arbor, Michigan.*

REFERENCES - Continued

13. Dendy, F. E. and L. E. Asmussen (1963). Permeability measurements with small well points. *Trans. ASAE*, 6: 297-300, 303.
14. Erickson, A. E., J. M. Fulton and G. H. Brandt (1964). New techniques for relating soil aeration and plant response. *Proc. 8th Intern. Congr. Soil Sci.*, 428-434.
15. Fair, A. M. and L. P. Hatch (1933). Fundamental factors governing the streamline flow of water through sand. *J. Amer. Water Works Assoc.*, Vol. 25.
16. Fang Ching, Seng. (1965). Field application of four well method of measuring hydraulic conductivity. M. S. thesis, North Carolina State University, Raleigh, North Carolina.
17. Folk, Y. S. (1970). A study of two-dimensional infiltration. *Trans., ASAE*, 13(5): 676.
18. Gardner, W. R., D. Hillel and Y. Benyamini (1970). Post-irrigation movement of soil water I: Redistribution. *Water Resources Res.*, 6(3): 851-861.
19. Green, W. H. and G. A. Ampt. (1911). Studies of soil physics. (1)I: The flow of air and water through soils. *J. Agric. Sci.*, 4: 1-24.
20. Holtan, H. N. (1961). A concept for infiltration estimates in watershed engineering. *ARS paper 41-51*. As quoted in reference 23.
21. Horton, R. E. (1940). An approach towards a physical interpretation of infiltration capacity. *Soil Sci. Soc. Amer. Proc.* 5: 339-417.
22. Hoveland, C. S. and H. L. Webster (1965). Flooding tolerance of annual clovers. *Agron. J.*, 57: 3-4.
23. Idike, F., D. C. Slack and R. A. Young (1977). Experimental evaluation of two infiltration equations. *ASAE paper No. 77-2558*. St. Joseph, Michigan.
24. Israelson, O. W. (1932). *Irrigation principles and practices*, p. 81, John Wiley and Sons, New York.
25. Jackson, R. D. (1963). Porosity and soil-water diffusivity relations. *Soil Sci. Soc. Am. Proc.*, 27: 123-126.

REFERENCES - Continued

26. James, L. A. (1976). Modeling infiltration and redistribution of soil water during intermittent application. *Trans. ASAE*, 19: 482-488.
27. Kohnke, H. (1968). *Soil physics*, pp. 321. McGraw-Hill, New York.
28. Kostikov, A. N. (1932). On the dynamics of the coefficient of water percolation in soils and on the necessity for studying it from a dynamic point of view for purposes of amelioration. *Trans. 6th Com. Intern. Soc. Soil Sci. Russian, Part A*: 17-21.
29. Kozeny, J. (1927). *Sitz Ber. Akad. Wiss. Wien. Abt. IIa*. As quoted in reference 30.
30. Laliberte, G. E. (1966). Properties of unsaturated porous media. Ph.D. thesis, Colorado State University, Fort Collins, Colorado.
31. Laliberte, G. E. (1969). A mathematical function of disturbed soil materials affected by porosity. *Soil Sci. Soc. Amer. Proc.*, 31: 451-454.
32. Laliberte, G. E., R. H. Brooks and A. T. Corey (1968). Permeability calculated from desaturation data. *J. Irr. and Drain. Div., ASCE*, Vol. 94, No. IR-1, Proc. Paper 5848, 54-71.
33. Mein, R. G. and C. L. Larson. (1971). Modeling infiltration during a steady rain. *Water Resources Res.*, 9: 384-394.
34. Michalyna, W. and R. E. Smith. (1972). Soils of the Portage la Prairie. Manitoba Soil Survey Soils Report No. 17. Manitoba Department of Agriculture, Manitoba.
35. Morel-Seytoux, H. J. and J. Khanji. (1974). Derivation of an equation of infiltration. *Water Resources Res.*, 10: 795-800.
36. Nielsen, D. R., J. W. Biggar and J. M. Davidson. (1962). Experimental consideration of diffusion analysis in unsaturated flow problems. *Soil Sci. Soc. Am. Proc.*, 26: 107-111.
37. Philip, J. R. (1954). An infiltration equation with physical significance. *Soil Sci.*, 77: 153-157.

REFERENCES - Continued

38. Philip, J. R. (1957). The theory of infiltration. 4: Sorptivity and algebraic infiltration equations. *Soil Sci.*, 88: 257-264.
39. Philip, J. R. (1958). The theory of infiltration. 7: *Soil Sci.*, 85: 333-337.
40. Richards, L. A. (1931). Capillary conduction of liquid through porous medium. *Physics I.* 318-338.
41. Richards, L. A. (1952). Report of the subcommittee on permeability and infiltration, Committee on Terminology, Soil Science Society of America. *Soil Sci. Soc. Am. Proc.*, 16: 85-88.
42. Richards, L. A. and D. C. Moore. (1952). Influence of the capillary conductivity and depth of wetting on moisture retention in soil. *Trans. Amer. Geo. Union* 33 (4): 531-540.
43. Rubin, J. (1966). Theory of rainfall uptake by soils initially drier than their field capacity and its application. *Water Resources Res.*, 2: 739-749.
44. Rubin, J. and R. Steinhardt. (1963). Soil water relations during rain infiltration: I Theory. *Soil Sci. Soc. Am. Proc.*, 27: 246-251.
45. Rubin, J. (1967). Numerical method for analyzing hysteresis-affected, post-infiltration of soil moisture. *Soil Sci. Soc. Amer. Proc.*, 31: 13-20.
46. Smiles, D. E. and E. G. Young. (1965). Hydraulic conductivity determinations by several field methods in a sand tank. *Soil Sci.*, 99: 83-87.
47. Snell, A. W. and Jan van Schilfgaarde. (1964). Four-well method of measuring hydraulic conductivity of the soil. *Trans. ASAE*, 1: 83-87, 91.
48. Staple, W. J. (1969). Comparison of computed and measured moisture redistribution following infiltration. *Soil Sci. Soc. Amer. Proc.*, 33: 840-847.
49. Su, Charles and R. H. Brooks. (1975). Soil hydraulic properties from infiltration tests. *Watershed Management Proc. Irrig. and Drain. Div. ASCE*, Logan, Utah, August 11-13.

50. Thomas, A. W. (1965). Application of four-well method of measuring hydraulic conductivity under field conditions. M. S. thesis, Clemson University, South Carolina.
51. van Schaik, J. C. and G. E. Laliberte. (1968). Soil hydraulic properties affected by several field methods in a sand tank. Soil Sci. Vol. 49, 95-102.
52. Whisler, F. D. and H. Bouwer. (1970). Comparison of methods for calculating vertical drainage and infiltration in soils. J. Hydrol., 10(1): 1-19.
53. White, N. F., D. K. Sunada, H. R. Duke and A. T. Corey. (1972). Boundary effects in desaturation of porous media. Soil Sci., 113: 80-85.
54. Williamson, R. E. (1964). The effect of root aeration on plant growth. Soil Sci. Soc. A., Proc., 28: 86-90.
55. Youngs, E. G. (1957). Moisture profiles during vertical infiltration. Soil Sci., 84: 283-290.
56. Youngs, E. G. (1958 a). Redistribution of moisture in porous materials after infiltration. Soil Sci., 86: 117-125.
57. Youngs, E. G. (1958 b). Redistribution of moisture in porous materials after infiltration. Soil Sci., 86: 202-207.

APPENDIX A
INFILTRATION DATA

TABLE A-1 ELAPSED TIME AND CUMULATIVE INFILTRATION DATA

Elapsed Time (min)	Cumulative Infiltration (cm)			
	<u>Experiment No.</u>			
	1	2	3	4
0	0.00	0.00	0.00	0.00
2	5.70	4.95	2.45	2.85
5	8.60	7.40	6.25	4.85
10	12.20	9.90	8.95	6.70
15	15.45	12.25	11.25	8.45
20	18.70	14.65	13.45	10.25
25	21.65	16.80	15.50	11.85
30	24.45	19.05	17.65	13.65
40	30.30	23.35	22.75	17.15
50	36.10	27.85	27.75	20.75
60	41.65	32.55	32.95	24.60
70	47.20	37.15	38.20	28.45
80	52.85	-	-	32.20
90	-	-	-	36.25

TABLE A-2 ELAPSED TIME AND CUMULATIVE INFILTRATION DATA

Elapsed Time (min)	Cumulative Infiltration (cm)			
	<u>Experiment No.</u>			
	5	6	7	8
0	0.00	0.00	0.00	0.00
2	1.50	3.80	4.50	4.15
5	3.60	6.35	6.80	5.60
10	5.40	8.15	8.60	6.75
15	6.80	9.50	9.90	7.75
20	8.00	10.70	11.00	8.75
25	9.25	11.60	12.10	9.75
30	10.50	12.85	13.30	10.80
40	12.95	15.35	15.55	12.90
50	15.30	17.65	17.65	15.00
60	17.80	20.10	20.35	17.10
70	20.30	22.45	22.85	18.25
80	22.80	24.95	-	-
90	25.30	27.40	-	-

TABLE A-3 ELAPSED TIME AND CUMULATIVE INFILTRATION DATA

Elapsed Time (min)	Cumulative Infiltration (cm)			
	<u>Experiment No.</u>			
	9	10	11	12
0	0.00	0.00	0.00	0.00
2	5.05	4.10	1.50	3.30
5	5.65	4.95	3.55	5.05
10	6.35	5.25	4.85	5.80
15	6.85	5.70	5.60	6.55
20	7.35	6.40	6.25	7.20
25	7.80	6.90	6.95	7.80
30	8.25	7.30	7.60	8.40
40	9.25	8.25	8.90	9.75
50	10.25	9.10	10.25	10.95
60	11.15	10.20	11.55	11.25
70	12.15	11.25	13.20	12.45
80	13.10	12.25	14.60	13.75
90	14.29	13.35	16.05	15.15

TABLE A-4 ELAPSED TIME AND INFILTRATION RATE

Elapsed Time (min)	Infiltration Rate (cm/min)			
	<u>Experiment No.</u>			
	1	2	3	4
0	-	-	-	-
2	2.85	2.47	1.22	1.42
5	0.96	0.82	1.26	0.66
10	0.72	0.51	0.54	0.37
15	0.65	0.46	0.46	0.35
20	0.65	0.48	0.44	0.36
25	0.59	0.43	0.41	0.32
30	0.56	0.45	0.43	0.36
40	0.58	0.43	0.51	0.35
50	0.58	0.45	0.50	0.36
60	0.55	0.47	0.52	0.38
70	0.55	0.46	0.52	0.38
80	0.56	-	-	0.37
90	-	-	-	0.40

TABLE A-5 ELAPSED TIME AND INFILTRATION RATE

Elapsed Time (min)	Infiltration Rate (cm/min)			
	<u>Experiment No.</u>			
	5	6	7	8
0	-	-	-	-
2	0.75	1.90	2.25	2.08
5	0.70	0.85	0.76	0.48
10	0.36	0.36	0.36	0.23
15	0.28	0.27	0.26	0.20
20	0.24	0.24	0.22	0.20
25	0.25	0.18	0.22	0.20
30	0.25	0.25	0.24	0.21
40	0.24	0.25	0.22	0.21
50	0.23	0.23	0.21	0.21
60	0.25	0.24	0.27	0.21
70	0.25	0.23	0.25	0.22
80	0.25	0.25	0.26	-
90	0.25	0.24	0.26	-

TABLE A-6 ELAPSED TIME AND INFILTRATION RATE

Elapsed Time (min)	Infiltration Rate (cm/min)			
	<u>Experiment No.</u>			
	9	10	11	12
0	-	-	-	-
2	2.02	2.05	0.75	1.65
5	0.20	0.28	0.68	0.58
10	0.14	0.06	0.26	0.15
15	0.10	0.09	0.15	0.15
20	0.10	0.12	0.13	0.13
25	0.09	0.10	0.15	0.12
30	0.09	0.08	0.13	0.13
40	0.10	0.09	0.13	0.12
50	0.10	0.08	0.13	0.13
60	0.09	0.11	0.13	0.13
70	0.10	0.10	0.16	0.12
80	0.09	0.10	0.14	0.14
90	0.10	0.11	0.14	0.14

TABLE A-7 INITIAL AND FINAL MOISTURE CONTENT DATA OF INFILTRATION EXPERIMENT

Depth (cm)	Moisture Content, Dry Weight Basis (%)					
	Experiment No.					
	1		2		3	
	Initial	Final	Initial	Final	Initial	Final
15	10.1	37.5	5.6	33.5	7.6	41.8
30	6.8	28.1	5.7	28.3	6.0	23.1
45	6.3	22.6	5.8	26.3	6.4	21.9
60	6.7	19.6	5.4	20.0	5.9	20.9

TABLE A-8 INITIAL AND FINAL MOISTURE CONTENT DATA OF INFILTRATION EXPERIMENT

Depth (cm)	Moisture Content, Dry Weight Basis (%)					
	Experiment No.					
	4		5		6	
	Initial	Final	Initial	Final	Initial	Final
15	10.4	40.8	11.5	32.7	5.6	31.2
30	8.1	36.7	9.4	27.6	5.7	22.1
45	8.0	26.2	8.3	26.5	5.8	18.8
60	7.0	20.5	8.3	23.0	5.4	16.0

TABLE A-9 INITIAL AND FINAL MOISTURE CONTENT DATA OF INFILTRATION EXPERIMENT

Depth (cm)	Moisture Content, Dry Weight Basis (%)					
	Experiment No.					
	7		8		9	
	Initial	Final	Initial	Final	Initial	Final
15	11.8	29.5	7.0	40.1	10.2	37.0
30	9.7	23.2	8.5	25.7	11.2	40.2
45	12.1	19.0	7.4	21.2	9.0	16.7
60	16.4	16.2	6.6	17.5	10.3	18.5

TABLE A-10 INITIAL AND FINAL MOISTURE CONTENT DATA OF INFILTRATION EXPERIMENT

Depth (cm)	Moisture Content, Dry Weight Basis (%)					
	Experiment No.					
	10		11		12	
	Initial	Final	Initial	Final	Initial	Final
15	11.9	33.7	11.8	27.4	7.0	43.9
30	8.4	31.3	9.7	24.5	8.5	25.0
45	7.6	18.5	12.1	16.8	7.4	22.5
60	6.3	17.0	16.4	14.8	6.7	18.6

TABLE A-11 MOISTURE CONTENT OF THE TRANSMISSION ZONE AFTER THE FLOODING ENDS AT SECTION I AND INITIAL MOISTURE CONTENT

Depth (cm)	Initial Moisture Content, Dry Weight Basis (%)	Moisture Content, Dry Weight Basis (%)							
		Elapsed Time (h)							
		0	1	2	3	6	10	24	
7.5	6.8	30.0	22.0	19.3	17.5	14.5	12.3	9.8	
15.0	7.0	28.5	21.9	19.7	17.3	14.0	12.0	9.6	
22.5	6.9	27.0	21.9	18.6	16.9	14.0	11.9	9.3	
30.0	6.9	26.5	21.8	18.6	16.7	13.5	11.8	9.3	

TABLE A-12 MOISTURE CONTENT OF THE TRANSMISSION ZONE AFTER THE FLOODING ENDS AT SECTION II AND INITIAL MOISTURE CONTENT

Depth (cm)	Initial Moisture Content, Dry Weight Basis (%)	Moisture Content, Dry Weight Basis (%)							
		Elapsed Time (h)							
		0	1	2	3	6	10	24	
7.5	7.0	29.0	20.5	17.0	15.0	12.5	10.8	9.0	
15.0	7.1	28.0	19.0	16.5	14.9	12.4	10.7	8.9	
22.5	7.1	26.0	19.0	16.5	14.8	12.2	10.7	8.9	
30.0	7.2	25.0	18.7	16.0	14.8	12.1	10.5	8.8	

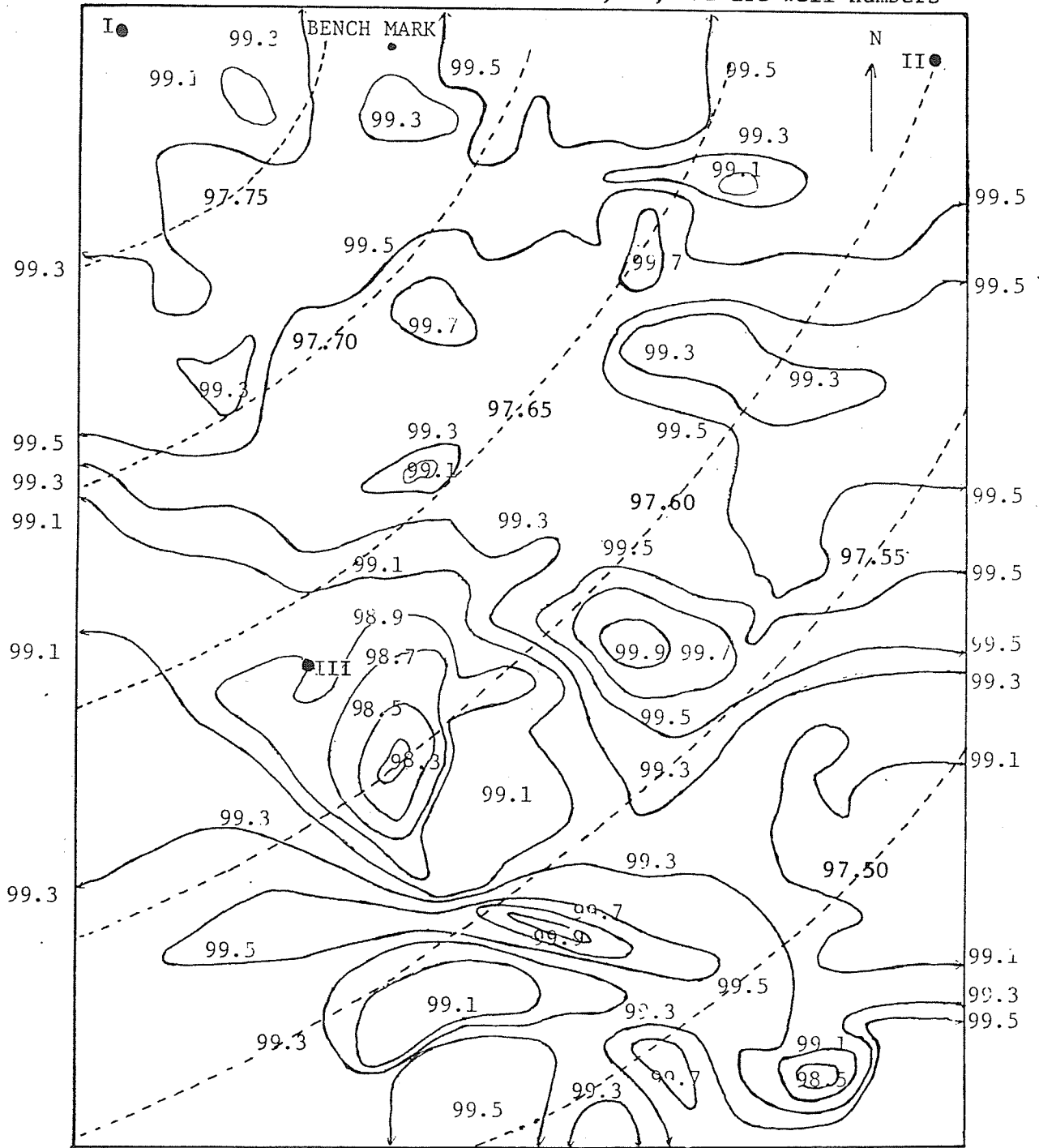
TABLE A-13 MOISTURE CONTENT OF THE TRANSMISSION ZONE AFTER THE FLOODING ENDS AT SECTION III AND INITIAL MOISTURE CONTENT

Depth (cm)	Initial Moisture Content, Dry Weight Basis (%)	Moisture Content, Dry Weight Basis (%)							
		Elapsed Time (h)							
		0	1	2	3	6	10	24	
7.5	7.1	29.5	24.3	22.0	20.0	16.6	14.9	12.0	
15.0	7.4	28.5	23.8	21.0	19.4	16.5	14.4	11.9	
22.5	7.6	27.0	23.5	20.6	19.0	16.4	14.4	11.8	
30.0	7.9	27.0	23.6	20.4	18.8	16.4	14.3	11.8	

APPENDIX B
CONTOUR MAP OF THE COUSINS FIELD

----- Equipotential Lines

I, II, III are well numbers



Scale 1:1650

Figure B1 Contour Map of the Cousins Field (E₂ 35-10-8W)

APPENDIX C

METHOD OF AVERAGES

Method of Averages

The method of averages was used to calculate average capillary pressure at the wetting front (P_{cav}) and saturated hydraulic conductivity (C_s) from the Green and Ampt function.

$$f_{(p)} = C_s \left[1 + \frac{(P_{cav} + h)IMD}{F} \right] \quad (I)$$

Rearranging equation (I), we obtain

$$f_{(p)} \cdot F = C_s [F + (P_{cav} + h)IMD] \quad (II)$$

The observed data includes the initial moisture deficit (IMD), the head of water above the soil surface (h) and a number of observations of the cumulative infiltration (F) corresponding to the infiltration rate $f_{(p)}$.

Let there be n data points. Substitute first $\frac{n}{2}$ data points in equation (II) to obtain $\frac{n}{2}$ equations. Add these equations to obtain equation (III) having a form

$$D = C_s \left[E + \frac{n}{2}(P_{cav} + h)IMD \right] \quad (III)$$

where $D = \sum_{J=1}^{\frac{n}{2}} f_{(p)J} \cdot F_J$

and $E = \sum_{J=1}^{\frac{n}{2}} F_J$

Similarly substitute $\frac{n}{2}$ data points in equation (II) and add $\frac{n}{2}$ equations to obtain another equation (IV) similar to equation (III). Equations (III) and (IV) are solved algebraically to obtain P_{cav} and C_s .